PREPARATION AND SURFACE CHARACTERIZATION OF PLASMA-TREATED AND BIOMOLECULAR-MICROPATTERNED POLYMER SUBSTRATES

by

BRYAN ALFRED LANGOWSKI

A Dissertation submitted to the

Graduate School-New Brunswick

Rutgers, The State University of New Jersey

in partial fulfillment of the requirements

for the degree of

Doctor of Philosophy

Graduate Program in Chemistry and Chemical Biology

written under the direction of

Kathryn E. Uhrich

and approved by

_____

_____

_____

_____

New Brunswick, New Jersey

May, 2007

ABSTRACT OF THE DISSERTATION

Preparation and Surface Characterization of Plasma-Treated and Biomolecular-Micropatterned Polymer Substrates

by Bryan Alfred Langowski

Dissertation Director:

Kathryn E. Uhrich

A micropatterning process creates distinct microscale domains on substrate surfaces that differ from the surfaces' original chemical/physical properties. Numerous micropatterning methods exist, each having relative advantages and disadvantages in terms of cost, ease, reproducibility, and versatility. Polymeric surfaces micropatterned with biomolecules have many applications, but are specifically utilized in tissue engineering as cell scaffolds that attempt to controlled tissue generation *in vivo* and *ex vivo*. As the physical and chemical cues presented by micropatterned substrates control resulting cellular behavior, characterization of these cues *via* surface-sensitive analytical techniques is essential in developing cell scaffolds that mimic complex *in vivo* physicochemical environments.

The initial focus of this thesis is the chemical and physical characterization of plasma-treated, microcontact-printed (μCP) polymeric substrates used to direct nerve cell behavior. Unmodified and oxygen plasma-treated poly(methyl methacrylate) (PMMA) substrates were analyzed by surface sensitive techniques to monitor plasma-induced

chemical and physical modifications. Additionally, protein-micropattern homogeneity and size were microscopically evaluated. Lastly, poly(dimethylsiloxane) (PDMS) stamps and contaminated PMMA substrates were characterized by spectroscopic and microscopic methods to identify a contamination source during microcontact printing.

The final focus of this thesis is the development of microscale plasma-initiated patterning (μPIP) as a versatile, reproducible micropatterning method. Using μPIP, polymeric substrates were micropatterned with several biologically relevant inks. Polymeric substrates were characterized following μPIP by surface-sensitive techniques to identify the technique's underlying physical and chemical bases. In addition, neural stem cell response to μPIP-generated laminin micropatterns was microscopically and biologically evaluated. Finally, enhanced versatility of μPIP in generating microscale poly-L-lysine gradients was demonstrated.

We are all destined for greatness, though it's not the kind that's famed
It's in the struggles and the battles and the fears that we have tamed
By living a life worth living, considering little of how it appears
to the judgments of the weaker who are paralyzed by their fears
To fear is only human, as we are that and never more
But it is in their final conquering that lets our true selves soar
To reach heights seemingly unattainable, reserved for the lucky few
Never knowing that heights are reached once you let yourself be you
No longer denying the presence of the person who patiently waits within
Now brazen, unapologetic, and living now that his life can at last begin
To break down inherited boundaries a single pebble at a time
Until the masses suddenly crumble, leaving an existence so sublime
Imagination without action is a gripping novel that's only half-read
Just as a man who conforms to fit leads a life that's half-dead
Starting with a lone thought, a single moment, a mere notion
But once begun, left to grow, how that puddle turns to ocean
How trickles turn to torrents and torrents turn to tides
Imparting strength to a gait that only shuffles and seldom strides
Perhaps dismiss me a dreamer but hold a mirror to your mind
Do the words remind you of the hopes you think you'll never find?
Or so you've thought all this time never knowing the real lessons
that wait for you to discover once you stand up to Their oppressions
Why the need to overly polish our scratches, the marks of our distinction
Polished to the point of common…polished individual extinction
I cherish my tarnish, my scuffs, my perfectly imperfect good
For the light reflects off of me in fashions that others never could
And though sometimes I may join the game only to prove that I can
It is in its eventual losing that will define me as a man
The fear of losing is not so horrible and no reason to despair
For I will have myself to rely on and that's all I really care

Dziadziu, Babci, Cioci Regina
Kocham Was
Zawsze będę o Was pamiętać

Acknowledgements

I would like to first thank Dr. Anne-Marie Sapse, my advisor from John Jay College, who first put the idea of obtaining a Ph.D. in Chemistry in my head. If it weren't for her encouragement ("You're very good at chemistry; you should think about getting a Ph.D."), I would not be here today. Thanks also go to Dr. Robert Rothchild, a reader on my Master's thesis, for all the support he has given to me over the years. I would also like to acknowledge Dr. Thomas Kubic, my analytical instrumentation professor from John Jay. His approach to teaching impacted me tremendously, and it is because of him that I have the teaching style that I do. At the same time, I'd like to thank Amy Stern, my Calculus I recitation instructor, who gave me so much of her time when I was an undergrad. When my students ask me why I am always so quick to help them out, I tell them that it's my way of thanking Amy. Thanks also go to Dr. Martha Cotter for all her support and confidence in me as a graduate student and as a teacher. Thank you to Dr. Don Siegel, Dr. Asbed Vassilian, and Dr. Ramesh Agarwal for their guidance and support; it was a pleasure working with each of you. Thanks also to Dr. Ken Breslauer for all your help, guidance and words of encouragement…all of which were given at the times when I needed them the most.

My appreciation goes out to Kris Wetter, Melissa Grunwerg, Ann Doeffinger, and Chris Luke for making things run as smoothly as can be. The life of graduate student has its stresses, but it was nice having you there to make things a little less hectic

Thank you to Dr. Boris Yakshinskiy, Ram Sharma, Dr. Luis Garfias, and Valentin Starovoytov for all of your help and guidance with the instrumentation aspects of my research.

Thanks to Kristi and Min Jung for your help and contributions to my project. Thank you also to Kenya, Marie, Evi, Anouska, and Leilani for making such a comfortable and enjoyable working environment. You are all really great people and it was wonderful getting to know you.

I would like to acknowledge Dr. Ted Madey, Dr. Kate Lee, and Dr. Prabhas Moghe, members of my thesis committee, for being such positive influences on me, and for validating me as a scientist. Thank you for all your kind words, votes of confidence, and support. I would especially like to thank Dr. Madey for all the times he stopped and listened to me when my life seemed to be going down the tubes…his advice and genuine interest in my welfare will never be forgotten.

To my advisor, Kathryn: I can honestly say that I am honored to have been one of your students, and I would like to express my deepest gratitude for *everything* you've done for me over the years. None of your patience, understanding, support, and interest went unnoticed. I am proud that "I'm one of Kathryn's Kids", and I hope that you are too.

Finally, I'd like to acknowledge the most important people in my life: my family. Mom, Pop, Michelle, Melissa, Glenn, Dave and Lorrie: There's no amount of words I can say that will capture how much you all mean to me. So rather than trying, I'll just leave it at this: I Love You and I will ALWAYS be there for you.

Table of Contents

List of Tables

List of Figures

CHAPTER 1: INTRODUCTION

1.1 General Overview

Biomolecular-micropatterned polymer substrates are currently used for a wide range of biotechnological applications,[1-3] including tissue engineering, bioassays, and biosensors. Numerous methods to micropattern polymers presently exist, however, each has its relative advantages and disadvantages with respect to ease, speed, cost-efficiency, reliability/consistency, and versatility. As all micropatterning methods employ substrate-surface modification, the identification/improvement of a particular method's shortcomings or the development of enhanced patterning techniques require in-depth knowledge of the chemistry occurring at the substrate surface/ink interface. This requirement promotes surface characterization following each step of a patterning procedure to ensure reliable and reproducible results, and allows application of a technique to a wider range of systems. In addition, surface characterization of biomolecular micropatterns with biotechnological applications may elucidate the mechanisms by which the patterns interact with biological systems (i.e., cells and other biological molecules), and give insight into ways in which the micropatterns may be modified to elicit more positive responses from biological systems.

This thesis focuses on the preparation and subsequent surface characterization of biomolecular micropatterned polymer substrates that may ultimately be used to engineer nerve tissues in peripheral and central nerve reparation. The first portion of this thesis (Chapters 2 and 3) addresses common challenges with and suggests remedies for

microcontact printing, a popular micropatterning technique widely used to produce biomolecular micropatterns. The remainder of the thesis (Chapters 4-7) documents the development of a novel micropatterning method, microscale plasma-initiated patterning, and its initial application for nerve tissue engineering *en route* to the development of an implantable nerve guide. Throughout this thesis, surface analytical techniques were used to monitor changes in polymer surface chemistry occurring during the patterning procedures to provide further understanding of the patterning procedures' scientific bases so that their performance may be improved.

1.2 Tissue Engineering

Tissue engineering is an interdisciplinary field that applies the principles of engineering and the life sciences toward the generation of new tissue or biological substitutes that restore, maintain, or improve tissue function.[4,5] Although the term *tissue engineering* had loosely been applied to the use of prosthetic devices and surgical manipulation of tissues,[5] significant advances in disciplines such as cell biology, materials science, and biochemistry have expanded the definition to encompass the *in vivo* and *ex vivo* creation of natural tissue. Tissue engineering has emerged as a promising approach to treat the loss or malfunction of a tissue or organ without the limitations of current therapies.[6] Organ transplants from one individual to another are severely limited by donor shortages and negative immune responses to the implanted organ/tissue that may lead to the transplant's "rejection".[4,7] Surgical reconstruction of the damaged organ/tissue can result in long-term complications and may not adequately restore proper function to the system,

causing additional pain and distress for the patient.[4,8,9] Use of mechanical devices, such as kidney dialyzers, remain an imperfect solution as they still limit a patient's quality of life and cannot perform all of the functions of a single organ and, therefore, cannot prevent progressive patient deterioration.[4] Although these therapies have saved and improved countless lives, they do not hold the promise for long-term health that tissue engineering offers.

Although tissue engineering holds immense potential, reaching this potential has been hampered by several issues.[7] A continuing challenge of tissue engineering is the development of constructs that more closely replicate the cells' complex *in vivo* dimensional, configurational, and compositional micro- and nano-environments.[10] It is well established that the extracellular environment within the body influences cell behavior with respect to morphology, cytoskeletal structure, and functionality during tissue/organ development.[10] Cellular processes such as adhesion, migration, growth, secretion, and gene expression are triggered, controlled, or influenced by the biomolecular, three-dimensional organization of neighboring surfaces.[11] Cells additionally respond to local concentrations of a variety of molecules that may be dissolved in the extracellular matrix (ECM) or present on the surfaces of adjacent cells.[11] Integrins, a widely expressed family of glycosylated transmembrane receptors, constitute the primary adhesion mechanism to ECM components (e.g., fibronectin, laminin, and type I collagen) and additionally mediate cell-cell adhesion.[12] Cell adhesion to ECM components, and the subsequent formation of focal adhesions combined with their interaction with growth factor receptors, activates signaling pathways that regulate the

survival, cell-cycle progression, and expression of differentiated phenotypes in multiple cell systems.[12] These complex cell/ECM interactions ultimately lead to tissue and organ formation, and it is the controlled re-creation of these events that tissue engineering seeks to achieve within the laboratory.

As tissue engineering approaches typically employ exogenous three-dimensional ECMs to engineer new natural tissues from isolated cells,[6] ultimate success relies greatly on the creation of cell scaffolds that accurately mimic the physiochemical cues that naturally control cell behavior during tissue/organ development. Although daunting and complex, this task may eventually be met through the use of fabrication techniques that can physically and chemically modify natural and synthetic materials at the spatial levels that control cell behavior, namely surface engineering at the micrometer and nanometer levels.

1.3 Micropatterning Techniques

Micropatterning methods include the physical and/or chemical modification of micrometer-sized spatial regions on a surface to create distinct, well-defined areas possessing different physical/chemical properties from the original surface. The modification can be purely physical,[10,13] purely chemical[14] (as in microfluidic networks,[2,15,16] micromolding,[17] or microcontact printing[18]), or a mixture of both.[19-21] Methods that have been employed to physically alter the surface topography at the microscale level include reactive ion etching,[22,23] micromachining,[10,13,24,25]

microroughening,[10,13,26] laser ablation,[10,19,27] and polymer-casting.[10,20,21,25,28] Current chemical modification methods are numerous and include photolithography,[29-32] microcontact printing,[18,32] microfluidic patterning,[15,16,32] micromolding,[17] and plasma lithography,[3,33,34] to name a few. Using these techniques, a vast array of organic- and inorganic-based surfaces have been modified at the microscale level. Micropatterned substrates have been used in many different applications and are commonly employed in the semiconductor industry,[3,18,29,30] as well as the biotechnology industry.[3,18,29,32,35,36] Substrates micropatterned with biologically relevant molecules (e.g., peptides, proteins, and polysaccharides) have led the advancement of biosensors,[18,32,36-39] bioassays,[3,15,18,40] tissue engineering,[14,35,37,41-43] and fundamental studies of cell biology.[3,14,18,21,36,43-47] With a micropatterned surface, a given substrate may interact with other biological entities in a controlled manner by presenting chemical and physical signals to approaching entities. These chemical and physical signals, though not present on the untreated substrate, can be introduced by a staggering combination of methods that will permit controlled interactions between the substrate surface and its surrounding environment. Figures 1-1 through 1-3 present schematic representations illustrating how micropatterns are applied to biosensors (Figure 1-1), tissue engineering (Figure 1-2), and bioassays (Figure 1-3).

As current micropatterning methods have relative advantages and disadvantages in terms of ease, reproducibility, cost, versatility, and need for specialized equipment, no single method is equally applicable to all substrate/ink combinations. The most appropriate method depends, in large part, on the specific system and the eventual application of the micropatterned substrates. For example, photolithography is extensively used for

microelectronic fabrication and requires the use of photoresists, developers, and other organic-based solvents which makes it less attractive for biomaterial applications, as the various organic compounds may be toxic to biological systems.[18] In contrast, soft lithographic methods[18,48,49] (e.g., microcontact printing and microfluidic patterning) do not usually require the use of harmful processing chemicals, and, therefore, have been very popular in generating micropatterns for biological systems.[1,3,18,32,42,47-52]

1.3.1 Microcontact Printing (μCP)

Microcontact printing[1,18,53] is a soft lithographic method that utilizes a micropatterned, elastomeric stamp to transfer inks to substrates. The micropatterned stamp is used in the same fashion as an office stamp, except that the raised features of the stamp are micrometer-sized (see Figure 1-4). The stamp, usually composed of poly(dimethylsiloxane) (PDMS), is immersed in a solution of the molecules to be patterned (i.e., "inked"). During inking, molecules from solution are deposited onto the stamp surface. Once dried of excess solution, the stamp is placed into contact with the substrate, where transfer of molecules from the raised portions of the stamp (i.e., the stamp pattern) to the underlying substrate occurs. Although the stamp surface is completely covered with ink molecules (Figure 1-4-ii), the recessed regions of the stamp never contact the substrate and transfer of ink molecules only occurs with direct stamp-substrate contact. The stamp pattern is typically formed by casting PDMS against a photolithographically fashioned mold (i.e., "master") having a "negative" pattern of the final stamp pattern.

Microcontact printing has been extensively used to pattern organic (i.e., polymeric)[21,41-43,54-60] and inorganic substrates (e.g., gold, silver, silicon, glass, copper, and palladium)[18,40,61,62] with a wide range of inks, including alkylthiols, alkylsilanes, polymer initiators, proteins and peptides.[18,21,35,41,43,55-57,59-62] Although μCP is a relatively uncomplicated technique, some significant issues must be considered when using this technique. For example, patterning with microcontact printing requires that the ink molecules interact with the final substrate more strongly than with the micropatterned stamp. If the ink interacts more strongly with the stamp, inadequate transfer to the substrate may occur, resulting in poor quality patterns.[61] This fact also requires that substrate surfaces be significantly derivatized so that adequate transfer does occur, which increases the number of processing steps. In addition, low molecular-weight PDMS fragments may be transferred from the stamp to the substrate during the microcontact printing process,[54,58,59,63-66] contaminating the resulting micropatterns and necessitating the search for methods that reduce or eliminate contamination.[64,65]

1.3.2 Microfluidic Patterning (μFP)

Microfluidic patterning[2,3,15,16,18,32] is similar to μCP in that a micropatterned, elastomeric stamp is used to define a micropattern on a substrate. However, the stamp is not used to transfer the inks, as in μCP. Instead, the stamp is contacted with a substrate to form microchannels, through which inking solutions can flow and deposit ink molecules in the areas of the substrate not protected by the stamp (see Figure 1-5). The elastic nature and hydrophobicity of PDMS enables self-sealing with the substrate.[15,16,32] Patterns can be

generated by restricting the fluid flow to selected areas of the substrate using the microchannels. This method has been used primarily for surface attachment of cells and deposition of biologically relevant molecules that either encourages or prevents subsequent cellular attachment.[3,16,32,36,67-71]

The success of μFP relies largely on the quality of the seal between the PDMS stamp and the substrate.[72] A weak seal may cause channel leakage and result in poor quality patterns. In addition, a pumping system is usually employed to force fluid through the channels,[2] making this method increasingly labor intensive and ill-suited for viscous liquids.[73]

1.4 Polymeric Biomaterials

Historically, micropatterning techniques were developed for the microelectronics industry, with a focus on inorganic substrates and organic-based inks for non-biological purposes. However, micropatterning methods developed by the microelectronics industry began to be utilized for biological issues. This evolution ushered in the micropatterning of aqueous-based biological ligands for biomaterial applications, first on inorganic substrates,[18,29-31,35,38,44,47,50,52,61,69,74] and then eventually to polymeric substrates.[21,40-43,54,56,58-60] This natural progression to biomolecular micropatterning onto polymeric substrates for biomaterial applications is understandable given the general physical and chemical characteristics of polymers.[75-78] Polymers are flexible, making them well suited as implant materials for applications where the rigidity and brittleness of

common inorganic materials (e.g., glass) would be a disadvantage. Polymers are more easily processed into different physical forms (i.e., fibers, meshes, thin films, etc.) than inorganic materials. Although most polymers are biocompatible, a new generation of polymers is emerging that are also biodegradable.[42,56,75,79,80] As biodegradation can be controlled, polymeric biomaterials are currently being fashioned that will perform a given function within the body for a specified length of time. Once the device has served its purpose and is no longer needed, natural degradation of the polymer occurs, eliminating the need for surgical explantation. Finally, polymer surfaces can be easily modified to better control their interactions with biomolecules and cells.[42,81-86] Currently, several chemical methods exist to modify polymer surface characteristics, including wet chemical techniques,[56,82-84,86,87] chemical vapor deposition,[37,85,88] polymer grafting,[75,84,89,90] and photochemical methods.[84,85,89,91,92]

1.5 Plasma Modification of Polymers

A widely used technique to physically and/or chemically modify polymer surfaces is plasma-treatment.[76,84,85,93-97] Plasma, which is considered the fourth state of matter, is essentially ionized gas.[3,98] Naturally occurring examples of plasma include flame, lightning, and stars.[98] In a laboratory setting, plasma is most commonly generated by irradiating a feed gas with radiofrequency waves (i.e., an RF discharge) or microwaves. Plasma is an energetic mixture of radicals, ions, electrons, photons, and metastable species.[93,94,98-100] Polymer surfaces exposed to the various components of plasma undergo a myriad of chemical and physical changes, including functional group

incorporation, etching, crosslinking, and ablation.[82,93,94,96,97,99,100] The exact modifications occurring at a substrate surface depend both on the chemical nature of the surface and the composition of the plasma. Plasma composition is controlled by several generator variables including feed gas, electrode/chamber configuration, power, and chamber pressure.[85,93,94,98,99,101-103] Plasma-treatment is an advantageous method to modify polymer surfaces for two reasons. First, as plasma only modifies the surface, the polymer's bulk mechanical properties remain unchanged.[76,82,93,103,104] Second, plasma-treatment is time efficient, generates little waste, and is generally safe.[104] Polymer surfaces treated with plasma have shown enhanced hydrophilicity, biocompatibility, and adhesivity.[76,81,93,94,97,102,105-107] Several studies have investigated and documented the chemical and physical modifications of plasma-treated polymers using surface-sensitive analytical techniques.[76,82,87,92,93,95,97,102,103,108,109]

A common feed gas used for plasma-treatment is oxygen. Oxygen plasma-treatment of polymer surfaces comprises substrate degradation and reactions with ions, atoms, ozone, electrons, and a broad electromagnetic spectrum.[82,94,105] Polymer surfaces exposed to oxygen plasma become oxidized and are incorporated with a variety of polar, oxygen-containing functional groups, including alcohols, ethers, esters, and acids. This, in turn, gives rise to increased surface hydrophilicity, as the surface presents a more polar environment. Most polymers tend to experience an increase in oxygen content at the surface during oxygen plasma-treatment; a notable exception is poly(tetrafluoroethylene) (PTFE or "Teflon"), for which no chemical change is observed, although the surface roughens.[94]

1.6 Surface Analysis

Surface analysis is used to understand the changes taking place on polymer surfaces during plasma modification.[92-94,108-110] In addition, physical and chemical characterization of micropatterned substrates is routinely performed to monitor topographical and chemical changes on the substrate surface caused by the patterning procedure and confirm pattern formation.[21,41,50,54,61,111,112] However, as each technique has its inherent advantages and disadvantages, it is vital that a multi-technique approach is used to characterize plasma-treated and/or micropatterned substrates.[51,58,65,94-96,109,113,114]

1.6.1 X-ray Photoelectron Spectroscopy (XPS)

X-ray photoelectron spectroscopy[81,87,113,115-117] is a surface-sensitive analytical technique based upon the photoelectric effect that provides surface elemental composition and identifies the chemical environments of the elements present. On the individual atomic scale, an x-ray photon of known frequency (ν) is used to irradiate a sample and eject an electron from one of the orbitals of an atom making up the sample surface, provided that the photon energy ($h\nu$) exceeds the electron binding energy (E_b). In XPS, the spectrometer analyzer separates the photoelectrons based upon their kinetic energies (E_k). Knowing the initial photon energy and a photoelectron's kinetic energy, the binding energy can be calculated simply by subtracting E_k from $h\nu$:

$$E_b = h\nu - E_k$$

As an electron's binding energy is mainly a function of the identity of the atom and the characteristic core energy level from which it originates, identification of the elements present at the sample surface is possible (apart from hydrogen). Signal intensities provide information concerning elemental surface concentration. In addition, as different chemical environments cause slight, but detectable shifts in binding energy, atoms in different chemical environments can be distinguished and identified. For example, aliphatic carbons can be distinguished from ether carbons, carbonyl carbons, and carboxylic carbons based upon their characteristic binding energy shifts.

XPS has been commonly employed to analyze untreated and plasma-treated polymer surfaces, assisting in the identification of unknown surface species created during plasma modification.[82,84,87,92,93,95,96,108-110] However, as samples must be analyzed under ultra-high vacuum environments (i.e., non-biologically relevant environments), XPS is not well suited for protein micropattern analysis.

1.6.2 Contact Angle Measurements (CAM)

A drop of water in contact with a sample surface will either spread out or bead up in response to the chemical environment of the underlying substrate.[84,118] Measurement of the angle between a solid surface and the liquid/gas tangent (i.e., the "contact angle", Figure 1-6) is an indication of the surface's hydrophilicity (i.e., water wettability).[81,84,118,119] Water droplets have small contact angles on hydrophilic surfaces, whereas droplets with larger contact angles form on hydrophobic surfaces. In addition, water contact angle measurements can give information regarding the polarity of functional

groups present at the surface/water interface. Highly polar groups (e.g., hydroxyls and amines) may cause a water droplet to spread to maximize the hydrophilic interactions between the droplet and surface, whereas the presence of non-polar groups (e.g., methyls) will cause a water droplet to bead up, minimizing the droplet's surface area and its interaction with the surface.

Water contact angle measurements are commonly used to monitor increases in polymer surface hydrophilicity following plasma-treatment, and suitably indicate differences in the chemical environments of polymer surfaces.[81,84,93-96,108,109,119]

1.6.3 Scanning Electron Microscopy (SEM)

Scanning electron microscopy[113,120] is a physical characterization technique that provides high magnification information about surface morphology and topography. In SEM, a surface is swept/scanned in a raster pattern with a finely focused electron beam. During the scanning process, backscattered and secondary electrons are produced from the sample, collected, and graphically converted to produce an image of the substrate surface.[113] The ultimate resolution of an electron microscope is largely limited by the diameters of the incident electron beam and backscattered electron beam.[113]

Although SEM can produce high magnification images and has a larger field of view than other high magnification microscopic methods (e.g., atomic force microscopy and near-field scanning optical microscopy, to be discussed), the technique is limited for polymeric/biological imaging. As in XPS, samples are analyzed under vacuum, making

SEM ill suited for protein micropatterns. Furthermore, insulating samples like polymers must be sputter-coated with a thin layer of metal prior to imaging to prevent charge accumulation during analysis. Sputter coating prevents further use of the sample following SEM analysis and, in the case of protein patterns, creates an unnatural environment that is not biologically relevant. Relatively fragile samples can be damaged by the high energy electron beam, and may introduce imaging artifacts.[29,121] Lastly, although SEM can provide qualitative topographical information, it only provides quantitative information in the *x* and *y* directions of the sample, yet is not accurate in the *z* direction. This issue deems SEM unsuitable to measure micropattern heights and topographical depths. However, SEM is commonly employed to analyze polymer surfaces and can document the physical changes induced on surfaces by plasma treatment.[94,96,102,104,114,122-124]

1.6.4 Atomic Force Microscopy (AFM)

Atomic force microscopy[113,115,125] is similar to SEM in that high magnification surface topographical data can be provided, but this technique affords additional information. In AFM, a sharp tip affixed to the end of a flexible cantilever is scanned in a raster pattern over a substrate surface. In "contact mode" AFM, the tip is dragged across the sample surface much like a stylus on a phonograph record. The cantilever, as it follows the surface topography, experiences vertical deflections in response to microscopic bumps and grooves on the surface. These vertical deflections are monitored by reflecting a laser off the cantilever onto a photodetector, which detects the laser movement in response to

the cantilever deflection. The vertical movement of the cantilever is recorded and used to produce surface images.

For biological samples that may be damaged by the dragging tip, intermittent contact (i.e., "tapping") is preferable. In "tapping mode", the cantilever is oscillated at its resonant frequency. The amplitude of the oscillating cantilever (i.e., the total distance swept during oscillation) is monitored by the same laser/photodetector assembly employed in contact mode. The amplitude is set at a certain value (i.e., the setpoint amplitude) and maintained by raising or lowering the sample surface relative to the oscillating cantilever. When the sample is brought close enough to the tip to decrease cantilever amplitude, the sample is moved away to reestablish the setpoint amplitude. If the sample is moved too far away, and the cantilever has an amplitude greater than the setpoint, the sample is brought closer until the setpoint amplitude is reestablished. The movement of the sample in the *z* direction is recorded and used to create a topographical image. As the tip is in contact with the sample only at the bottom of each oscillation cycle, less damage occurs as compared to "contact mode".[113,125]

In addition to surface topography visualization, AFM provides quantitative measurements of surface roughness and feature height. As deflections at the nanometer scale can be detected, AFM gives high spatial resolution images at the near-atomic level. Because the spatial resolution of AFM is largely dictated by the tip's radius of curvature, micron and sub-micron features can be easily detected with common AFM tips, as their radii of curvatures typically range from 10-40 nm.[125] Additionally, samples can be imaged in wet

and dry environments, allowing for protein pattern analysis under biologically relevant conditions. Unfortunately, AFM has a relatively narrow field of view,[126] with most systems capturing areas no larger than 100 μm × 100 μm at a time. This limitation ensures that topographical overviews of large (e.g., 1 cm^2) samples are difficult and extremely time-consuming. Despite its limitations, AFM is routinely used to analyze biomaterial surfaces, interfaces and biomolecular micropatterns.[17,50,58,69,94,96,111,112,125,127-131]

1.6.5 Near-Field Scanning Optical Microscopy (NSOM)

Near-field scanning optical microscopy[125,132,133] is a physical characterization technique similar to AFM in that surface topography is analyzed by scanning a probe across a surface and images generated by monitoring the tip/sample distance. However, instead of a tip/cantilever assembly, NSOM utilizes a finely tapered fiber optic probe capable of capturing both topographical and complimentary optical information. Like AFM, the ultimate spatial resolution of NSOM is dictated by tip dimensions. As typical NSOM probes have approximate diameters of 50 nm, micron and sub-micron surface features can be routinely detected when measuring surface topography.[125] In addition, as the complimentary optical information is from the near field, no diffraction limit is apparent as is common to many other forms of optical microscopy.[125] When rastered over the sample surface, the fiber optic probe maintains a set distance from the surface and moves in response to surface morphology, thus, generating quantitative topographical information. Simultaneously, the probe illuminates the substrate and captures the reflected light from the area directly below it. As the opening of the fiber is on the

nanometer scale, only small portions of the sample are illuminated and analyzed by the photodector that generates the optical image.[125]

Like AFM, NSOM can be performed in both wet and dry environments. However, unlike AFM, NSOM is truly non-contact, as the probe never touches the sample surface. This occurrence is due to the different mechanisms and instrumental components by which tip/sample distance is maintained in NSOM.[125] Although NSOM does not have as good resolution compared to AFM, the fact that NSOM is non-contact makes it very suitable for analyzing fragile, biological specimens that may normally be damaged or disrupted during AFM analysis. Due to its advantages, NSOM is gaining popularity for polymer and biomaterial analysis.[31,132-138] The limitations of NSOM are similar to those of AFM, namely small fields of view, time-consuming data capture, and difficulty in maintaining constant tip/sample distances.

1.6.6 Confocal Laser Scanning Microscopy (CLSM)

In confocal laser scanning microscopy, [132,139,140] an illumination source (i.e., laser) is scanned over a stationary sample. The light from the sample, originating from either reflection or sample fluorescence (depending upon instrument mode), is captured by a photodector that generates an optical image. A pinhole aperture placed in front of the photodector allows samples to be optically sectioned, thus, allowing photodection in a single focal plane. After several focal planes are captured, these sections are combined to form three-dimensional images. Samples that naturally fluoresce can be imaged without further preparation, while non-fluorescent samples must be tagged prior to imaging with

a fluorescent molecule. Because CLSM is an optical microscopic technique, its resolution is ultimately limited by the wavelength of light illuminating the sample, making CLSM most suitable for microscale analysis. Also, as most samples are fluorescently tagged, excessive exposure to outside sources of light should be minimized and avoided. CLSM is routinely used for biomolecule and cellular imaging.[17,29,43,54,58,60,69,70,121,129,130,140-142]

1.7 An Overview of Forthcoming Chapters

This section presents an overview with the intent of guiding the reader through the experiments in this thesis and unifying the relevant issues, goals, findings and scientific significance of the various chapters into a single, self-contained body of work. The forthcoming chapters are organized chronologically, and where applicable, highlight the pertinent experimental findings that laid the groundwork for the eventual experiments contained in later chapters. This thesis is organized to demonstrate the unforeseen nature of research and mirrors how the path of research is defined by the scientific findings, and not by the scientist. In addition to a presentation of the author's work, succeeding chapters also contain findings from experiments not necessarily performed by the author.

Chapter 2 covers the surface characterization of plasma-treated polymeric substrates, the use of microcontact printing (μCP) to produce protein micropatterns on polymer surfaces for directed nerve cell attachment, and the subsequent chemical/physical characterization of these micropatterned substrates. The findings from this chapter illustrate the various

physical and chemical changes occurring on polymer surfaces due to plasma exposure, and lay the historical and theoretical bases for the development of microscale plasma-initiated patterning (discussed in greater detail in Chapters 4-6). In addition, the findings from Chapter 2 identify two significant drawbacks of microcontact printing: the unwanted silicone transfer that occurs during the printing procedure and the unreliability of μCP for protein pattern generation. The discovery of silicone transfer, and the need to minimize it, led to the experiments in Chapter 3. The unreliability of μCP and the challenges associated with this technique enabled the discovery of microscale plasma-initiated patterning.

Chapter 3 focuses in-depth on the unwanted silicone transfer that occurs during microcontact printing, and describes studies to identify its origins, and methods to minimize its occurrence.

The topic of Chapter 4, microscale plasma-initiated patterning (μPIP), is a direct result of the second significant drawback of μCP identified in Chapter 2, namely, the unreliability of μCP to consistently generate protein micropatterns on polymer substrates. The versatility and enhanced reliability of μPIP in generating simple protein micropatterns, as well as the physical and chemical concepts behind the technique are discussed.

Chapter 5 illustrates the bioactivity of μPIP protein patterns using cell response as an indicator of biological activity. This chapter further demonstrates the "real world" utility of μPIP to generate biologically active micropatterns.

Chapter 6 shows the enhanced versatility of μPIP by demonstrating the generation of microscale biomolecular gradients - micropatterns that show gradual changes in biomolecule amounts along their length. As chemical gradients naturally occur *in vivo* to control cell behavior, their facile generation by μPIP will encourage further controlled, *in vitro* studies on the effects of chemical gradients on cell behavior.

Chapter 7 identifies unresolved issues that must be addressed regarding μPIP and future directions to further increase the utility and versatility of μPIP.

1.8 References

(1) Bernard, A.; Renault, J. P.; Michel, B.; Bosshard, H. R.; Delamarche, E. *Adv. Mater.* **2000**, *12*, 1067-1070.

(2) Delamarche, E.; Juncker, D.; Schmid, H. *Adv. Mater.* **2005**, *17*, 2911-2933.

(3) Falconnet, D.; Csucs, G.; Grandin, H. M.; Textor, M. *Biomaterials* **2006**, *27*, 3044-3063.

(4) Langer, R.; Vacanti, J. P. *Science* **1993**, *260*, 920-926.

(5) Vacanti, C. A. *Tissue Eng.* **2006**, *12*, 1137-1142.

(6) Kim, B. S.; Mooney, D. J. *TIBTECH* **1998**, *16*, 224-230.

(7) Nerem, R. M. *Tissue Eng.* **2006**, *12*, 1143-1150.

(8) Seckel, B. R. *Muscle & Nerve* **1990**, *13*, 785-800.

(9) Kim, B. S.; Baez, C. E.; Atala, A. *World J. Urol.* **2000**, *18*, 2-9.

(10) Desai, T. A. *Med. Eng. Phys.* **2000**, *22*, 595-606.

(11) Folch, A.; Toner, M. *Annu. Rev. Biomed. Eng.* **2000**, *2*, 227-256.

(12) Garcia, A. J. *Adv. Polym. Sci.* **2006**, *2003*, 171-190.

(13) Ito, Y. *Biomaterials* **1999**, *20*, 2333-2342.

(14) Corey, J. M.; Feldman, E. L. *Experimental Neurology* **2003**, *184*, S89-S96.

(15) Delamarche, E.; Bernard, A.; Schmid, H.; Bietsch, A.; Michel, B.; Biebuyck, H. *J. Am. Chem. Soc.* **1998**, *120*, 500-508.

(16) Folch, A.; Toner, M. *Biotechnol. Prog.* **1998**, *14*, 388-392.

(17) Suh, K. Y.; Khademhosseini, A.; Yang, J. M.; Eng, G.; Langer, R. *Adv. Mater.* **2004**, *16*, 584-588.

(18) Xia, Y.; Whitesides, G. M. *Angew. Chem. Int. Ed.* **1998**, *37*, 550-575.

(19) Clark, P.; Dunn, G. A.; Knibbs, A.; Peckham, M. *Int. J. Biochem. Cell Biol.* **2002**, *34*, 816-825.

(20) Recknor, J. B.; Recknor, J. C.; Sakaguchi, D. S.; Mallapragada, S. K. *Biomaterials* **2004**, *25*, 2753-2767.

(21) Recknor, J. B.; Sakaguchi, D. S.; Mallapragada, S. K. *Biomaterials* **2006**, *27*, 4098-4108.

(22) Meyle, J.; Wolburg, H.; von Recum, A. F. *J. Biomater. Appl.* **1993**, *7*, 362-374.

(23) Gray, B. L.; Lieu, D. K.; Collins, S. D.; Smith, R. L.; Barakat, A. I. *Biomedical Microdevices* **2002**, *4*, 9-16.

(24) Chehroudi, B.; Gould, T. R.; Brunette, D. M. *J. Biomed. Mater. Res.* **1988**, *22*, 459-473.

(25) Borenstein, J. T.; Terai, H.; King, K. R.; Weinberg, E. J.; Kaazempur-Mofrad, M. R.; Vacanti, J. P. *Biomedical Microdevices* **2002**, *4*, 167-175.

(26) Itälä, A.; Ylänen, H. O.; Yrjans, J.; Heino, T.; Hentunen, T.; Hupa, M.; Aro, H. T. *J. Biomed. Mater. Res.* **2002**, *62*, 404-411.

(27) Barbucci, R.; Lamponi, S.; Pasqui, D.; Rossi, A.; Weber, E. *Mater. Sci. Eng. C* **2003**, *23*, 329-335.

(28) Mata, A.; Boehm, C.; Fleischman, A. J.; Muschler, G.; Roy, S. *J. Biomed. Mater. Res.* **2002**, *62*, 499-506.

(29) Blawas, A. S.; Reichert, W. M. *Biomaterials* **1998**, *19*, 595-609.

(30) Tai, H.; Buettner, H. M. *Biotechnol. Prog.* **1998**, *14*, 364-370.

(31) Schmalenberg, K. E.; Thompson, D. M.; Buettner, H. M.; Uhrich, K. E.; Garfias, L. F. *Langmuir* **2002**, *18*, 8593-8600.

(32) Park, T. H.; Shuler, M. L. *Biotechnol. Prog.* **2003**, *19*, 243-253.

(33) Goessl, A.; Garrison, M. D.; Lhoest, J.-B.; Hoffman, A. S. *J. Biomater. Sci. Polymer Edn.* **2001**, *12*, 721-738.

(34) Goessl, A.; Golledge, S. L.; Hoffman, A. S. *J. Biomater. Sci. Polymer Edn.* **2001**, *12*, 739-753.

(35) James, C. D.; Davis, R. C.; Kam, L.; Craighead, H. G.; Isaacson, M.; Turner, J. N.; Shain, W. *Langmuir* **1998**, *14*, 741-744.

(36) Reyes, D. R.; Perruccio, E. M.; Becerra, S. P.; Locascio, L. E.; Gaitan, M. *Langmuir* **2004**, *20*, 8805-8811.

(37) Manso, M.; Rossini, P.; Malerba, I.; Valsesia, A.; Gribaldo, L.; Ceccone, G.; Rossi, F. *J. Biomater. Sci. Polymer Edn.* **2004**, *15*, 161-172.

(38) St. John, P. M.; Davis, R.; Cady, N.; Czajka, J.; Batt, C. A.; Craighead, H. G. *Anal. Chem.* **1998**, *70*, 1108-1111.

(39) Orth, R. N.; Clark, T. G.; Craighead, H. G. *Biomedical Microdevices* **2003**, *5*, 29-34.

(40) Howell, S. W.; Inerowicz, H. D.; Regnier, F. E.; Reifenberger, R. *Langmuir* **2003**, *19*, 436-439.

(41) Lin, C.-C.; Co, C. C.; Ho, C.-C. *Biomaterials* **2005**, *26*, 3655-3662.

(42) McDevitt, T. C.; Woodhouse, K. A.; Hauschka, S. D.; Murry, C. E.; Stayton, P. S. *J. Biomed. Mater. Res.* **2003**, *66A*, 586-595.

(43) Schmalenberg, K. E.; Uhrich, K. E. *Biomaterials* **2005**, *26*, 1423-1430.

(44) Mrksich, M.; Whitesides, G. M. *Annu. Rev. Biophys. Biomol. Struct.* **1996**, *25*, 55-78.

(45) Mrksich, M. *Chem. Soc. Rev.* **2000**, *29*, 267-273.

(46) Chen, C. S.; Mrksich, M.; Huang, S.; Whitesides, G. M.; Ingber, D. E. *Science* **1997**, *276*, 1425-1428.

(47) Kam, L.; Shain, W.; Turner, J. N.; Bizios, R. *Biomaterials* **2001**, *22*, 1049-1054.

(48) Whitesides, G. M.; Ostuni, E.; Takayama, S.; Jiang, X.; Ingber, D. E. *Annu. Rev. Biomed. Eng.* **2001**, *3*, 335-373.

(49) Kane, R. S.; Takayama, S.; Ostuni, E.; Ingber, D. E.; Whitesides, G. M. *Biomaterials* **1999**, *20*, 2363-2376.

(50) Sgarbi, N.; Pisignano, D.; Di Benedetto, F.; Gigli, G.; Cingolani, R.; Rinaldi, R. *Biomaterials* **2004**, *25*, 1349-1353.

(51) Csucs, G.; Michel, R.; Lussi, J. W.; Textor, M.; Danuser, G. *Biomaterials* **2003**, *24*, 1713-1720.

(52) Kam, L.; Boxer, S. G. *J. Biomed. Mater. Res.* **2001**, *55*, 487-495.

(53) Kumar, A.; Whitesides, G. M. *Appl. Phys. Lett.* **1993**, *63*, 2002-2004.

(54) Yang, Z.; Chilkoti, A. *Adv. Mater.* **2000**, *12*, 413-417.

(55) Zheng, H.; Berg, M. C.; Rubner, M. F.; Hammond, P. T. *Langmuir* **2004**, *20*, 7215-7222.

(56) Lee, K.; Kim, D. J.; Lee, Z.; Woo, S. I.; Choi, I. S. *Langmuir* **2004**, *20*, 2531-2535.

(57) Inglis, W.; Sanders, G. H. W.; Williams, P. M.; Davies, M. C.; Roberts, C. J.; Tendler, S. B. *Langmuir* **2001**, *17*, 7402-7405.

(58) Csucs, G.; Künzler, T.; Feldman, K.; Robin, F.; Spencer, N. D. *Langmuir* **2003**, *19*, 6104-6109.

(59) Yang, Z.; Belu, A. M.; Liebmann-Vinson, A.; Sugg, H.; Chilkoti, A. *Langmuir* **2000**, *16*, 7482-7492.

(60) Schmalenberg, K. E.; Buettner, H. M.; Uhrich, K. E. *Biomaterials* **2004**, *25*, 1851-1857.

(61) Tan, J. L.; Tien, J.; Chen, C. S. *Langmuir* **2002**, *18*, 519-523.

(62) Chen, C. S.; Mrksich, M.; Huang, S.; Whitesides, G. M.; Ingber, D. E. *Biotechnol. Prog.* **1998**, *14*, 356-363.

(63) Hyun, J.; Chilkoti, A. *J. Am. Chem. Soc.* **2001**, *123*, 6943-6944.

(64) Glasmästar, K.; Gold, J.; Andersson, A. S.; Sutherland, D. S.; Kasemo, B. *Langmuir* **2003**, *19*, 5475-5483.

(65) Graham, D. J.; Price, D. D.; Ratner, B. D. *Langmuir* **2002**, *18*, 1518-1527.

(66) Dukovic, G. In *Department of Chemistry and Chemical Biology*; Rutgers University: New Brunswick, 2001; p 49.

(67) Shin, M.; Matsuda, K.; Ishii, O.; Terai, H.; Kaazempur-Mofrad, M.; Borenstein, J.; Detmar, M.; Vacanti, J. P. *Biomedical Microdevices* **2004**, *6*, 269-278.

(68) Cuvelier, D.; Rossier, O.; Bassereau, P.; Nassoy, P. *Eur. Biophys. J.* **2003**, *32*, 342-354.

(69) Patel, N.; Sanders, G. H. W.; Shakesheff, K. M.; Cannizzaro, S. M.; Davies, M. C.; Langer, R.; Roberts, C. J.; Tendler, S. J. B.; Williams, P. M. *Langmuir* **1999**, *15*, 7252-7257.

(70) Khademhosseini, A.; Suh, K. Y.; Jon, S.; Eng, G.; Yeh, J.; Chen, G.; Langer, R. *Anal. Chem.* **2004**, *76*, 3675-3681.

(71) Ma, N.; Koelling, K. W.; Chalmers, J. J. *Biotechnol. Bioeng.* **2002**, *80*, 428-437.

(72) Bhattacharya, S.; Datta, A.; Berg, J. M.; Gangopadhyay, S. *J. Microelectromech. Sys.* **2005**, *14*, 590-597.

(73) Pisignano, D.; Di Benedetto, F.; Persano, L.; Gigli, G.; Cingolani, R. *Langmuir* **2004**, *20*, 4802-4804.

(74) Chang, J. C.; Brewer, G. J.; Wheeler, B. C. *Biomaterials* **2003**, *24*, 2863-2870.

(75) Allcock, H. R.; Lampe, F. W. *Contemporary polymer chemistry*, Second ed.; Prentice Hall: Englewood Cliffs, 1990.

(76) Oehr, C. *Nucl. Instr. and Meth. in Phys. Res. B* **2003**, *208*, 40-47.

(77) Angelova, N.; Hunkeler, D. *Trends Biotechnol.* **1999**, *17*, 409-421.

(78) Klee, D.; Höcker, H. *Adv. Polym. Sci.* **2000**, *149*, 1-57.

(79) Kannan, R. Y.; Salacinski, H. J.; Butler, P. E. M.; Seifalian, A. M. *Biotechnol. Appl. Biochem.* **2005**, *41*, 193-200.

(80) Schmeltzer, R. C.; Schmalenberg, K. E.; Uhrich, K. E. *Biomacromolecules* **2005**, *6*, 359-367.

(81) Ratner, B. D., Ed. *Surface characterization of biomaterials*, First ed.; Elsevier: Amsterdam, 1988; Vol. 6.

(82) Feast, W. J.; Munro, H. S., Eds. *Polymer surfaces and interfaces*, First ed.; John Wiley & Sons: Chichester, 1987.

(83) Lohse, D. J.; Russell, T. P.; Sperling, L. H., Eds. *Interfacial aspects of multicomponent polymer materials*; Plenum Press: New York, 1997.

(84) Garbassi, F.; Morra, M.; Occhiello, E. *Polymer surfaces: from physics to technology*, First ed.; John Wiley & Sons: Chichester, 1994.

(85) Lee, W. W.; d'Agostino, R.; Wertheimer, M. R., Eds. *Plasma deposition and treatment of polymers*; Materials Research Society: Warrendale, 1999; Vol. 544.

(86) Feast, W. J.; Munro, H. S.; Richards, R. W., Eds. *Polymer surfaces and interfaces II*, First ed.; John Wiley & Sons: Chichester, 1993.

(87) Briggs, D.; Seah, M. P., Eds. *Practical surface analysis*, Second ed.; John Wiley & Sons: Chichester, 1990; Vol. 1.

(88) Hozumi, A.; Saito, T.; Shirahata, N.; Yokogawa, Y.; Kameyama, T. *J. Vac. Sci. Technol. A* **2004**, *22*, 1836-1841.

(89) Chen, Y.; Liu, P. *J. Appl. Polym. Sci.* **2004**, *93*, 2014-2018.

(90) Delamarche, E.; Donzel, C.; Kamounah, F. S.; Wolf, H.; Geissler, M.; Stutz, R.; Schmidt-Winkel, P.; Bruno, M.; Mathieu, H. J.; Schaumburg, K. *Langmuir* **2003**, *19*, 8749-8758.

(91) Zhang, D.; Dougal, S. M.; Yeganeh, M. S. *Langmuir* **2000**, *16*, 4528-4532.

(92) Foerch, R.; McIntyre, N. S.; Hunter, D. H. *J. Polym. Sci. A Polym. Chem.* **1990**, *28*, 193-204.

(93) Inagaki, N. *Plasma surface modification and plasma polymerization*, First ed.; Technomic Publishing Co., Inc.: Lancaster, 1996.

(94) Wheale, S. H.; Badyal, J. P. S. In *Interfacial Science*; Roberts, M. W., Ed.; Blackwell Science Ltd: Oxford, 1997; pp 237-255.

(95) Øiseth, S. K.; Krozer, A.; Kasemo, B.; Lausmaa, J. *Appl. Surf. Sci.* **2002**, *202*, 92-103.

(96) Olde Riekerink, M. B.; Terlingen, J. G. A.; Engbers, G. H. M.; Feijen, J. *Langmuir* **1999**, *15*, 4847-4856.

(97) Liston, E. M. *J. Adhesion* **1989**, *30*, 199-218.

(98) Eliezer, S.; Eliezer, Y. *The fourth state of matter: an introduction to plasma science*, Second ed.; Institute of Physics Publishing: Bristol, 2001.

(99) Hollahan, J. R.; Bell, A. T., Eds. *Techniques and applications of plasma chemistry*, First ed.; John Wiley & Sons: New York, 1974.

(100) Hippler, R.; Pfau, S.; Schmidt, M.; Schoenbach, K. H., Eds. *Low temperature plasma physics: fundamental aspects and applications*, First ed.; Wiley-VCH: Berlin, 2001.

(101) Olander, B.; Wirsén, A.; Albertsson, A. *J. Appl. Polym. Sci.* **2003**, *90*, 1378-1383.

(102) Owen, M. J.; Smith, P. J. *J. Adhesion Sci. Technol.* **1994**, *8*, 1063-1075.

(103) Gerenser, L. J. *J. Adhesion Sci. Technol.* **1993**, *7*, 1019-1040.

(104) Fritz, J. L.; Owen, M. J. *J. Adhesion* **1995**, *54*, 33-45.

(105) Whitaker, A. F.; Jang, B. Z. *J. Appl. Polym. Sci.* **1993**, *48*, 1341-1367.

(106) Ohl, A.; Schröder, K. *Surf. Coat. Technol.* **1999**, *116-119*, 820-830.

(107) Hegemann, D.; Brunner, H.; Oehr, C. *Nucl. Instr. and Meth. in Phys. Res. B* **2003**, *208*, 281-286.

(108) Murakami, T.; Kuroda, S.; Osawa, Z. *J. Coll. Int. Sci.* **1998**, *202*, 37-44.

(109) Morra, M.; Occhiello, E.; Marola, R.; Garbassi, F.; Humphrey, P.; Johnson, D. *J. Coll. Int. Sci.* **1990**, *137*, 11-24.

(110) Tóth, A.; Bertóti, I.; Blazsó, M.; Bánhegyi, G.; Bognar, A.; Szaplonczay, P. *J. Appl. Polym. Sci.* **1994**, *52*, 1293-1307.

(111) Kumar, N.; Hahm, J. *Langmuir* **2005**, *21*, 6652-6655.

(112) Biasco, A.; Pisignano, D.; Krebs, B.; Pompa, P. P.; Persano, L.; Cingolani, R.; Rinaldi, R. *Langmuir* **2005**, *21*, 5154-5158.

(113) Skoog, D. A.; Holler, F. J.; Nieman, T. A. *Principles of instrumental analysis*, Fifth ed.; Harcourt Brace College Publishers: Philadelphia, 1998.

(114) Wei, Q. F.; Gao, W. D.; Hou, D. Y.; Wang, X. Q. *Appl. Surf. Sci.* **2005**, *245*, 16-20.

(115) Woodruff, D. P.; Delchar, T. A. *Modern techniques of surface science*, Second ed.; Cambridge University Press: Cambridge, 1994.

(116) Barr, T. L. *Modern ESCA: the principles and practice of x-ray photoelectron spectroscopy*, First ed.; CRC Press: Boca Raton, 1994.

(117) Beamson, G.; Briggs, D. *High resolution XPS of organic polymers: the Scienta ESCA300 database*, First ed.; John Wiley & Sons: Chichester, 1992.

(118) Israelachvili, J. *Intermolecular & surface forces*, Second ed.; Academic Press: San Diego, 1991.

(119) Andrade, J. D., Ed. *Polymer surface dynamics*, First ed.; Plenum Press: New York, 1988.

(120) Goldstein, J. I.; Newbury, D. E.; Echlin, P.; Joy, D. C.; Romig, A. D.; Lyman, C. E.; Fiori, C.; Lifshin, E. *Scanning electron microscopy and x-ray microanalysis*, Second ed.; Plenum Press: New York, 1992.

(121) McKinlay, K. J.; Allison, F. J.; Scotchford, C. A.; Grant, D. M.; Oliver, J. M.; King, J. R.; Wood, J. V.; Brown, P. D. *J. Biomed. Mater. Res.* **2004**, *69A*, 359-366.

(122) Hillborg, H.; Ankner, J. F.; Gedde, U. W.; Smith, G. D.; Yasuda, H. K.; Wikström, K. *Polymer* **2000**, *41*, 6851-6863.

(123) Hillborg, H.; Sandelin, M.; Gedde, U. W. *Polymer* **2001**, *42*, 7349-7362.

(124) Weikart, C. M.; Yasuda, H. K. *J. Polym. Sci. A Polym. Chem.* **2000**, *38*, 3028-3042.

(125) Bonnell, D., Ed. *Scanning probe microscopy and spectroscopy: theory, techniques, and applications*, Second ed.; Wiley-VCH: New York, 2001.

(126) Chung, Y. *Practical guide to surface science & spectroscopy*, First ed.; Academic Press: San Diego, 2001.

(127) Wang, M. S.; Palmer, L. B.; Schwartz, J. D.; Razatos, A. *Langmuir* **2004**, *20*, 7753-7759.

(128) Li, J.; Cassell, A. M.; Dai, H. *Surf. Interface Anal.* **1999**, *28*, 8-11.

(129) Patel, N.; Bhandari, R.; Shakesheff, K. M.; Cannizzaro, S. M.; Davies, M. C.; Langer, R.; Roberts, C. J.; Tendler, S. B.; Williams, P. M. *J. Biomater. Sci. Polymer Edn.* **2000**, *11*, 319-331.

(130) Feng, X.; Roberts, C. J.; Armitage, D. A.; Davies, M. C.; Tendler, S. J. B.; Allen, S.; Williams, P. M. *Analyst* **2001**, *126*, 1100-1104.

(131) Jandt, K. D. *Surf. Sci.* **2001**, *491*, 303-332.

(132) Navratil, M.; Mabbott, G. A.; Arriaga, E. A. *Anal. Chem.* **2006**, *78*, 4005-4020.

(133) de Lange, F.; Cambi, A.; Huijbens, R.; de Bakker, B.; Rensen, W.; Garcia-Parajo, M.; van Hulst, N.; Figdor, C. G. *J. Cell Sci.* **2001**, *114*, 4153-4160.

(134) Aoki, H.; Ito, S. *J. Phys. Chem. B* **2001**, *105*, 4558-4564.

(135) Gunning, A. P.; Mackie, A. R.; Kirby, A. R.; Morris, V. J. *Langmuir* **2001**, *17*, 2013-2018.

(136) Teetsov, J. A.; Vanden Bout, D. A. *J. Am. Chem. Soc.* **2001**, *123*, 3605-3606.

(137) Liao, X.; Higgins, D. A. *Langmuir* **2001**, *17*, 6051-6055.

(138) Valaskovic, G. A.; Holton, M.; Morrison, G. H. *Ultramicroscopy* **1995**, *57*, 212-218.

(139) Merrett, K.; Cornelius, R. M.; McClung, W. G.; Unsworth, L. D.; Sheardown, H. *J. Biomater. Sci. Polymer Edn.* **2002**, *13*, 593-621.

(140) Cooke, P. M. *Anal. Chem.* **2000**, *72*, 169R-188R.

(141) Xu, C.; Taylor, P.; Ersoz, M.; Fletcher, P. D. I.; Paunov, V. N. *J. Mater. Chem.* **2003**, *13*, 3044-3048.

(142) Sapsford, K. E.; Ligler, F. S. *Biosens. Bioelectron.* **2004**, *19*, 1045-1055.

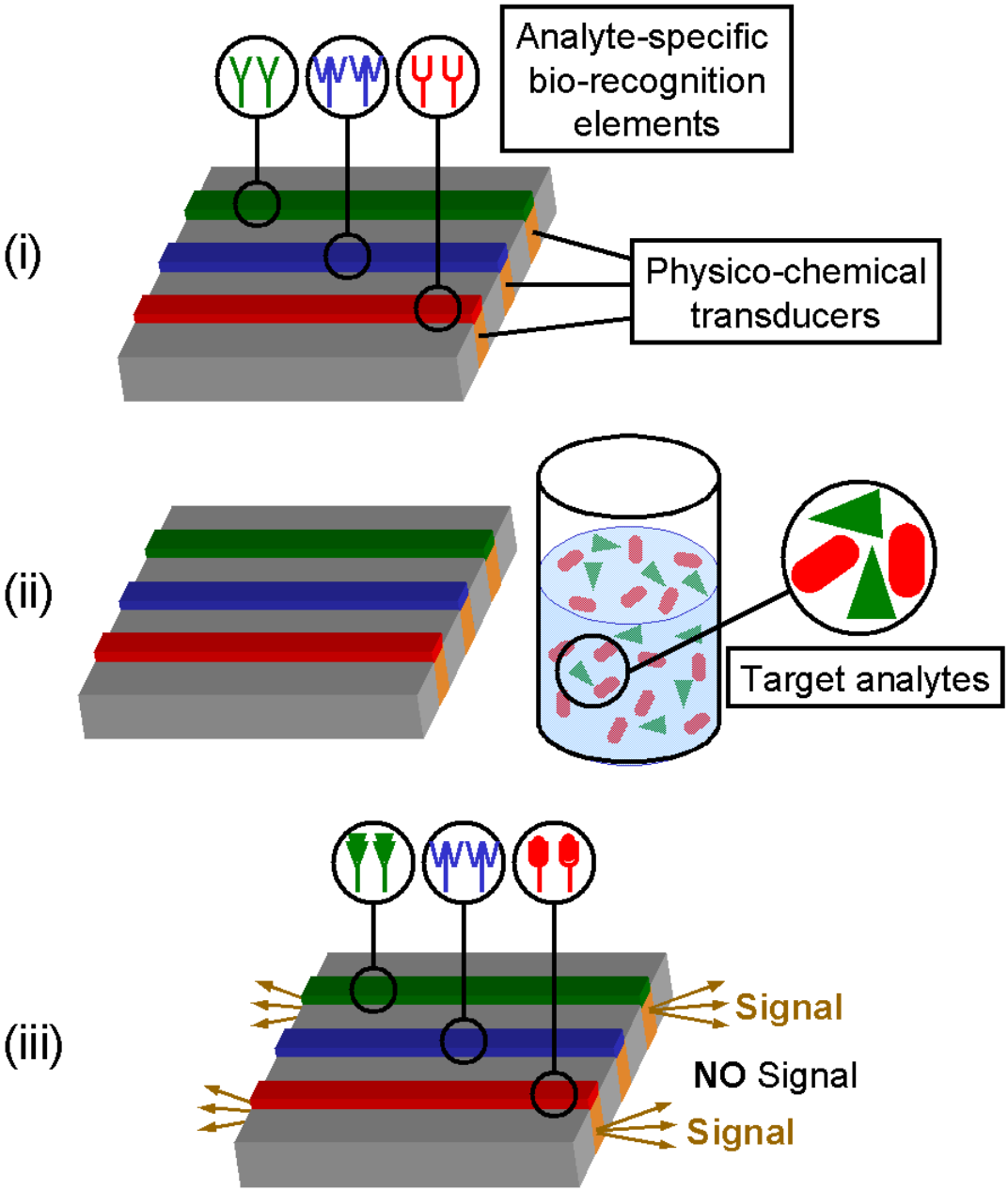

Figure 1-1: Schematic of a general biosensor: (i) analyte-specific bio-recognition elements are coupled to physico-chemical transducers, (ii) sample containing target analytes to be detected, and (iii) interaction of analytes with the specific bio-recognition elements cause transducers to form detectable signals, indicating the presence of analytes.

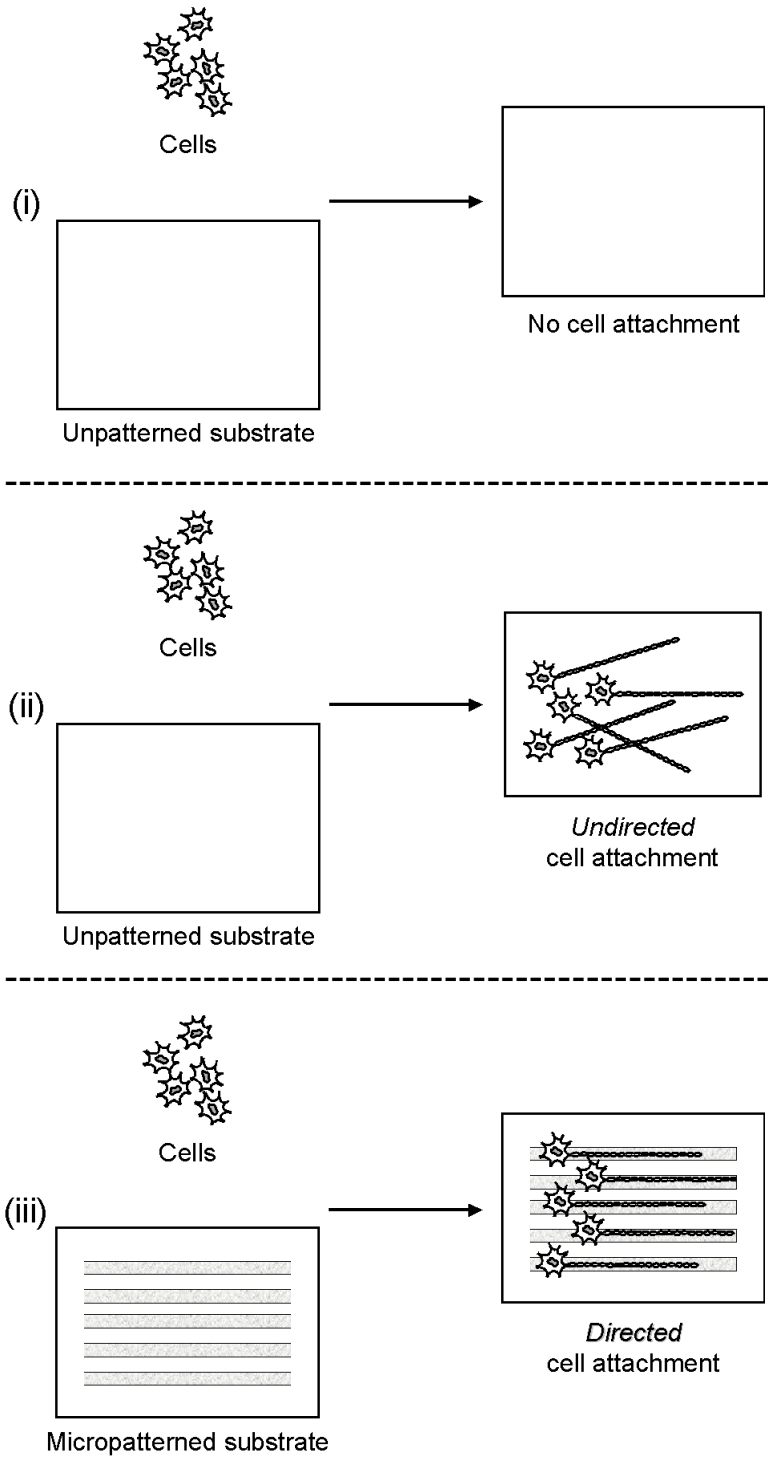

Figure 1-2: Schematic of a general two-dimensional tissue scaffold used to direct nerve cell attachment and outgrowth. Cells on unpatterned substrates may (i) not attach to the substrate, or may (ii) attach to the substrate with random orientations and undirected outgrowth, whereas cells on micropatterned substrates will (iii) attach to the substrate with directed orientations and outgrowth.

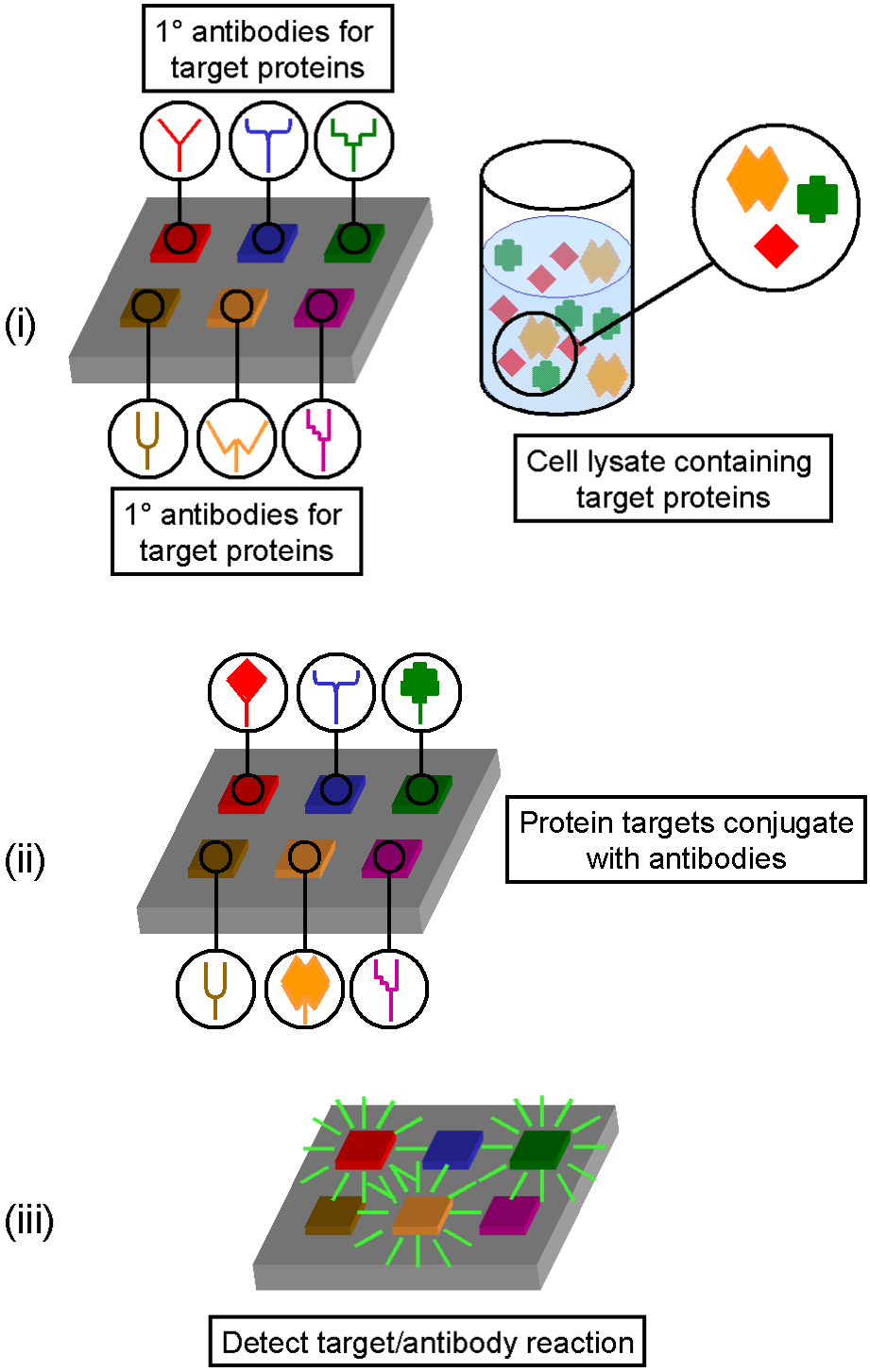

Figure 1-3: Schematic of a general antibody bioassay: (i) primary antibodies for the target proteins are micropatterned onto a support, (ii) target proteins conjugate with their specific antibody, and (iii) target protein/antibody reaction is detected by various methods indicating the presence of specific target proteins.

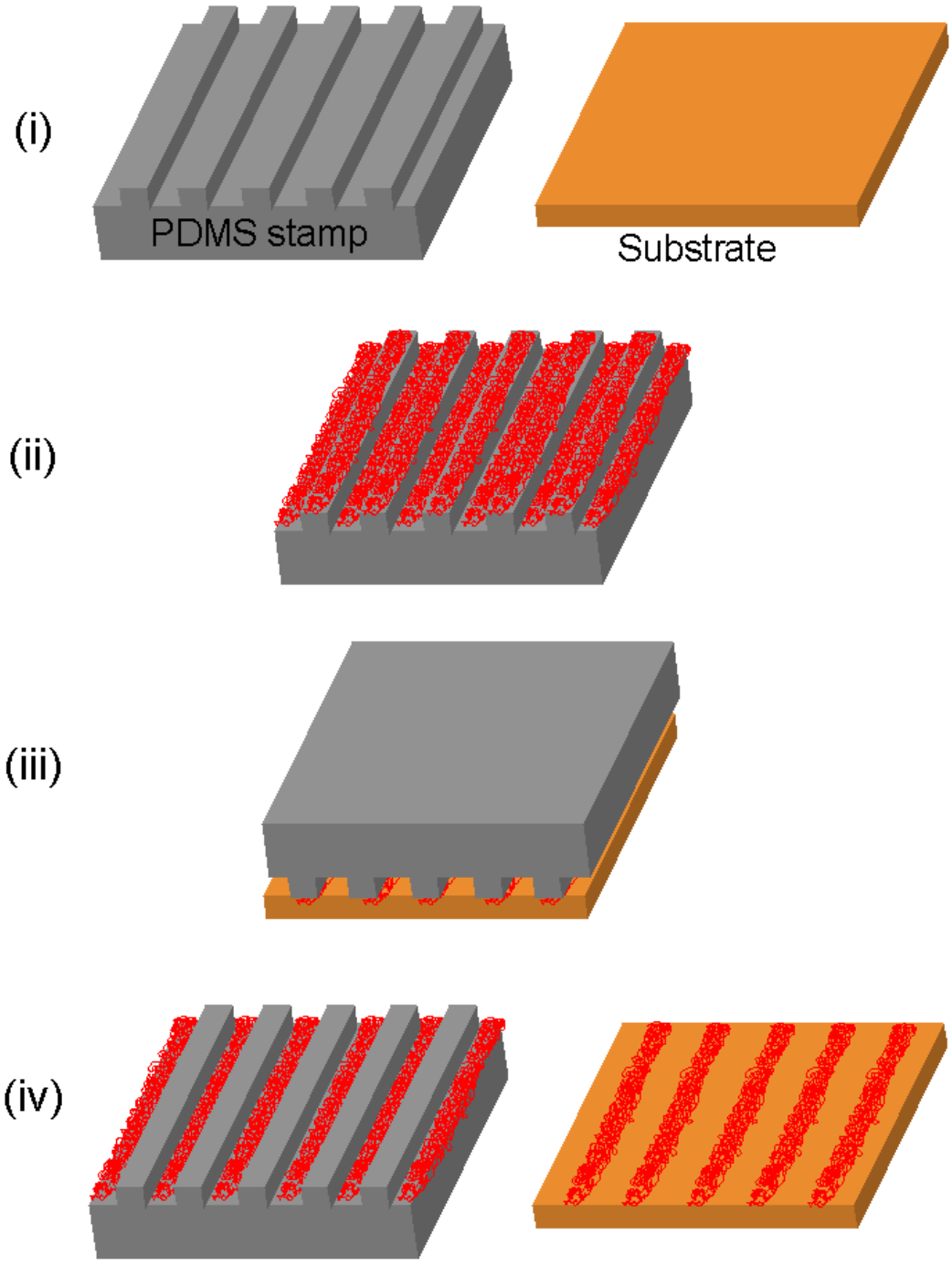

Figure 1-4: Schematic of general microcontact printing procedure: (i) patterned PDMS stamp and substrate, (ii) stamp is inked with molecules to be patterned, (iii) stamp is placed into contact with substrate where ink transfer occurs, and (iv) stamp is removed, leaving an ink-micropatterned substrate.

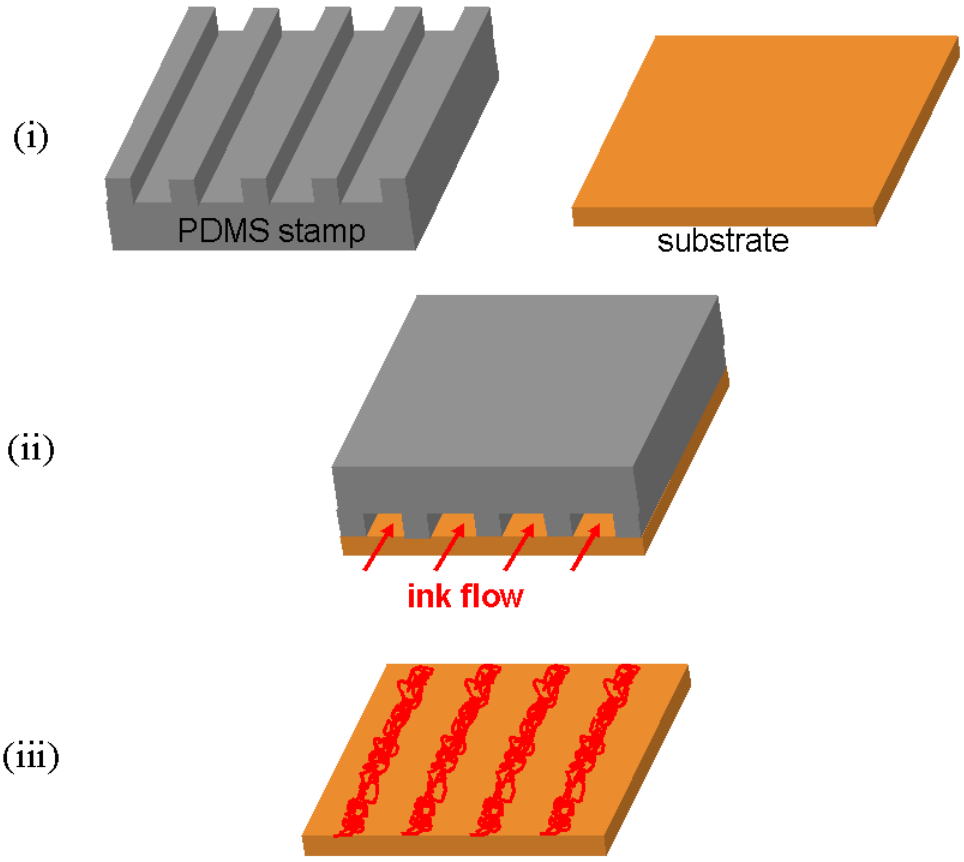

Figure 1-5: Schematic of general microfluidic patterning procedure: (i) patterned PDMS stamp and substrate, (ii) stamp is placed into contact with substrate and ink is flowed through channels formed by the stamp, where ink is deposited, and (iii) stamp is removed, leaving a micropatterned substrate.

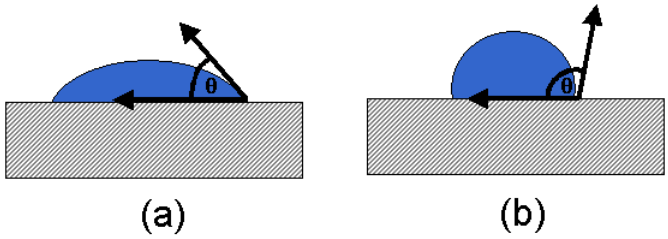

Figure 1-6: Cartoon representation of water contact angles (θ) on: (a) a hydrophilic surface, and (b) a relatively hydrophobic surface.

CHAPTER 2: SURFACE CHARACTERIZATION OF OXYGEN PLASMA-TREATED POLY(METHYL METHACRYLATE) (PMMA) AND RESULTING MICROCONTACT PRINTED (μCP) LAMININ PATTERNS

2.1 Abstract

Unmodified and oxygen plasma-treated poly(methyl methacrylate) (PMMA) substrates were analyzed by surface-sensitive techniques to monitor the chemical and physical modifications due to plasma exposure. X-ray photoelectron spectroscopy (XPS) and water contact angle measurements (CAM) were used to evaluate plasma-induced chemical changes occurring on the PMMA surfaces, whereas atomic force microscopy (AFM) analysis documented plasma-induced topographical changes. XPS results indicate that oxygen plasma increased the amount of oxygen on PMMA, and that the amount of oxygen incorporation can be maximized by systematically optimizing the specific set of plasma parameters (i.e., power, chamber pressure, and duration) used to generate the plasma. AFM results reveal significant roughening of PMMA upon plasma-treatment, and the formation of a loosely bound layer of oxidized PMMA particles that was removed by rinsing in deionized H_2O.

Additionally, microcontact printing (μCP) was used to micropattern laminin stripes onto oxygen plasma-treated PMMA. Laminin-patterned PMMA substrates were subsequently analyzed by confocal laser scanning microscopy (CLSM), XPS, AFM and near-field optical microscopy (NSOM). Although CLSM analysis confirmed the presence of well-formed, widespread laminin stripes in only a few cases, repeated analysis revealed that the *vast* majority (~ 80 %) of detectable patterns were of poor quality. In cases where

good quality patterns were obtained, the patterns were stable on PMMA for four weeks, when stored either under wet or dry conditions at 37 °C. Most importantly, CLSM results demonstrated the unreliability of μCP as a method for laminin micropatterning on PMMA. XPS analysis of laminin-patterned PMMA, indicated by the lack of nitrogen on PMMA, confirmed poor laminin transfer during μCP. XPS also detected the presence of silicon on PMMA surfaces, in addition to carbon and oxygen. As either untreated PMMA or laminin do not inherently contain Si, the appearance of Si indicates possible contamination from the poly(dimethylsiloxane) stamp used in μCP. AFM results showed that laminin stripes, when present, were not homogeneous. AFM analysis also showed that laminin stripe heights (~ 5 nm) were independent of the ink concentration used during μCP. NSOM results confirmed pattern presence, but showed that the stripe heights were significantly greater than those obtained by AFM. This discrepancy is attributed to differences in imaging environments and instrumental data-capturing methods. As both AFM and NSOM analyses determined that laminin stripes present only slight physical cues, it was determined that laminin stripes direct nerve cell attachment and outgrowth predominantly by presenting chemical cues to cells.

2.2 Introduction

Polymer substrates micropatterned with cytophilic (i.e., "cell-loving") proteins are commonly used for tissue engineering applications.[1-10] A popular micropatterning method used to generate such patterns is μCP.[11-14] In most cited instances of protein patterning on polymer surfaces via μCP, the polymers surfaces must first be "activated"

or chemically modified prior to μCP to ensure adequate protein transfer from the elastomeric stamp.[15-20] Although wet chemical methods have been routinely used to activate polymer surfaces, they often expose polymer surfaces to organic-based solvents and compounds which may create a less biologically permissive surface to proteins and/or cells.[15,16,19,21] Previous work by Schmalenberg et al. had shown polymer activation by oxygen plasma as a more biologically friendly alternative to wet chemical methods.[19,20] In these studies, PMMA was exposed to oxygen plasma (200 W, 175 mTorr, for 60 s) prior to μCP with laminin. The resulting laminin stripes were shown to support Schwann cell growth and direct cell orientation and outgrowth. However, aside from CAM and CLSM, the aforementioned studies did not employ any other surface-sensitive techniques to characterize oxygen plasma-treated PMMA or laminin-micropatterned PMMA, leaving many unresolved issues. For example, as the specific plasma parameters (i.e., power, chamber pressure, and duration) used in these studies were arbitrarily chosen, the question as to whether oxygen plasma at 200 W, 175 mTorr, for 60 s is optimal for PMMA activation persisted. Optimization of the plasma-activation process (i.e., oxygen incorporation onto the PMMA surface) may maximize the amount of laminin transferred to the PMMA substrate during μCP which, in turn, would produce micropatterns that are more effective in controlling Schwann cell behavior. Unpublished results by Schmalenberg revealed that Schwann cells did not always attach to the micropatterned substrate areas, and that cells did not always proliferate along a given micropattern after attachment.[22] As an additional example, although the biological activity of the laminin micropatterns was illustrated based upon positive Schwann cell response, little information as to the stability of these patterns or pattern dimensions (e.g.,

width and height) was presented. Therefore, to better understand the role of oxygen plasma-treatment in laminin pattern formation/quality, PMMA substrates were exposed to oxygen plasma and characterized by XPS, CAM, and AFM. The results from these studies could be used to improve/maximize laminin transfer during μCP, particularly for polymer/biomolecule systems. In addition, laminin-micropatterned substrates were analyzed by CLSM, XPS, AFM, and NSOM to evaluate pattern quality, stability, homogeneity and to gain more insight into the physical/chemical cues presented by the micropatterns to nerve cells. These studies could be used to improve cellular response to the micropatterns and add to the general knowledge regarding directed cell attachment for tissue engineering applications.

2.3 Materials and Methods

2.3.1 Materials

Sheets of poly(methyl methacrylate) (Goodfellow, Huntingdon, England, 0.7 mm thick, CQ grade) were cut into squares (1 cm^2) using a razor blade and rinsed with HPLC grade ethanol (Sigma-Aldrich, St. Louis, MO) prior to analysis, plasma-treatment or plasma-treatment/μCP. Laminin from Engelbreth-Holm-Swarm murine sarcoma (Sigma) was serially diluted with phosphate buffered saline (PBS, pH 7.4, MP Biomedicals, Aurora, OH) to concentrations of 500 and 100 μg/mL. Rabbit anti-laminin primary antibody (α-laminin, Sigma) and fluorescein isothiocyanate (FITC)-conjugated goat anti-rabbit immunoglobulin G secondary antibody (α-rabbit IgG, Sigma) were diluted 1:100 in PBS.

2.3.2 Patterned PDMS Stamps

Patterned poly(dimethylsiloxane) (PDMS) stamps were made using Sylgard 184 silicone elastomer kit (Dow Corning, Midland, MI). Elastomer base and curing agent were combined in a 10:1 ratio (w\w), after which prepolymer was placed under vacuum to remove entrapped air. The prepolymer was poured, and allowed to cure, over lithographically created masters. The masters were produced in collaboration with Mr. Octavio Hurtado (BioMEMS Resource Center, Massachusetts General Hospital, Charlestown, MA). In brief, masters were created by exposing photoresist-coated silicon wafers through a photomask producing a relief pattern on the silicon surface. The relief pattern consists of a series of raised, parallel lanes (20 μm wide) separated by 20 μm spaces. Upon curing, the PDMS was peeled off the master, and the patterned regions were cut using a razor blade into stamps (8 mm × 8 mm).

2.3.3 Oxygen Plasma-Treatment (OPT)

PMMA substrates and PDMS stamps were treated with oxygen plasma using a March PX-250 plasma cleaning system (March Plasma, Concord, CA). Prior to sample treatments, the plasma chamber was purged of contaminants adhering to the chamber walls by running a "cleaning cycle" of 300 W, 580 mTorr for 900 s (recommended by the manufacturer). For microcontact printing experiments, the PMMA substrates and PDMS stamps were oxygen plasma-treated simultaneously. PMMA substrates simultaneously treated with PDMS showed no contamination, as evidenced by the lack of Si established by XPS analysis (results not shown). The specific set of parameters used to generate

oxygen plasma (i.e., power, chamber pressure and duration) was varied and will be discussed in more detail.

2.3.3.1 Oxygen Plasma-Treatment Optimization

PMMA substrates were treated under various plasma conditions to ascertain the optimal treatment for activation. Substrates were then analyzed with XPS to monitor changes in oxygen amounts on the PMMA surfaces (see below). The initial starting point for oxygen plasma-treatment optimization was 200 W, 175 mTorr, 60 s, as suggested by Schmalenberg et al.[19,20] Fresh substrates were oxygen plasma-treated at 200 W for 60 s under various chamber pressures: 78, 110, 300, 485, 510, 660, 830, and 996 mTorr. The chamber pressure that yielded the greatest increase in oxygen on PMMA was then used as the chamber pressure for the subsequent studies on power and duration.

To establish the effect of plasma power on oxygen incorporation, fresh PMMA substrates were analyzed by XPS (as described below) after being oxygen plasma-treated at 660 mTorr for 60 s under various powers: 50, 75, 100, 150, and 200 W. The power that caused the greatest increase in oxygen was then used, along with the optimized chamber pressure, to study the effect of plasma duration. Specifically, PMMA substrates were oxygen plasma-treated at 50 W, 660 mTorr for various durations (e.g., 10, 60, 120, and 300 s) and analyzed by XPS (as described below).

2.3.3.2 Microcontact Printed Laminin on PMMA

PMMA substrates were micropatterned with laminin following the μCP procedure described below under "Microcontact Printing (μCP)". Oxygen plasma-treatments at

either 200 W, 175 mTorr, 60 s or 50 W, 660 mTorr, 300 s were used to activate the PMMA substrates prior to patterning and subsequent analysis by XPS, CLSM, AFM, and NSOM (to be described).

2.3.4 Microcontact Printing (μCP)

PMMA substrates were micropatterned with laminin following the procedure outlined in Figure 2-1, a modified protocol of the one suggested by Schmalenberg et al.[19] PMMA and patterned PDMS stamps were simultaneously oxygen plasma-treated at either 200 W, 175 mTorr for 60 s or 50 W, 660 mTorr for 300 s (Figure 2-1i). Following plasma-treatment, the PDMS stamp was covered with ~ 100 μL of laminin solution (100 or 500 μg/mL) and allowed to incubate at room temperature for 15 min (Figure 2-1ii). Excess laminin solution was removed using an aspirator and the stamp dried for 1-2 min using filtered N_2 (Fig. 2-1iii). The stamp was then placed under a 40-g weight and into contact with plasma-treated PMMA for 15 min (Figure 2-1iv). Upon stamp removal, the patterned substrates were analyzed with XPS, CLSM, AFM, and NSOM (as described below).

2.3.5 X-Ray Photoelectron Spectroscopy (XPS)

XPS analysis of PMMA substrates (untreated, oxygen plasma-treated, and laminin micropatterned; described above) was performed with a Kratos XSAM 800 spectrometer using unmonochromatized Mg Kα radiation (8 mA, 12 kV). Due to instrumental constraints, samples were analyzed *no less than 90 min* following modification. The analysis chamber was kept at 1×10^{-8} Torr or below during data collection. The angle

between the sample normal and analyzer was set at 0° for all specimens. Pass energies of 80 eV and 20 eV were used for survey and narrow energy range spectra, respectively. For narrow energy range spectra, peak binding energies were referenced to the hydrocarbon C 1s peak at 285.0 eV. As PMMA contains carbon atoms in slightly different chemical environments, it was necessary to peak fit the C 1s envelopes using published deconvolution guidelines.[23-28]

2.3.6 Water Contact Angle Measurements (CAM)

The wettabilities of untreated and oxygen plasma-treated PMMA substrates were established by contact angle measurements recorded at room temperature using an NRL contact angle goniometer (Rame-Hart Instruments, Netcong, NJ). Measurements were taken separately on untreated substrates or PMMA substrates oxygen plasma-treated at either 200 W, 175 mTorr, 60 s or 50 W, 660 mTorr, 300 s. In each experiment, a drop of deionized, doubly distilled water was placed on the sample, and two contact angle measurements per drop were taken by direct reading. Reported values are an average of *at least* 6 measurements per sample type.

2.3.7 Confocal Laser Scanning Microscopy (CLSM)

To confirm micropattern formation, μCP PMMA substrates were imaged using a Zeiss LSM 410 confocal laser scanning microscope, with a computer-controlled laser scanning assembly attached to the microscope. An Omnichrome 3 line Ar/Kr laser operating at 488 nm was used as the excitation source. The images were processed with Zeiss LSM control software. Prior to imaging, laminin micropatterns were fluorescently tagged by

immersing the patterned PMMA substrates in a primary antibody solution of rabbit anti-laminin (1 h), followed by three rinses in PBS. The patterns were then immersed in a secondary antibody solution of FITC-conjugated goat anti-rabbit IgG for 1 h (under Al foil to minimize light exposure), and rinsed three times in PBS. Patterned substrates were imaged dry.

To establish the stability of laminin micropatterns under biologically relevant storage conditions, PMMA substrates were microcontact printed with laminin (ink concentration: 100 μg/mL) as described above and imaged with CLSM. Areas with good quality micropatterns were imaged. Following initial imaging, samples were immersed in PBS or placed in dry Petri dishes, wrapped in Al foil, and stored in an incubator at 37 °C for a period of 30 days. Following 30 days, immersed samples were removed from PBS and dried. All samples (dry- vs. wet-storage) were imaged again with CLSM in the same general areas that the initial images were taken. This task was performed by recording the approximate locations of distinctive pattern features present in the initial images, and relocating these unique features during re-imaging.

2.3.8 Atomic Force Microscopy (AFM)

To monitor plasma-induced topographical changes, untreated PMMA substrates were analyzed using a BioScope atomic force microscope (Veeco Instruments, Santa Barbara, CA) in intermittent contact mode (i.e., “tapping mode”) under ambient conditions (e.g., room temperature, in air). PMMA substrates were affixed to glass microscope slides with double-sided tape. Silicon cantilevers (model TESP, Veeco) having a nominal

resonance frequency of 320 kHz and a nominal tip radius of <10 nm were used. For a given substrate, over 10 separate areas were imaged at various scan sizes to obtain representative topographical data. Once thoroughly analyzed, the untreated PMMA samples were oxygen plasma-treated at 50 W and 660 mTorr for 300 s, and re-imaged using the same imaging conditions as before (e.g., tapping mode, scan sizes, cantilever, and ambient environment). The plasma-treated samples were then immersed in PBS for 40 min, thoroughly dried, and imaged as before using the same conditions. Finally, substrates were immersed in deionized water (DI H_2O) for 10 min, dried, and imaged a fourth time under the same conditions. The resulting images were identically processed and/or analyzed using BioScope data analysis software.

To characterize the laminin stripes and evaluate the role of ink concentration on pattern height, PMMA substrates were oxygen plasma-treated (50 W, 660 mTorr, 300 s), and micropatterned with laminin using two different ink concentrations: 100 and 500 μg/mL. As before, samples were imaged in air, using tapping mode and a new Si cantilever that was used throughout the experiment. Prior to AFM analysis, the presence of micropatterns first had to be confirmed with CLSM, as micropattern formation was found to be extremely variable and unreliable.

2.3.9 Near-Field Scanning Optical Microscopy (NSOM)

Laminin micropatterns were formed on oxygen plasma-treated PMMA (50 W, 660 mTorr, 300 s) using an ink concentration of 100 μg/mL and subsequently analyzed at room temperature under wet conditions (i.e., PBS) using a custom-modified Topometrix

Aurora near-field scanning optical microscope (Thermomicroscopes-Veeco Instruments, Santa Barbara, CA). All NSOM probe tips were prepared from type F-AS optical fibers (SiO_2, 3.7 μm core diameter, 125 μm cladding, and 245 μm polymer coating) obtained from Newport Corporation (Irvine, CA). The optical fibers were pulled with a commercial micropipette puller (Sutter Instruments, Novato, CA) to form NSOM probes with apexes ranging from 50-100 nm.

2.4 Results and Discussion

2.4.1 CLSM and XPS Analysis: Laminin Stripes on Oxygen Plasma-Treated (OPT) PMMA (200 W, 175 mTorr, 60 s)

Over the course of several months, numerous oxygen plasma-treated PMMA substrates microcontact printed with laminin were imaged with CLSM. Laminin micropatterns were not present on a large majority of substrates (~ 75 – 85 %). For example, it was common for 10 substrates to be patterned at one time, with only one or two exhibiting *any* micropatterns. Furthermore, when micropatterns were present, they occupied a small fraction of the expected area based on the PDMS stamp. Representative images of laminin stripes, when present, are shown in Figure 2-2. The quality of the patterned stripes was considered poor as they exhibited several bare areas within a stripe (Figure 2-2a,b,d, and e) or discontinuities (i.e., gaps) along the stripes (Figure 2-2c and e).

The poor transfer of laminin to PMMA during μCP was also evident by XPS analysis of laminin micropatterned substrates, as performed by G. Dukovic.[29] The XPS survey

spectrum (shown in Figure 2-3) showed peaks consistent with the presence of carbon and oxygen (to be discussed further). However, the absence of a peak at ~ 400 eV indicates the absence of nitrogen on the supposedly protein-patterned PMMA. As proteins contain significant amounts of nitrogen due to the large number of amide bonds, the lack of nitrogen indicates little or no laminin present on the substrate. Table 2-1 quantitatively shows that the micropatterned PMMA surface consisted mainly of carbon and oxygen, with no nitrogen. In addition, the appearance of two intense peaks at ~ 100 eV and ~ 150 eV (Figure 2-3) indicates a significant presence of silicon (15.0 %, Table 2-1). As PMMA, laminin, or phosphate buffered saline do not contain silicon, its presence indicates possible substrate contamination during microcontact printing, likely originating from the PDMS stamp. The origin of this silicon-containing contamination, as well as its reduction by oxygen plasma-treatment, is addressed in greater detail in Chapter 3 of this thesis.

As a significant number of substrates showed no micropatterns, the ability of oxygen plasma at 200 W, 175 mTorr, 60 s to effectively activate and increase oxygen concentration on PMMA was evaluated.

2.4.2 XPS and CAM Analysis: Untreated vs. OPT PMMA (200 W, 175 mTorr, 60 s)

Figure 2-4a shows a representative XPS survey spectrum for untreated PMMA. The peaks at ~ 285 eV and ~ 532 eV are due to photoelectron ejection from the C 1s and O 1s orbitals, respectively, and indicate the presence of carbon and oxygen on the untreated PMMA surface. As shown in Table 2-1, untreated PMMA was composed of 71.1 % C

and 28.9 % O, with a C\O ratio of 2.5 : 1. These results are in excellent agreement with the theoretical results expected from PMMA's repeat unit (Figure 2-5). A narrow energy scan of the C 1s region for untreated PMMA is shown in Figure 2-6a, and indicates the presence of carbons in different chemical environments. Based on the structure of PMMA, the C 1s envelope was deconvoluted with peaks at 285.0, 285.8, 287.0, and 289.0 eV to measure the relative amounts of carbon-containing functional groups. Aliphatic carbons, numbered "1" in Figure 2-5, have binding energies at 285.0 eV. Singly bound oxygens cause shifts in the carbon binding energy by ~ 2 eV, and are indicated by a peak at ~ 287.0 eV. This type of carbon is numbered "3" in Figure 2-5. Carbons triply bound to oxygen, numbered "4" in Figure 2-5, have binding energies at ~ 289.0 eV. In addition, the C 1s envelope was fitted with a fourth peak at ~ 285.8 eV, consistent with the binding energy of a carbon adjacent to a carbonyl carbon, and numbered "2" in Figure 2-5. Quantification of the peak-fitted C 1s envelope showed that 44.7 % of the total amount of carbons were aliphatic (i.e., "C1"), 21.7 % were "C2" carbons (i.e., carbons adjacent to carbonyls), 14.2 % were "C3" carbons (i.e., singly bound to oxygen), and 19.4 % were "C4" carbons (i.e., triply bound to oxygen). The ratio of C1\C2\C3\C4 carbons was 3.1:1.5:1:1.4. This deviation from the theoretically expected ratio of 2:1:1:1 is most likely due to the peak-fitting procedure followed or the presence of hydrocarbon contaminants on the PMMA surface. The average water contact angle measurement on untreated PMMA was 60.8° ± 2.4°, indicating a moderately hydrophobic surface. This value is somewhat lower than published values[19,21,29-32] that range from 65-86°, and may be attributed to differences in polymer source and sample preparation methods prior to analysis.

Figure 2-4b shows a representative XPS survey spectrum for PMMA oxygen plasma-treated (OPT) at 200 W, 175 mTorr, for 60 s. As with untreated PMMA, the peaks at ~ 285 eV and ~ 532 eV indicate the presence of carbon and oxygen, respectively. However, qualitative comparison of the O 1s and C 1s peak heights on OPT PMMA relative to those of untreated PMMA indicate an increase in oxygen in the former case. As shown in Table 2-1, this qualitative finding was quantitatively confirmed. The OPT PMMA surface was composed of 67.6 % C and 32.4 % O, with a C\O ratio of 2.1:1. This result indicates that oxygen plasma minimally increased the surface concentration of oxygen by 3.5 %. The narrow energy scan of the C 1s region for OPT PMMA, shown in Figure 2-6b, and subsequent quantification of the C 1s envelope further supports plasma-induced incorporation of oxygen on PMMA. As with untreated PMMA, the C 1s envelope of OPT PMMA was deconvoluted with peaks at 285.0, 285.8, 287.0, and 289.0 eV. Quantification of the peak-fitted C 1s envelope gave the following percentages of the total carbon amount: 37.4 % "C1", 16.4 % "C2", 20.3 % "C3", and 25.9 % "C4". Relative to untreated PMMA, increased amounts of carbons bound to oxygen ("C3" and "C4"), and decreased amounts of carbons bonded to either hydrogen or carbon ("C1" and "C2") were observed. These results indicate the formation of oxygen-containing species on PMMA during oxygen plasma-treatment. This contention is further confirmed by contact angle measurements. The average water contact angle measurement on OPT PMMA was 52.3° ± 2.4°. Although this value is much higher compared with other published values for OPT PMMA,[19,29,30] which range from 20°-30°, the modest decrease in contact angle still indicates an increase in hydrophilicity and an increase in surface polarity due to plasma-induced oxygen incorporation. As hydrophilicity was increased to

some extent, these results generally agree with other published studies evaluating the effect of oxygen plasma on PMMA[33-35] and other common polymers.[34-41] As plasma-treatment only minimally increased oxygen amounts on PMMA compared to other published studies, PMMA may not be sufficiently activated for reliable micropatterning, causing patterns shown in Figure 2-2. Further, increasing the amount of oxygen incorporation onto PMMA by systematically optimizing plasma-treatment chamber pressure, power, and duration may improve laminin transfer onto PMMA during the μCP process.

2.4.3 Optimized Oxygen Plasma-Treatment

2.4.3.1 Chamber Pressure

PMMA substrates were oxygen plasma-treated at 200 W for 60 s at the following chamber pressures and analyzed by XPS to determine oxygen concentrations (% O is shown in parentheses following the chamber pressure): 78 mTorr (34.4 %), 110 mTorr (34.5 %), 300 mTorr (35.0 %), 485 mTorr (35.0 %), 510 mTorr (36.9 %), 660 mTorr (37.5 %), 830 mTorr (37.4 %), and 996 mTorr (35.1 %). The survey spectra of all samples showed the presence of only carbon and oxygen. The data illustrates no correlation between chamber pressure and oxygen amounts as the highest pressure (996 mTorr) did not necessarily introduce the most oxygen on the PMMA surface. However, the general trends in oxygen amounts show that higher chamber pressures are more favorable for oxygen incorporation than lower pressures. As 660 mTorr gave the largest oxygen concentration, this pressure was used for power and duration optimization.

2.4.3.2 Plasma Power

PMMA samples were oxygen plasma-treated for 60 s at 660 mTorr under the following powers (% O is shown in parentheses): 50 W (37.7 %), 75 W (35.8 %), 100 W (36.2 %), 150 W (36.3 %), and 200 W (34.8 %). As with chamber pressure, no defined correlation between power and oxygen amounts was observed. As 50 W gave the largest oxygen concentration, this power setting was used for optimization.

2.4.3.3 Plasma Duration

PMMA samples were oxygen plasma-treated at 50 W, 660 mTorr for the following durations (% O is shown in parentheses): 10 s (37.8 %), 60 s (37.5 %), 120 s (38.5 %), and 300 s (38.9 %). Even though the difference in oxygen incorporation among the studied durations was negligible, 300 s was chosen as the optimized duration as it empirically gave the highest oxygen concentration. Treatment-times longer than 300 s were not evaluated, as noted by the minimal 0.4 % increase in oxygen when the duration was increased from 120 to 300 s. Several samples exposed to the optimized oxygen plasma treatment of 50 W, 660 mTorr, 300 s were analyzed with XPS to evaluate variability. As shown in Table 2-1, PMMA substrates had oxygen amounts of 38.5 ± 0.5 %, an increase in oxygen incorporation by almost 10 % compared to untreated PMMA. The average water contact angle measurement on PMMA treated at 50 W, 660 mTorr, 300 s was 38.8° ± 4.4°, indicating a substantially more hydrophilic surface than plasma treatment at 200 W, 175 mTorr, 60 s (52.3°).

2.4.4 CLSM Analysis: Laminin Stripes on OPT PMMA (50 W, 660 mTorr, 300 s)

To establish if optimizing the oxygen plasma-treatment used to activate PMMA affected pattern transfer during μCP, numerous samples were imaged with CLSM over the course of several weeks. As with μCP using the initial plasma-treatment (200 W, 175 mTorr, and 60 s), laminin micropatterns were still not present on a large majority of substrates. Although patterning appeared to be more widespread compared to the unoptimized plasma-treatment, its occurrence was still rare and inconsistent. As before, the large majority of patterns were poor quality, as shown in Figure 2-7. Comparison of Figure 2-7 and Figure 2-2 illustrates that using the optimized oxygen plasma-treatment did little to improve laminin transfer during μCP, and indicates that this poor transfer may be due to factors other than PMMA plasma-treatment conditions.

However, when patterns *were* present, they were found to be stable under physiologically relevant conditions. Figure 2-8 shows that laminin patterns remained intact and well defined after 4 weeks of storage at body temperature (37 °C) under wet or dry conditions. As shown, the laminin stripes did not merge over time into a continuous monolayer, nor did they desorb from the PMMA surface. These findings were encouraging, and illustrated that laminin micropatterns could be utilized for long term cell response studies.

2.4.5 t-AFM Analysis: Laminin Stripe-Height as a Function of Ink Concentration

As cell behaviors can be directed by physical/topographical cues present on the substrate[42-55] in addition to chemical cues, the physical environment that μCP laminin

stripes present to direct Schwann cell attachment was observed. Laminin stripes were made on OPT PMMA (50 W, 660 mTorr, 300 s) using two different ink concentrations: 100 μg/mL and 500 μg/mL. Representative tapping-AFM images are shown in Figure 2-9. Typical stripe widths ranged between 16-22 μm, regardless of the ink concentration used. The height difference between patterned and unpatterned PMMA regions of 100 μg/mL stripes (Figure 2-9a) was 5.1 ± 1.1 nm. Interestingly, pattern-height for 500 μg/mL stripes (Figure 2-9b) was 4.9 ± 1.0 nm. These results demonstrate that pattern height is independent of the ink concentration used during μCP, and give further insight into the μCP procedure. As increased ink concentration would be expected to deposit thicker protein layers onto the PDMS stamp surface than more dilute concentrations, it was anticipated that 500 μg/mL stripes would be steeper than 100 μg/mL stripes, assuming all of the protein from the PDMS stamp is transferred to PMMA during μCP. As this was not the case, it indicates that either total protein transfer is not occurring during μCP, or if total ink transfer is occurring, the intramolecular forces among laminin molecules may be insufficient to prevent a large portion of laminin molecules from being washed away during fluorescent tagging. As many bare areas (i.e., devoid of laminin) were detected within the stripes (Figure 2-9b), it is more probable that total ink transfer is not occurring. In either case, excessive ink concentrations may be unnecessary and wasteful when performing μCP. In addition, these results indicate that μCP laminin stripes provide negligible physical cues, and that their ability to control Schwann cell attachment[19,20] is largely due to the chemical signals provided to approaching cells. However, as laminin stripes were analyzed with AFM under ambient (i.e., dry)

conditions, the physical cues provided by laminin stripes under wet conditions may give a more accurate representation of what approaching cells encounter *in vitro*.

2.4.6 NSOM Analysis: Laminin Stripe-Height under Wet Conditions

Micropatterns of laminin (ink concentration: 100 μg/mL) were created on OPT PMMA (50 W, 660 mTorr, 300 s) and imaged with NSOM under wet conditions. Figure 2-10a and 2-10b respectively show the topographical and optical images of a representative laminin stripe. In addition to the laminin stripe (outlined in red for easier viewing), Figure 2-10 shows some common morphological features of the underlying PMMA substrate. For example, the black arrows in Figure 2-10 point to linear raised portions of the PMMA substrate. These features, along with micron-sized scratches, were commonly encountered on other areas of the substrate and occurred in regions not patterned with laminin. These features are most likely introduced onto the PMMA surface during polymer processing, when the polymer sheets are made by the manufacturer. Features similar to this were also detected by AFM and can be seen going across the bottom left corner of Figure 2-9a. The features in Figure 2-10 appear slightly curved due to the non-linear motion of the piezo scanner that moves the sample during NSOM analysis. This non-linear movement, however, does not impact pattern height determination by NSOM. NSOM analysis showed that μCP laminin stripes had heights of 26.2 ± 2.6 nm, which are significantly greater than the heights determined by AFM (5.1 nm). This difference can be explained by the different imaging environments. NSOM analysis was done under wet conditions, where the protein patterns remained hydrated. As a result, it would be expected that the protein patterns would swell and give a greater pattern height than the

dry protein stripes imaged by AFM. This swelling during wet NSOM analysis has been previously observed and documented.[56] A second explanation for the height differential measured by AFM and NSOM is the manner in which the images are captured. As NSOM analysis is truly non-contact, the scanning probe does not touch the sample or significantly modify the dimensions of the pattern. However, in tapping-AFM, the resonating probe tip, although not in constant contact, does make contact with the sample at the bottom of each oscillation cycle. The tapping of the AFM tip on the protein stripes may be compacting the stripes in the process, thus resulting in shorter heights compared to NSOM results. Although NSOM analysis revealed that laminin stripes were several times higher/deeper in an aqueous environment, the stripes likely do not present significant physical cues to approaching cells.[19,20] Hence, laminin stripes direct cell attachment primarily by chemical means.

It was the intent of the author to analyze pattern height of μCP laminin stripes produced using an ink concentration of 500 μg/mL, however, this was not accomplished due to the unexpected and untimely end of a collaboration with Dr. Luis Garfias (Lucent Technologies, Murray Hill, NJ), who provided access to the NSOM.

2.4.7 t-AFM Analysis: Untreated vs. OPT PMMA (50 W, 660 mTorr, 300 s)

As poor laminin transfer during μCP was not improved by optimizing plasma-induced chemical modification, it was necessary to explore the plasma-induced physical modifications that may affect laminin transfer. Figure 2-11 shows representative t-AFM images of PMMA prior to oxygen plasma-treatment (Figure 2-11a), immediately after

plasma-treatment (Figure 2-11b), and after plasma-treatment and subsequent rinsing in PBS (Figure 2-11c) or PBS, then DI H_2O (Figure 2-11d). Initially, the PMMA surface is relatively featureless, with the exception of linear raised or grooved regions. These features were detected by NSOM, and previously discussed. Roughness measurements on untreated PMMA averaged 3.6 ± 2.5 nm, indicating a smooth surface. As shown in Figure 2-11b, oxygen plasma-treatment (50 W, 660 mTorr, 300 s) dramatically alters the PMMA surface, forming countless raised particles, and resulting in an average roughness of 39.3 ± 3.3 nm. To determine if these particles were firmly attached to the underlying substrate, the plasma-treated substrate was immersed in PBS for 40 min, dried and reanalyzed. This rinsing step produced the PMMA surface shown in Figure 2-11c. Although fewer particles are shown in Figure 2-11b, the particles are significantly larger when deposited onto the surface. These particles, which were initially presumed to be buffer salts, were commonly encountered when analyzing μCP laminin stripes, and resulted in an average roughness of 98.8 ± 19.5 nm. Immersing the sample in DI H_2O for 10 min, which resulted in the surface shown in Figure 2-11d, removed the extremely large particles, which supports their identification as buffer salts. In addition, compared to Figure 2-11b, significantly fewer small particles were observed. This observation was also quantitatively confirmed by a decrease in surface roughness to 16.8 ± 0.4 nm. Therefore, these results show that oxygen plasma-treatment significantly damages the PMMA surface and forms a weakly bound surface layer of presumably oxidized PMMA particles that can be easily removed by post-treatment rinsing. These findings may explain why poor laminin transfer during μCP was commonly observed. If laminin was transferred to the PMMA substrates, the proteins were likely attaching to the particle

layer. As the particle layer was later removed by rinsing, the particles were likely washed away, resulting in the poor micropatterns shown in Figure 2-7. This hypothesis, however, was not tested further due to a change in research focus brought about by the development of microscale plasma-initiated patterning (μPIP, to be discussed in greater detail in Chapters 4-7).

2.5 Conclusions

XPS and CAM analysis of PMMA substrates exposed to oxygen plasma showed increased oxygen incorporation and increased hydrophilicity, respectively. The extents of oxygen incorporation and hydrophilicity increase were shown to be greater when using an optimized plasma-treatment of 50 W, 660 mTorr, 300 s. However, CLSM results show that laminin transfer to PMMA during μCP was not significantly improved by increased hydrophilicity and oxygen concentration. The poor transfer is likely due to other factors, such as the physical surface modifications introduced by plasma-treatment. AFM analysis demonstrated that oxygen plasma-treatment of PMMA caused significant topographical changes and the formation of a weakly bound particle layer that can be removed with rinsing. This particle layer was hypothesized to be responsible, in part, for poor laminin transfer during μCP. However, when laminin stripes were present on the PMMA surfaces, they were stable for at least 4 weeks when stored at body temperature under wet or dry environments. AFM analysis showed that μCP laminin stripe-height averaged 5 nm and was independent of the ink concentration used during μCP. NSOM analysis demonstrated that laminin stripes in aqueous environments had heights several

times larger than stripes imaged in dry environments by AFM. However, both AFM and NSOM analyses demonstrated that laminin stripe-heights were extremely small and offers only slight physical cues to cells. In addition, XPS analysis of laminin-patterned PMMA confirmed poor laminin transfer during μCP, further illustrating the unreliability of this patterning technique. This finding provided the impetus for future experiments that sought to improve μCP and experiments that led to the development of microscale plasma-initiated patterning (μPIP). Lastly, the XPS results introduced the possibility of substrate contamination by the PDMS stamps used during μCP, and led to future experiments to minimize this contamination. This minimization is covered in greater detail in the next chapter.

2.6 Acknowledgements

The author would like to acknowledge Gordana Dukovic for performing XPS analysis on laminin micropatterned PMMA, Dr. Boris Yakshinskiy for XPS training and assistance in XPS data analysis, Dr. Theodore Madey for support and assistance in XPS data analysis, Ram Sharma for CLSM and AFM training, Dr. Alex Semenov for AFM training and healthy adversity, Dr. Luis Garfias for NSOM instrument access, training, and analysis assistance, Dr. Kristi Schmalenberg for helpful discussions, The Laboratory for Surface Modification for instrument access (XPS), The N.J. Confocal Microscopy and Cell Culture Facility for Biomaterials for instrument access (CLSM and AFM), and Dr. Das Bolikal for goniometer access. The research presented in this chapter was funded by DuPont, Rutgers University BioMEMS SROA, and NIH (DE 13205).

2.7 References

(1) Detrait, E.; Lhoest, J.-B.; Bertrand, P.; van den Bosch de Aguilar, P. *J. Biomed. Mater. Res.* **1999**, *45*, 404-413.

(2) DeFife, K. M.; Colton, E.; Nakayama, Y.; Matsuda, T.; Anderson, J. M. *J. Biomed. Mater. Res.* **1999**, *45*, 148-154.

(3) Dewez, J.-L.; Lhoest, J.-B.; Detrait, E.; Berger, V.; Dupont-Gillain, C. C.; Vincent, L.-M.; Schneider, Y.-J.; Bertrand, P.; Rouxhet, P. G. *Biomaterials* **1998**, *19*, 1441-1445.

(4) Matsuda, T.; Sugawara, T. *J. Biomed. Mater. Res.* **1996**, *32*, 165-173.

(5) Ito, Y. *Biomaterials* **1999**, *20*, 2333-2342.

(6) Corey, J. M.; Feldman, E. L. *Experimental Neurology* **2003**, *184*, S89-S96.

(7) Folch, A.; Toner, M. *Biotechnol. Prog.* **1998**, *14*, 388-392.

(8) Blawas, A. S.; Reichert, W. M. *Biomaterials* **1998**, *19*, 595-609.

(9) Park, T. H.; Shuler, M. L. *Biotechnol. Prog.* **2003**, *19*, 243-253.

(10) Recknor, J. B.; Recknor, J. C.; Sakaguchi, D. S.; Mallapragada, S. K. *Biomaterials* **2004**, *25*, 2753-2767.

(11) Kumar, A.; Whitesides, G. M. *Appl. Phys. Lett.* **1993**, *63*, 2002-2004.

(12) Xia, Y.; Whitesides, G. M. *Angew. Chem. Int. Ed.* **1998**, *37*, 550-575.

(13) Bernard, A.; Renault, J. P.; Michel, B.; Bosshard, H. R.; Delamarche, E. *Adv. Mater.* **2000**, *12*, 1067-1070.

(14) Falconnet, D.; Csucs, G.; Grandin, H. M.; Textor, M. *Biomaterials* **2006**, *27*, 3044-3063.

(15) Yang, Z.; Belu, A. M.; Liebmann-Vinson, A.; Sugg, H.; Chilkoti, A. *Langmuir* **2000**, *16*, 7482-7492.

(16) Yang, Z.; Chilkoti, A. *Adv. Mater.* **2000**, *12*, 413-417.

(17) Lee, K.; Kim, D. J.; Lee, Z.; Woo, S. I.; Choi, I. S. *Langmuir* **2004**, *20*, 2531-2535.

(18) Hyun, J.; Zhu, Y.; Liebmann-Vinson, A.; Beebe, J., T. P.; Chilkoti, A. *Langmuir* **2001**, *17*, 6358-6367.

(19) Schmalenberg, K. E.; Buettner, H. M.; Uhrich, K. E. *Biomaterials* **2004**, *25*, 1851-1857.

(20) Schmalenberg, K. E.; Uhrich, K. E. *Biomaterials* **2005**, *26*, 1423-1430.

(21) Henry, A. C.; Tutt, T. J.; Galloway, M.; Davidson, Y. Y.; McWhorter, C. S.; Soper, S. A.; McCarley, R. L. *Anal. Chem.* **2000**, *72*, 5331-5337.

(22) Personal communication.

(23) Briggs, D.; Seah, M. P., Eds. *Practical surface analysis*, Second ed.; John Wiley & Sons: Chichester, 1990; Vol. 1.

(24) Beamson, G.; Briggs, D. *High resolution XPS of organic polymers: the Scienta ESCA300 database*, First ed.; John Wiley & Sons: Chichester, 1992.

(25) Gröning, P.; Küttel, O. M.; Collaud Coen, M.; Dietler, G.; Schlapbach, L. *Appl. Surf. Sci.* **1995**, *89*, 83-91.

(26) Collaud, M.; Groening, P.; Nowak, S.; Schlapbach, L. *J. Adhesion Sci. Technol.* **1994**, *8*, 1115-1127.

(27) Ben Amor, S.; Baud, G.; Jacquet, M.; Nansé, G.; Fioux, P.; Nardin, M. *Appl. Surf. Sci.* **2000**, *153*, 172-183.

(28) Watts, J. F.; Leadley, S. R.; Castle, J. E.; Blomfield, C. J. *Langmuir* **2000**, *16*, 2292-2300.

(29) Dukovic, G. In *Department of Chemistry and Chemical Biology*; Rutgers University: New Brunswick, 2001; p 49.

(30) Lim, H.; Lee, Y.; Han, S.; Cho, J.; Kim, K. J. *J. Vac. Sci. Technol. A* **2001**, *19*, 1490-1496.

(31) Dupont-Gillain, C. C.; Nysten, B.; Rouxhet, P. G. *Polym. Int.* **1999**, *48*, 271-276.

(32) Schmalenberg, K. E. In *Chemistry and Chemical Biology*; Rutgers University: New Brunswick, 2003; p 196.

(33) Süzer, S.; Özden, N.; Akaltan, F.; Akovali, G. *Appl. Spectrosc.* **1997**, *51*, 1741-1744.

(34) Lianos, L.; Parrat, D.; Hoc, T. Q.; Duc, T. M. *J. Vac. Sci. Technol. A* **1994**, *12*, 2491-2498.

(35) Kodama, J.; Foerch, R.; McIntyre, N. S.; Castle, G. S. P. *J. Appl. Phys.* **1993**, *74*, 4026-4033.

(36) Gröning, P.; Collaud, M.; Dietler, G.; Schlapbach, L. *J. Appl. Phys.* **1994**, *76*, 887-892.

(37) Gerenser, L. J. *J. Adhesion Sci. Technol.* **1987**, *1*, 303-318.

(38) Wells, R. K.; Badyal, J. P. S.; Drummond, I. W.; Robinson, K. S.; Street, F. J. *J. Adhesion Sci. Technol.* **1993**, *7*, 1129-1137.

(39) Hopkins, J.; Boyd, R. D.; Badyal, J. P. S. *J. Phys. Chem.* **1996**, *100*, 6755-6759.

(40) Wheale, S. H.; Badyal, J. P. S. In *Interfacial Science*; Roberts, M. W., Ed.; Blackwell Science Ltd: Oxford, 1997; pp 237-255.

(41) Owen, M. J.; Smith, P. J. *J. Adhesion Sci. Technol.* **1994**, *8*, 1063-1075.

(42) Brunette, D. M. *Exp. Cell. Res.* **1986**, *164*, 11-26.

(43) Britland, S.; Clark, P.; Connolly, P.; Moores, G. *Exp. Cell. Res.* **1992**, *198*, 124-129.

(44) Meyle, J.; Wolburg, H.; von Recum, A. F. *J. Biomater. Appl.* **1993**, *7*, 362-374.

(45) Clark, P.; Dunn, G. A.; Knibbs, A.; Peckham, M. *Int. J. Biochem. Cell Biol.* **2002**, *34*, 816-825.

(46) Lam, M. T.; Sim, S.; Zhu, X.; Takayama, S. *Biomaterials* **2006**, *27*, 4340-4347.

(47) Chen, C. S.; Mrksich, M.; Huang, S.; Whitesides, G. M.; Ingber, D. E. *Biotechnol. Prog.* **1998**, *14*, 356-363.

(48) Chen, C. S.; Mrksich, M.; Huang, S.; Whitesides, G. M.; Ingber, D. E. *Science* **1997**, *276*, 1425-1428.

(49) Lukashev, M. E.; Werb, Z. *Trends Cell Bio.* **1998**, *8*, 437-441.

(50) Ranucci, C. S.; Moghe, P. V. *J. Biomed. Mater. Res.* **2001**, *54*, 149-161.

(51) Dunn, G. A.; Brown, A. F. *J. Cell Sci.* **1986**, *83*, 313-340.

(52) Clark, P.; Connolly, P.; Curtis, A. S. G.; Dow, J. A. T.; Wilkinson, C. D. W. *J. Cell Sci.* **1991**, *99*, 73-77.

(53) Folch, A.; Toner, M. *Annu. Rev. Biomed. Eng.* **2000**, *2*, 227-256.

(54) Desai, T. A. *Med. Eng. Phys.* **2000**, *22*, 595-606.

(55) Garcia, A. J. *Adv. Polym. Sci.* **2006**, *2003*, 171-190.

(56) Schmalenberg, K. E.; Thompson, D. M.; Buettner, H. M.; Uhrich, K. E.; Garfias, L. F. *Langmuir* **2002**, *18*, 8593-8600.

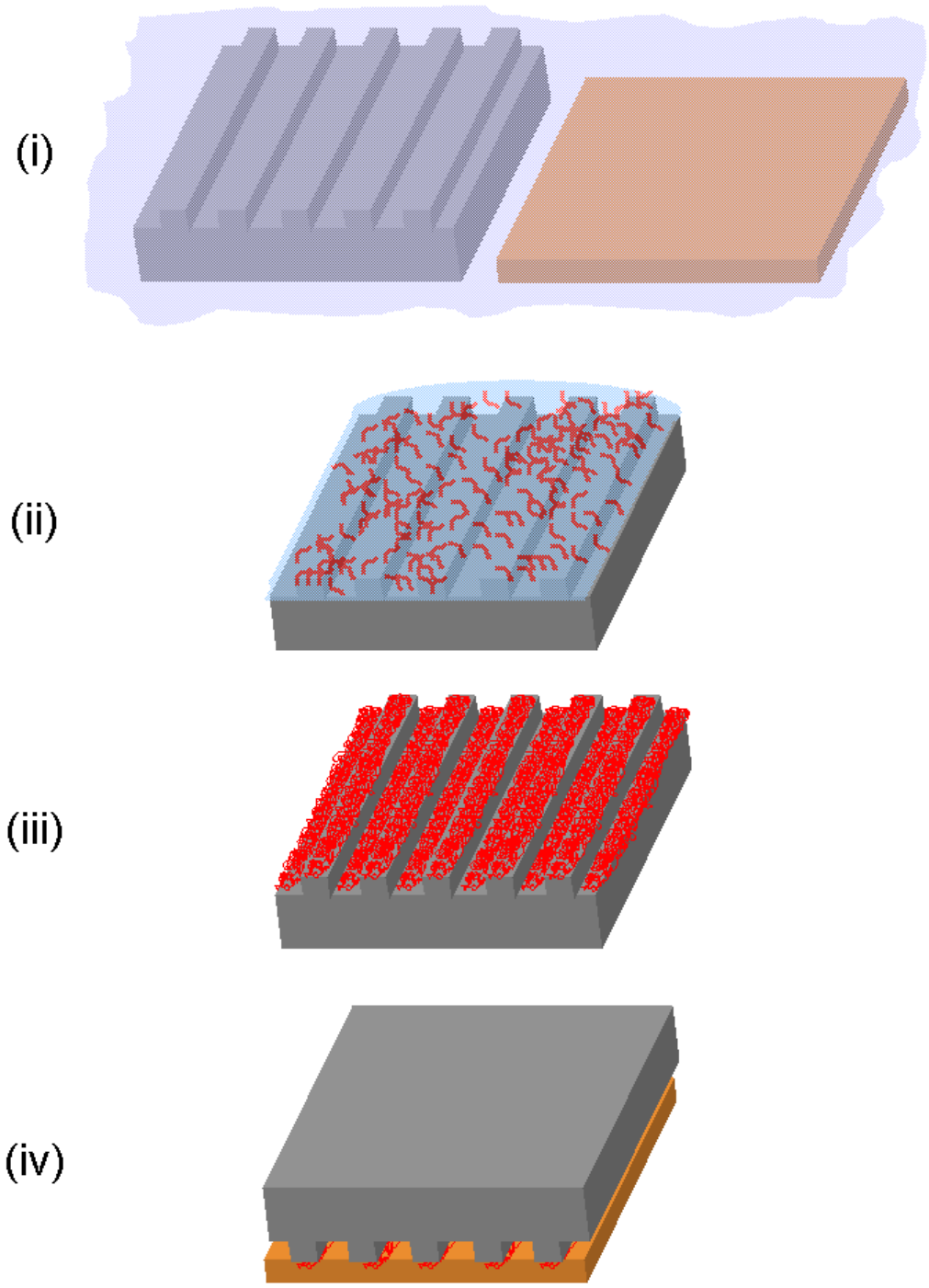

Figure 2-1: Schematic of microcontact printing procedure to produce laminin micropatterns on PMMA: (i) simultaneously expose PDMS stamp and PMMA substrate to oxygen plasma, (ii) stamp is inked with laminin solution for 15 min, (iii) excess solution is removed and stamp is dried, and (iv) stamp is placed into contact with substrate for 15 min.

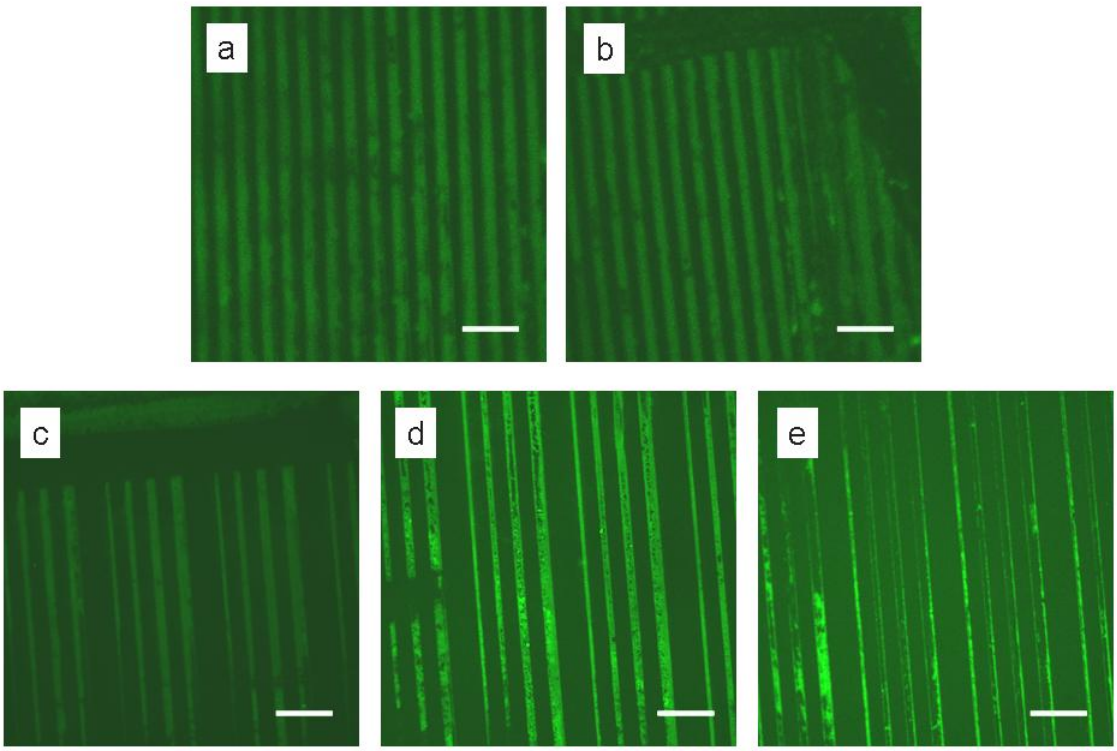

Figure 2-2: Representative fluorescent micrographs of microcontact printed laminin stripes on oxygen plasma-treated PMMA (200 W, 175 mTorr, 60 s). Micropatterns in (a) and (b) were made using a pattered PDMS stamp with different dimensions than the stamps used to make the patterns in (c)-(e). Micropatterns in (a), (b), (d), and (e) exhibit numerous dark spots within, indicating inhomogeneous laminin coverage. In addition, micropatterns in (c) and (e) exhibit several discontinuities (i.e., gaps) along the patterns where laminin was not transferred. Scale bars indicate 100 μm.

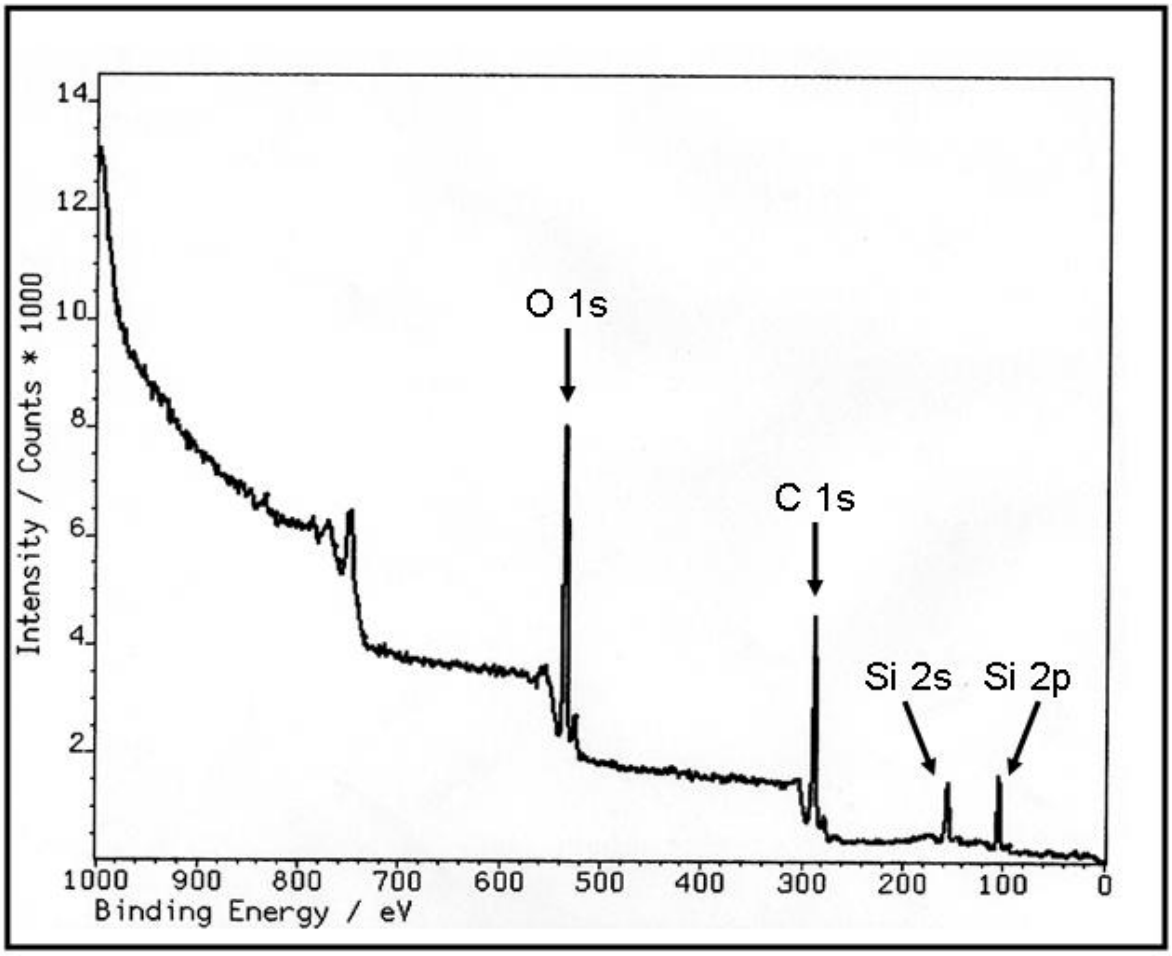

Figure 2-3: XPS survey spectrum of oxygen plasma-treated PMMA microcontact-printed with laminin. Results obtained by G. Dukovic (see Reference 29).

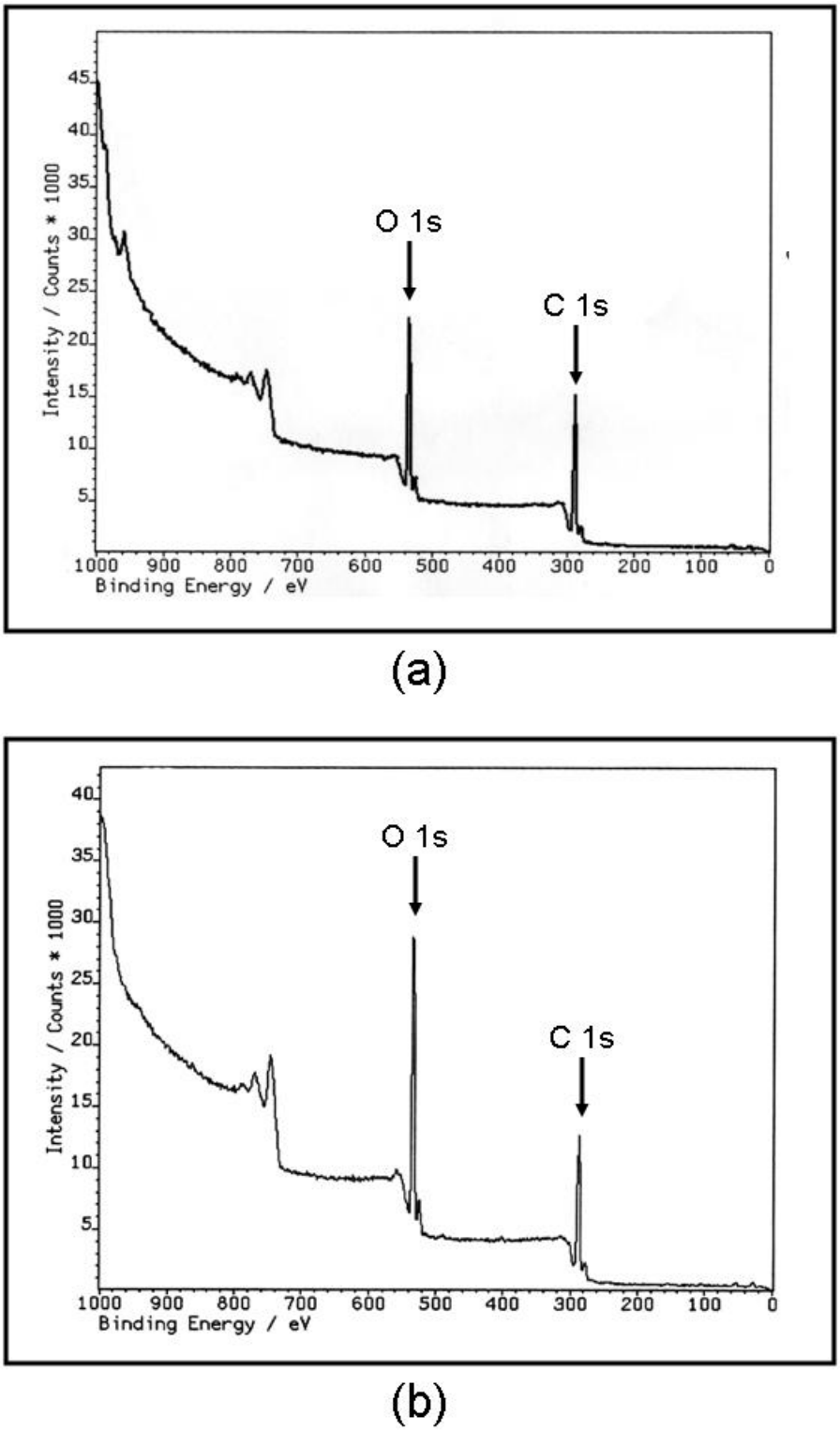

Figure 2-4: Representative XPS survey spectra of PMMA: (a) untreated and (b) oxygen plasma-treated at 200 W and 175 mTorr for 60 s.

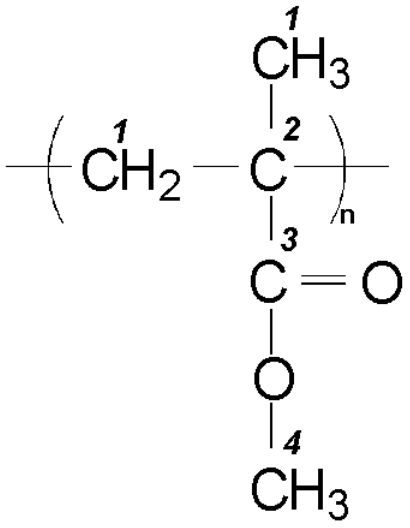

poly(methyl methacrylate)

Figure 2-5: Chemical structure of PMMA. Carbons are numbered according to the chemical environments that give rise to binding energy differences as detected by XPS.

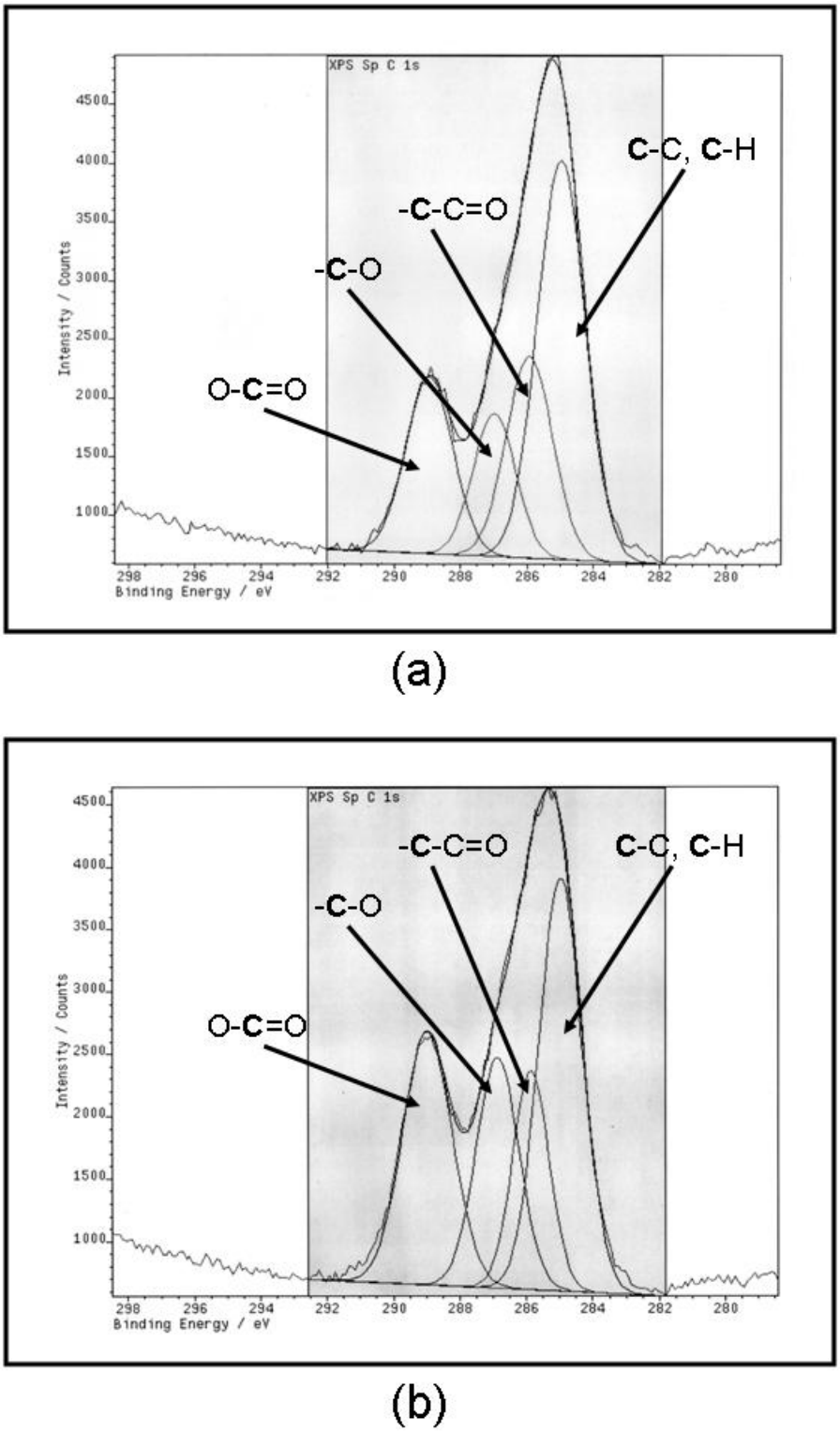

Figure 2-6: Representative C 1s XPS spectra of PMMA with peak-fitted C 1s envelopes: (a) untreated and (b) oxygen plasma-treated at 200 W, 175 mTorr for 60 s.

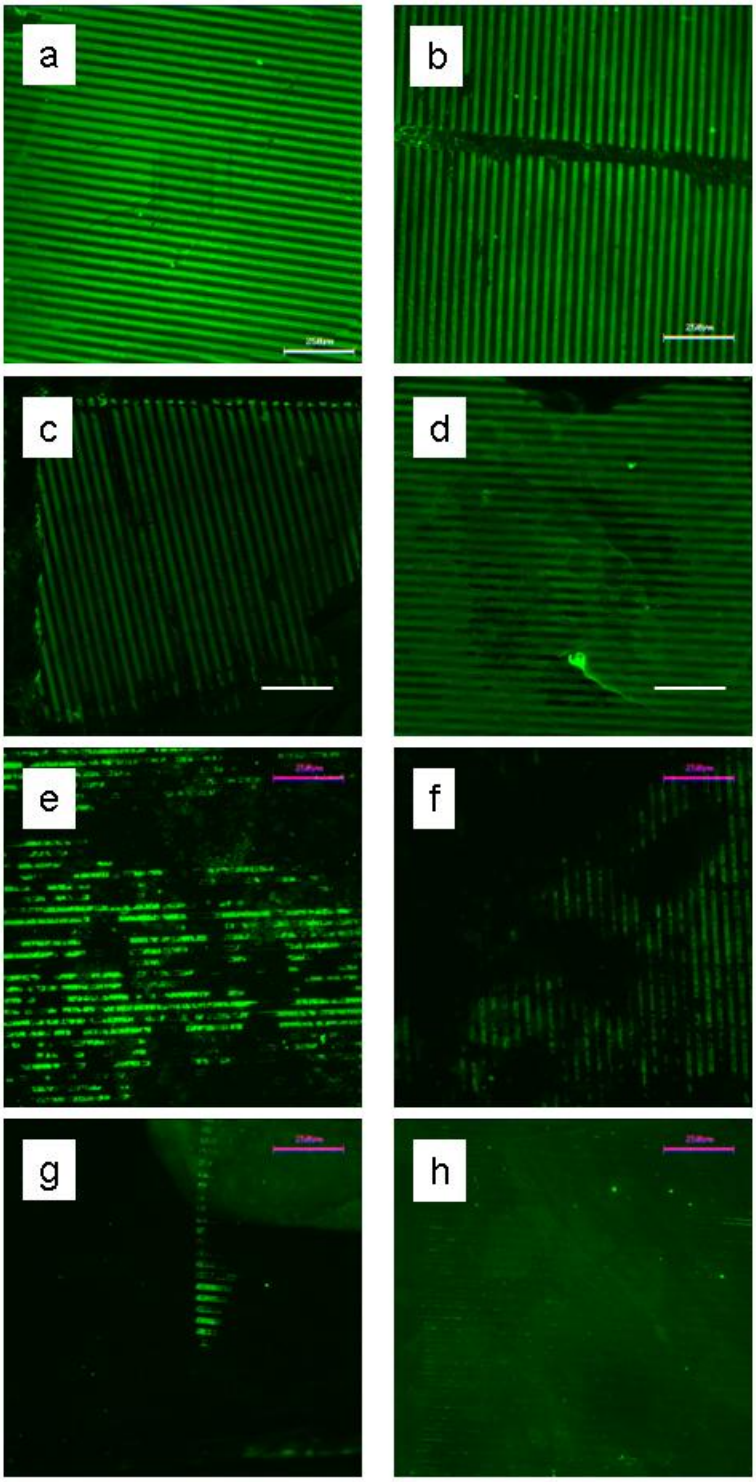

Figure 2-7: Representative fluorescent micrographs of μCP laminin stripes on oxygen plasma-treated PMMA (50 W, 660 mTorr, 300 s). Patterns in (a)-(c) are considered acceptable quality, whereas patterns in (d)-(h) are poor quality. Scale bars indicate 250 μm.

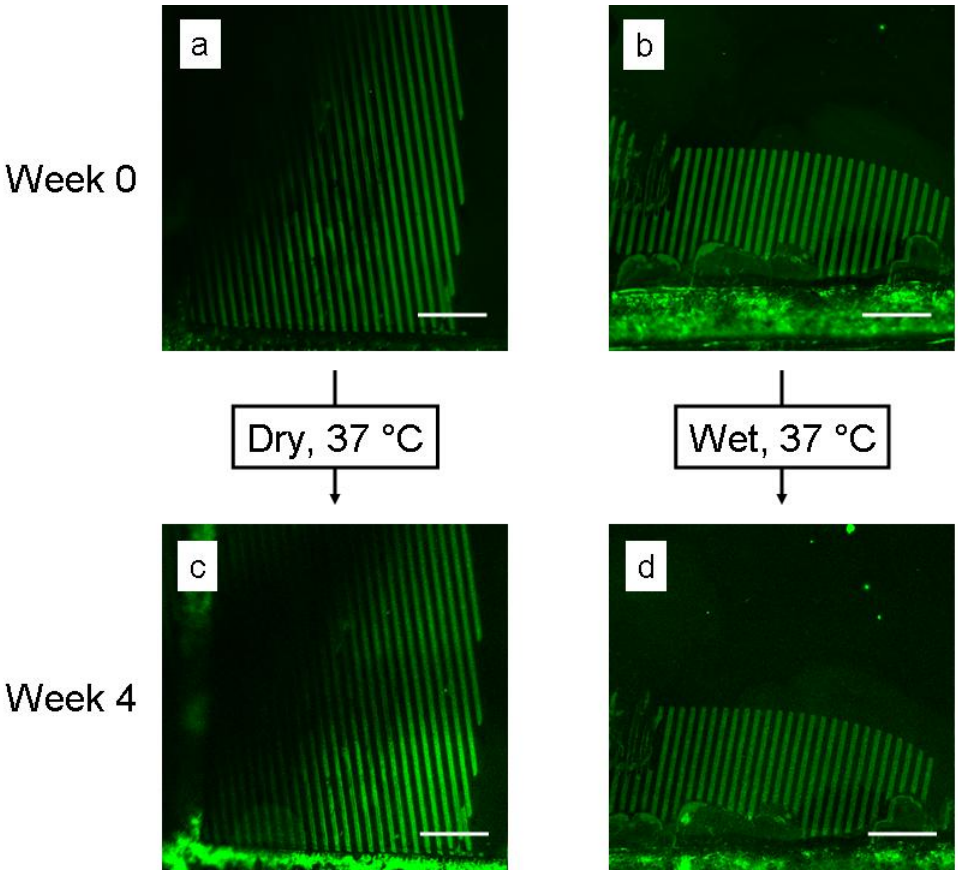

Figure 2-8: Fluorescent micrographs of μCP laminin stripes on oxygen plasma-treated PMMA (50 W, 660 mTorr, 300 s): at week 0 (a & b) and after 4 weeks of storage at 37 °C (c & d) under dry (c) and wet (d) environments. Scale bars indicate 250 μm.

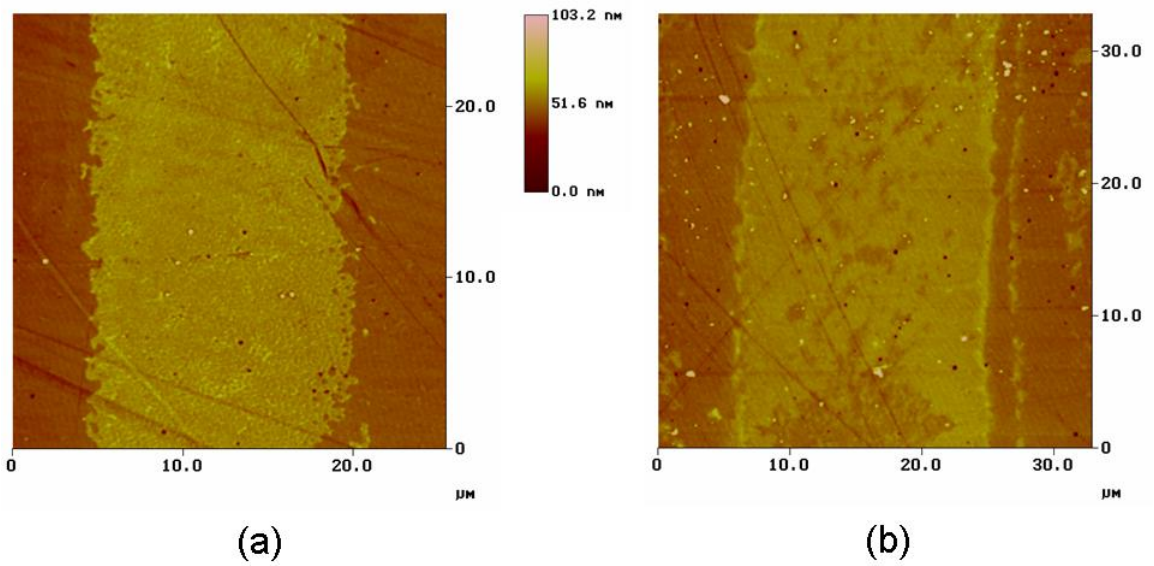

Figure 2-9: Representative t-AFM images of laminin stripes on PMMA made by μCP utilizing different ink concentrations: (a) 100 μg/mL and (b) 500 μg/mL. Scan sizes are approximately 30 μm × 30 μm.

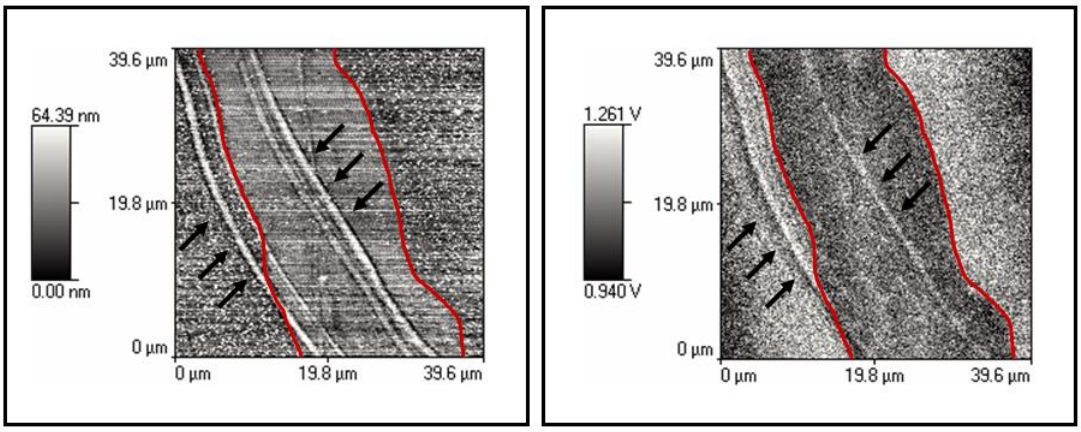

(a) (b)

Figure 2-10: Representative NSOM micrographs of a μCP laminin stripe on oxygen plasma-treated (50 W, 660 mTorr, 300 s) PMMA imaged under wet conditions: (a) topographical image, and (b) complementary optical image. Scan size is 40 μm × 40 μm. For easier viewing, the laminin stripe is outlined in red. The black arrows point to topographical features on PMMA commonly encountered during both AFM and NSOM analyses.

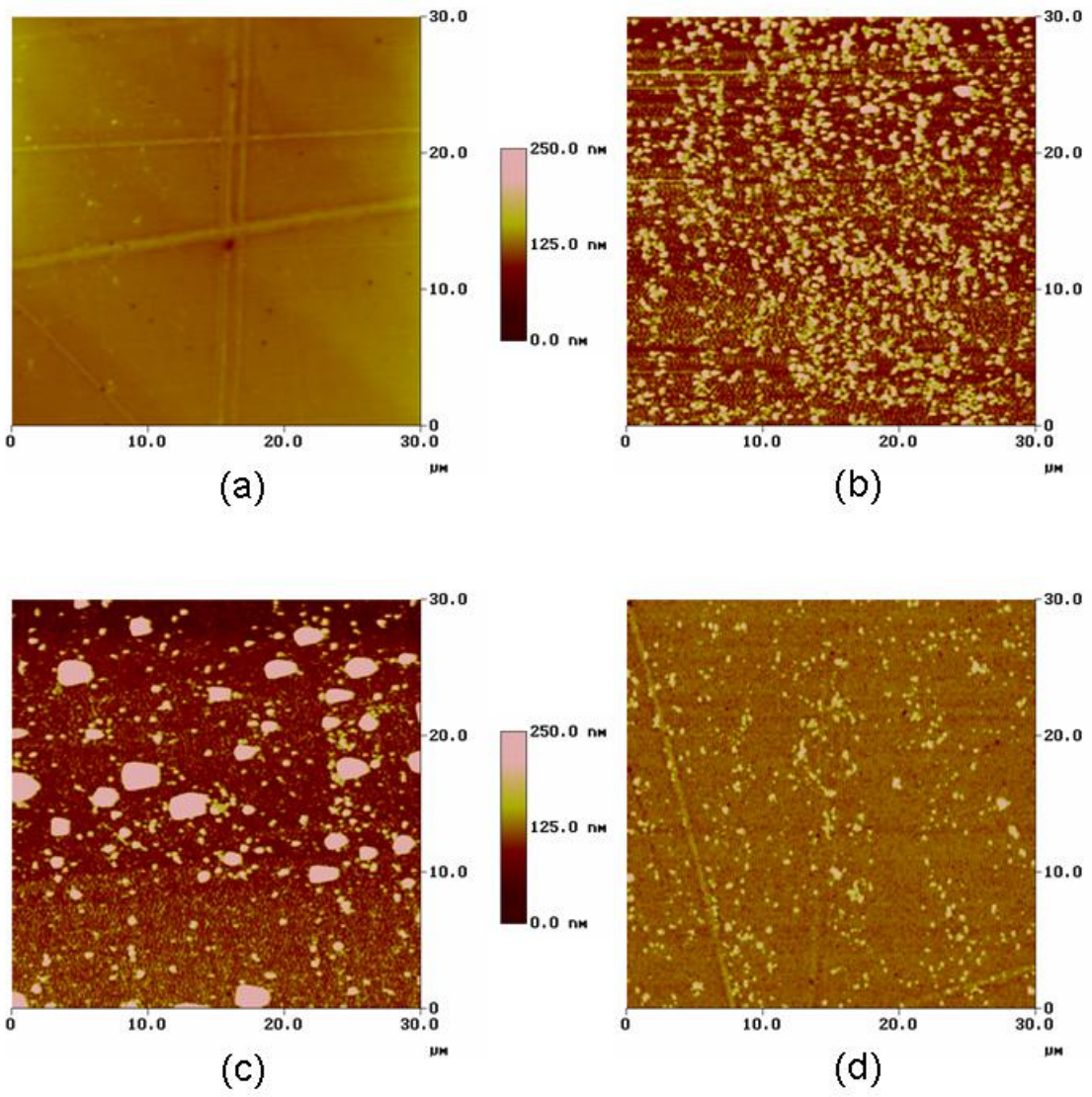

Figure 2-11: t-AFM images of PMMA: (a) untreated, (b) oxygen plasma-treated (50 W, 660 mTorr, 300 s), (c) OPT/rinsed in PBS, and (d) OPT/rinsed in PBS/rinsed in DI H_2O. Scan sizes are 30 μm × 30 μm.

		% C	% O	% Si	C:O Ratio
Untreated PMMA		71.1 ± 0.7	28.9 ± 0.7	n. d.[a]	2.5 ± 0.1
Oxygen plasma-treated PMMA	**200 W, 60 s, 175 mTorr**	67.6 ± 1.0	32.4 ± 1.0	n. d.[a]	2.1 ± 0.1
	50 W, 300 s, 660 mTorr	61.5 ± 0.5	38.5 ± 0.5	n. d.[a]	1.6 ± 0.1
μCP laminin/PMMA[b]		51.6	33.4	15.0	1.5

Table 2-1: XPS compositional data for PMMA: untreated vs. oxygen plasma-treated vs. laminin-printed. [a]not detected. [b]Results obtained by G. Dukovic (see Reference 29).

CHAPTER 3: OXYGEN PLASMA-TREATMENT EFFECTS ON Si TRANSFER

3.1 Abstract

Oxygen plasma-treatment is commonly used to increase the hydrophilicity of poly(dimethylsiloxane) (PDMS) stamps used for microcontact printing (μCP) aqueous-based inks. Review of the literature reveals that a wide range of plasma parameters are currently employed to modify stamp surfaces. However, little is known about the effect of these parameters (e.g., power, chamber pressure, duration) on the undesirable transfer of low-molecular-weight silicon-containing fragments from the stamps that commonly occurs during μCP. To study the effect of oxygen plasma-treatment on Si transfer, unpatterned PDMS stamps were treated with oxygen plasma under various conditions and used to stamp deionized water on plasma-activated poly(methyl methacrylate) (PMMA) substrates. Once stamped, the PMMA substrates were analyzed with X-ray photoelectron spectroscopy (XPS) to quantify and characterize silicon present on the substrate surface. In addition, used PDMS stamps were analyzed with scanning electron microscopy (SEM) to observe topographical changes that occur during oxygen plasma-treatment.

XPS results show that all plasma-treatments studied significantly reduced the amount of Si transfer from the treated stamps during μCP as compared to untreated PDMS stamps, and that the source of transfer is residual PDMS fragments not removed by oxygen plasma. SEM results show that although the treated stamps undergo a variety of

topographical changes, no correlation exists between stamp topography and extent of Si transfer from the stamps.

3.2 Introduction

Microcontact printing (μCP)[1,2] is a patterning technique that has been extensively used to produce well-defined, chemically specific patterns on a wide range of substrates. Its ease, cost-efficiency, and applicability to chemically different surfaces has made it an attractive alternative to other patterning methods,[3-7] such as photolithography,[8,9] which can be time-consuming and require specialized equipment not commonly found in a standard lab. In μCP, a patterned, elastomeric stamp is used to transfer molecules (i.e., "inks") to a particular substrate, much like an office stamp, except that the raised features of the stamp have micrometer-sized dimensions. The raised portions of the stamp (i.e., the stamp pattern) are formed by casting an elastomeric polymer, most often poly(dimethylsiloxane) (PDMS), over a photolithographically fashioned mold or master. Stamps are incubated or inked with a solution of the molecules to be stamped, ultimately producing a pattern of molecules that is identical to the stamp pattern.

Although μCP was initially used to pattern inorganic substrates (e.g., gold,[10-12] silver,[10] silicon,[13] glass,[13]) with organic-based inks (e.g., alkylthiols,[10-12] silanes,[13]), its range of applicability has been successfully expanded to include polymeric substrates[14-24] and aqueous-based inks (e.g., proteins,[14-16,18-21,23-35] RGD peptides,[17] DNA-surfactant arrays,[22] amphiphilic comb polymers[36]). Patterning of organic-based inks is relatively

straightforward in that the stamps do not require pretreatment prior to inking. However, due to the hydrophobic nature of the PDMS stamps, aqueous-based inks require modification of the patterning procedure. For example, PDMS stamp surfaces are chemically treated/oxidized to increase hydrophilicity prior to inking to ensure even distribution of molecules. Although several examples are described in the literature where non-modified stamps have been used to pattern aqueous-based inks,[14-16,18,19,21,25,27] it has been claimed that oxidized stamps exhibit better protein adsorption,[28,35] more efficient transfer of ligand molecules to the stamp during inking[37] and more homogeneous pattern production.[34,38-41] To modify the PDMS surface properties, stamps are derivatized with polar functional groups using traditional wet chemical methods;[22,39,40] however, increased PDMS hydrophilicity can be more quickly achieved by treatment with plasma,[2,17,20,23,24,28-35,37,38,41] corona discharge[42-46] or UV/ozone,[47] although few instances could be found in the literature of the latter two methods being used in conjunction with μCP.

Plasma is commonly employed because treatment takes only a few minutes, the chemical modifications are consistent and reproducible, and no special chemicals or waste removal is needed as gaseous byproducts are removed under vacuum. Air[23,24,30,33,34,37,41] and oxygen[17,20,28,32,38] are the most common feed gases used for treatment, though other gases have been employed to increase PDMS hydrophilicity.[48-50] Oxygen radicals formed within the plasma oxidize the PDMS surface to produce a polar, silica-like surface that is easily wettable with polar solvents.[45,48,49] However, the extent of oxidation and subsequent hydrophilicity increase are largely dependent upon the specific parameters

used to generate the plasma (e.g., feed gas, power, chamber pressure, duration),[48-50] and results may vary among different generators despite the use of similar parameters.[51,52] A review of the literature regarding stamp plasma-treatment reveals that a wide range of parameters are used and frequently the plasma treatment parameters are either unknown or not stated within the studies.[17,20,23,24,28-38,41,53] As all of these various treatments presumably increased stamp hydrophilicity as intended, the need to investigate and optimize these individual plasma parameters during stamp treatment did not exist.

However, plasma-treatment may play a larger role in the *quality* of microcontact- printed patterns beyond providing a simple method for increasing a PDMS stamp's wettability. For example, it was observed that plasma-treatment also affects the transfer of low-molecular-weight PDMS fragments from the stamp to the substrate during the microcontact printing process.[54] Although PDMS transfer has been reported during the stamping of various substrates (e.g., carboxylic acid derivatized poly(ethylene terephthalate),[23] gold,[47,55] polystyrene,[14] TiO_2 and SiO_x[47]), only a few studies have made any recommendations regarding its control or elimination.[47,55] Using X-ray photoelectron spectroscopy (XPS) and time of flight secondary ion mass spectrometry (ToF-SIMS), Graham et al. demonstrated that low-molecular-weight silicone compounds were transferred from flat, featureless (i.e., unpatterned) PDMS stamps during the stamping of self-assembled monolayers (SAMs) of dodecanethiol onto gold.[55] Because transfer of PDMS-related fragments compromises the advantages of using SAM substrates to produce clean and well-defined surfaces, Graham et al. suggested a rigorous, week-long extraction procedure for the stamps prior to μCP to significantly reduce the

transfer of low-molecular-weight oligomers from the PDMS stamp surface. However, as the extracted stamps were used to pattern organic-based inks and required no additional pre-stamping treatments, the above cleaning procedure may not suitably eliminate Si transfer from PDMS stamps used to pattern aqueous-based inks and subjected to surface modification (e.g., plasma-treatment to increase hydrophilicity) prior to use.

More recently, Glasmästar et al. used XPS and ToF-SIMS to measure the amount and character of PDMS transferred from both unpatterned and patterned PDMS stamps to substrates of gold, TiO_2 and SiO_2 during μCP with water or buffer.[47] They demonstrated that UV/ozone-treatment of PDMS stamps prior to μCP significantly reduced transfer of PDMS-related material to all three inorganic substrates. Although similarities exist between oxygen plasma and UV/ozone treatments, significant differences also exist such that translation of parameters between the two treatments is not available.

Because μCP is often used to create patterns that present markedly different chemical characteristics from the unpatterned substrate surface, the transfer of PDMS-related material from the stamp can adversely affect the chemical homogeneity of the patterned areas, which in turn, may influence their intended function. For example, when μCP is used to ink biological ligands onto biocompatible substrates for directed cell growth,[15-21,25,29,30,32,33] the transfer of silicon-containing fragments may interfere with the bioactivity of the ligand pattern or the proliferation and long-term function of the overlying cells. Consequently, means to reduce Si transfer during μCP must be

investigated to maintain the chemical integrity of patterned substrates and preserve pattern function.

Although plasma-treatment is a common method used to increase PDMS stamp hydrophilicity, a wide range of plasma-parameters are currently utilized and their effect on the transfer of PDMS-fragments is unknown. Therefore, the role of oxygen plasma-treatment on Si transfer during the μCP of poly(methyl methacrylate) (PMMA) is discussed in this chapter. As previous studies[47,55] have only addressed Si transfer to inorganic substrates, this study is the first to address the minimization of Si transfer on polymeric substrates. This study is further motivated by the observation of significant Si transfer[56] during the exploration of μCP as an alternative to photolithography[8] for the protein-patterning of biocompatible, plasma-activated polymeric substrates used to direct nerve cell attachment and outgrowth[20] (previously discussed in Chapter 2).

Unpatterned PDMS stamps were treated with oxygen plasma over a range of power levels , chamber pressures and durations most commonly employed in the literature and used to stamp plasma-activated PMMA.[20] The stamped PMMA substrates were analyzed with XPS to evaluate the amount and nature of PDMS fragments transferred from the stamp during μCP. In addition, scanning electron microscopy (SEM) was utilized to analyze the surfaces of the used PDMS stamps following μCP to evaluate topographical changes induced by the specific plasma system (i.e., power, chamber pressure and duration) employed.

3.3 Materials and Methods

3.3.1 Substrate and Stamp Preparation

Sheets of poly(methyl methacrylate) (Goodfellow, Huntingdon, England, 0.7 mm thick, CQ grade) were cut into pieces (8 mm × 10 mm) using a razor blade, sonicated in HPLC grade ethanol (Sigma-Aldrich, St. Louis, MO) for 10 minutes and air-dried. Unpatterned PDMS stamps were made using Sylgard 184 silicone elastomer kit (Dow Corning, Midland, MI). Elastomer base and curing agent were combined in a 10:1 ratio (w\w) after which prepolymer was placed under vacuum to remove entrained air. Thin layers of uncured elastomer (~ 10 mm) were poured into petri dishes (150 mm × 10 mm) and allowed to cure for 24 h under vacuum (-0.98 bar, room temperature). Once cured, PDMS sheets were cut with a razor blade into stamps (10 mm × 10 mm), sonicated in HPLC grade ethanol for 10 min, and air-dried.

Prior to stamping, PDMS stamps were treated with oxygen plasma (parameters described below), incubated with deionized water for 15 min, dried with filtered N_2 and placed into contact with oxygen plasma-treated PMMA (parameters described below) for 15 minutes (see Figure 3-1). To ensure that stamps made complete contact with substrates, PDMS stamps were placed on the PMMA substrates and pressed down with moderate, though not excessive, finger-pressure. In addition, weights (~ 13 g) were placed on top of the PDMS stamps to provide constant pressure throughout the procedure. Additional experiments that evaluated the effect of stamping pressure on Si transfer were performed (results not included); however there was no significant difference in transfer amounts

even between extremes in pressure (e.g., no additional pressure vs. over-excessive finger pressure). Upon removal of stamps, PMMA substrates were analyzed with X-ray photoelectron spectroscopy (XPS) to measure Si concentration (see below) on the PMMA surface. The surfaces of the used PDMS stamps were imaged with scanning electron microscopy (SEM) to evaluate topographical changes (see below) occurring during plasma-treatment and stamping.

3.3.2 Oxygen Plasma-Treatment

Stamps and substrates were treated with oxygen plasma using a March PX-250 plasma cleaning system (March Plasma, Concord, CA). Prior to substrate and stamp treatments, the plasma chamber was purged of contaminants adhering to the chamber walls by running a "cleaning cycle" of 300 W, 580 mTorr for a duration of 900 s (recommended by the manufacturer). In each stamping experiment, PMMA substrates were plasma-treated before the PDMS stamps to ensure that any Si found on PMMA could be attributed to transfer of stamp materials and not to plasma chamber contamination. All PMMA substrates were treated at 50 W, 660 mTorr for 300 s.

To evaluate the effect of individual plasma parameters (e.g., power, chamber pressure and duration) on Si transfer, stamps were subjected to treatments in which one plasma parameter was varied, keeping the other two parameters constant. Four different power settings were evaluated (50, 100, 200, 300 W), using three different chamber pressures (225, 660, 980 mTorr). When power or pressure was varied, duration was constant at 60 s. Treatment duration (10, 30, 60, 120 s) was evaluated at both 50 W, 980 mTorr and 300

W, 225 mTorr. These ranges of power, chamber pressure and duration were chosen because they encompass the various sets of parameters that are typically encountered in the literature. One sample for each set of parameters was subsequently analyzed with XPS. In addition, Si transfer from four stamps simultaneously treated at 300 W, 225 mTorr and 120 s was monitored with XPS to evaluate transfer variability.

3.3.3 XPS Analysis of PMMA Substrates

Si concentration was monitored with a Kratos XSAM 800 spectrometer using unmonochromatized Mg Kα radiation (8 mA, 12 kV). To enhance surface-sensitivity, the angle between sample normal and analyzer was set at 75°. Pass energies of 80 eV and 20 eV were used for survey and narrow energy range spectra, respectively. Four substrates stamped with *untreated* PDMS were analyzed in addition to substrates stamped with plasma-treated PDMS. For narrow energy range spectra, peak binding energies were referenced to the hydrocarbon C 1s peak at 285.0 eV. Due to the limited spatial resolution of XPS, the homogeneity of fragment coverage on the PMMA substrates could not be evaluated.

3.3.4 SEM Analysis of PDMS Stamps

Topographical changes on used stamp surfaces were evaluated with an Amray 1830I scanning electron microscope, using an acceleration potential of 10 kV. Prior to imaging, stamps were sputter-coated with gold and palladium using a Balzers SCD004 sputter coater (working pressure, 0.05 mbar; working distance, 50 mm; current, 30 mA; time, 120 s).

3.4 Results

3.4.1 XPS Analysis

Survey scans of untreated PMMA detected only carbon and oxygen at the polymer surface present in a 2.6:1 ratio (Table 3-1), which is in close agreement with the expected ratio based on PMMA's repeat unit (2.5:1). Plasma-treatment introduced oxygen-containing functionalities onto the PMMA surface and increased oxygen concentration by 7.1 %, lowering the C\O ratio to 1.8:1. Survey scans of plasma-treated PMMA did not show the presence of Si, indicating that the plasma chamber is free of Si-containing contaminants that are commonly deposited onto chamber walls during PDMS plasma-treatment and which can be subsequently contaminate PMMA substrates during their plasma-activation. Survey scans of untreated PDMS (Figure 3-2a) detected the presence of silicon (two peaks at ~ 100 eV and ~ 150 eV), in addition to carbon and oxygen (peaks at ~ 285 eV and ~ 532 eV, respectively), with a C\O\Si ratio of 2:1.3:1, in good agreement with the expected ratio of 2:1:1 based on the repeat unit of PDMS:

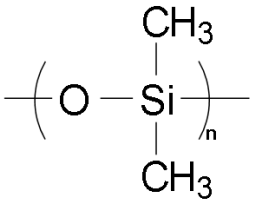

As shown in Figure 3-3a, the binding energy of the Si 2p peak was 102.6 eV, which is in good agreement with published values for PDMS[42,45,47,57-59] and indicates the presence of Si species doubly bound to oxygen. Plasma-treatment of PDMS increased oxygen concentration by 21 % (Table 3-1 and Figure 3-2b) indicating significant surface

oxidation. The shift in binding energy of Si 2p to 104.3 eV, shown in Figure 3-3b, indicates the presence of highly oxidized silica-like species that are formed during plasma-treatment.

Figure 3-4 shows the XPS results of PMMA substrates stamped with either untreated or plasma-exposed PDMS stamps under various treatments. Significant amounts of Si (7.0-11.1 %) were detected on PMMA substrates stamped with untreated PDMS stamps. As either PMMA or deionized water does not contain inherent Si, the source of Si is PDMS transferred from the stamp onto PMMA during microcontact printing. Figure 3-5a shows that the Si detected on the PMMA substrates stamped with untreated PDMS stamps had Si 2p binding energies consistent with untreated PDMS (~ 102.6 eV). Analysis of Si amounts from stamps that were plasma-treated at four powers (50, 100, 200 and 300 W) and three chamber pressures (225, 630 and 980 mTorr) showed several instances of Si transfer. However, no correlation between power or chamber pressure and Si transfer was observed for 60 s treatments (Figure 3-4).

The effect of treatment duration on Si transfer was evaluated with two sets of treatments: 50 W, 980 mTorr and 300 W, 225 mTorr. These treatments were used to evaluate duration with plasma systems exhibiting different chemical- and physical-modification abilities. Figure 3-4 shows that treatment duration does not affect Si transfer in either plasma system.

Stamps simultaneously treated under identical plasma conditions exhibited variable amounts of Si transfer, ranging from 2.2 to 4.3 %, thus indicating inconsistent transfer. In *all* cases of Si transfer from plasma-treated stamps, the Si 2p binding energy was consistent with untreated PDMS (~ 102.6 eV) and not plasma-treated PDMS (~ 104.3 eV). Figure 3-5b shows a representative Si 2p spectra of PMMA stamped with an oxygen plasma-treated PDMS stamp. As shown, the binding energy was consistent with Si that is doubly bound to oxygen, similar to the Si found in untreated PDMS (Figures 3-3a and 3-5a).

3.4.2 SEM Analysis

Stamps used to generate the data contained in Figure 3-4 were imaged with SEM to evaluate topographical changes caused by plasma-treatment; Table 3-2 summarizes the results. Although the topographical features varied widely among stamps, certain features consistently appeared, allowing stamp surfaces to be grouped into four main classifications.

As shown in representative images, stamp topographies consisted of extremely smooth surfaces devoid of features (Figure 3-6A), smooth surfaces interspersed with cracks several micrometers wide (Figure 3-6B), rippled surfaces (Figure 3-6C) and rippled surfaces with shallow indentations and sub-micrometer cracks (Figure 3-6D). These topographical changes are consistent with other published studies reporting PDMS cracking[45,46,48,49,60] and rippling[61] after exposure to oxygen plasma. In many cases,

topographical features were not uniformly distributed and several stamps exhibited regions of differing topographies. Topographical comparisons of stamps that transferred Si onto PMMA substrates, or not, typically displayed topographies A, C and D. However, deep cracking (topography B) was only observed on stamps that had exhibited Si transfer and was never was found on "nontransfer" stamps. Still, not every stamp exhibiting transfer showed deep cracking, implying that the extent of Si transfer is not related to the appearance of these cracks.

3.5 Discussion

3.5.1 Previous Studies on Si Transfer

Although μCP is a widely used patterning technique, the related disadvantage of Si transfer during stamping has received relatively little attention in the literature. Thus far, its control and reduction have been partially addressed by only a few studies.[47,55] Using XPS and ToF-SIMS, Graham et al. illustrated Si transfer from unpatterned PDMS stamps onto gold during the microcontact printing of thiol SAMs.[55] They demonstrated that low molecular weight PDMS, if present, can easily be transferred onto the SAM, thereby compromising the advantages of using SAM substrates to create clean, well-defined surfaces. The authors suggested a rigorous precleaning procedure whereby stamps are extracted in hexanes overnight, dried, and sonicated in ethanol/water. The entire process of extraction, drying and sonication is repeated three times, with the whole cleaning procedure taking approximately one week.

A more recent study by Glasmästar et al. investigated UV/ozone-treatment as a means to reduce Si transfer.[47] The authors used XPS and ToF-SIMS to measure the amount and character of PDMS transfer from unpatterned and patterned stamps to substrates of gold, TiO_2 and SiO_2 during μCP with water or buffer. In addition, they explored whether UV/ozone-treatment of the PDMS stamps could reduce the amount of transferred material. XPS results showed that UV/ozone-treatment oxidized the stamp surface causing (1) an increase in oxygen concentration by 7 % and (2) the modification of stamp surface chemistry to a state somewhere between PDMS and silica (SiO_2). The authors proposed a likely mechanism for the observed reduction of PDMS transfer by UV/ozone treatment whereby reactive oxygen radicals formed by UV light have two effects on the surface of the stamp: (i) they oxidize hydrocarbon groups that could contaminate the stamped surface and (ii) they reduce the hydrogen and carbon content in the surface region and cause a larger number of Si-O bonds. This glassy, SiO_x-like surface is likely to reduce the PDMS transfer to the stamped substrate.

3.5.2 Extent of Si Transfer: Untreated vs. Plasma-Treated PDMS

Results from Figure 3-4 indicate extensive transfer of PDMS-related materials from untreated, flat PDMS stamps (7-11 % Si). This range of transfer is consistent with results from the aforementioned studies by Graham et al. and Glasmästar et al., where untreated, unextracted stamps exhibited transfer amounts up to 12 % Si. However, once oxygen plasma-treated, all stamps showed marked increases in hydrophilicity and significant reduction in transfer amounts that were well below the range exhibited by untreated

stamps (see Figure 3-4). The highest amount of Si transferred onto the PMMA substrates from plasma-treated PDMS stamps (4.3 % Si, Figure 3-4) was significantly less than the amount of Si transferred from the untreated PDMS stamps, indicating that each plasma-treatment removes residual oligomers and PDMS-related fragments to *some* extent. Significant Si transfer was always observed when using untreated stamps; thus, it is likely that plasma-treatment is partly responsible for the removal of low-molecular-weight silicone fragments from the PDMS stamp surface.

It should be noted that during the course of early experiments, significant amounts of Si were observed on PMMA substrates that were *never in direct contact* with PDMS. It was discovered that PMMA could be contaminated with Si by simply plasma-treating the substrates immediately after plasma-treating PDMS without running an energetic cleaning cycle between stamp and substrate treatments. Plasma-treating the PDMS caused the chamber to be contaminated with Si-containing compounds that were transferred to PMMA during subsequent plasma-treatment. Moreover, the binding energy of Si 2p on the PMMA substrates was consistent with highly oxidized Si. Therefore, it was concluded that Si-containing compounds are removed from the PDMS surface and deposited onto the chamber walls. Thus, when a cleaning cycle was included between PDMS stamp and PMMA substrate treatments, XPS data of the PMMA substrates showed no presence of Si. For all the experiments presented in this chapter, a cleaning cycle was performed following each plasma-treatment to eliminate the transfer of volatile species in the plasma generator.

3.5.3 Si Transfer Variability

Figure 3-4 presents several examples in which Si transfer was eliminated, yet many examples exist where detectable transfer occurred. Furthermore, significant variability in transfer among stamps treated with identical plasma conditions is observed, illustrating an apparent inconsistency with which oxygen plasma removes low-molecular-weight fragments from PDMS surfaces. Of the possible explanations for the variability in Si transfer amounts among identically treated stamps, it is believed that the main factor may be the variability in the initial concentrations of PDMS fragments on the stamp surface prior to plasma-treatment. Results from Figure 3-4 indicate that the initial amount of fragments vary on stamps originating from the same sheet of PDMS. Therefore, the varying amounts of Si reported for plasma-treated stamps are primarily due to differences in initial PDMS fragment concentrations rather than the ability of plasma-treatment to remove/oxidize silicone. With samples simultaneously treated under identical conditions, variations in plasma composition may be responsible for the differences in transfer and this heterogeneity may treat samples differently based on their locations in the chamber. To address this issue, samples were always placed on the same area within the chamber and subjected to plasma whose composition should be homogeneous over such a small treatment area (~ 3 cm^2). In addition, plasma-treatment of other polymers (PE, PP, PS, and PMMA; results not shown) demonstrates that samples treated under the same plasma conditions but on different days are chemically modified to the same extent, thereby ruling out the possibility that variations in plasma-generator operation are responsible.

Thus, each plasma-treatment method exhibits approximately the same ability to remove PDMS fragments.

3.5.4 Role of Plasma-Treatment in Si Transfer Reduction

Although all treatments reduced Si transfer onto the PMMA substrates (Figure 3-4), none of the plasma-treatment parameters appear to be solely responsible for silicone removal. For example, both the lowest and highest powers (50 and 300 W) showed no or trace amounts of Si. In another example, high (980 mTorr) and low (225 mTorr) chamber pressures produced samples with no Si transferred. Although these results may indicate that plasma compositions do not differ significantly over the power and chamber pressure ranges employed, it is more likely that the relative amounts of ions and radicals within the plasma is not a factor in silicone removal and that plasma removes residual fragments predominantly by chemical reaction of oxygen radicals, rather than physical ablation by ions. Plasma, a mixture of radicals, ions, electrons, photons and meta-stable species, can simultaneously modify surfaces both chemically and physically.[51,52,62] Studies have shown that radicals formed within plasma are primarily responsible for chemically modifying polymers by their reaction with polymer-surface functional groups, whereas ions formed within plasma are primarily responsible for physically modifying surfaces by ablation.[51,52,63] Therefore, plasma having more radicals than ions would chemically modify a substrate more than plasma having a relatively higher presence of ions, which would exhibit more physical modification and relatively less chemical incorporation. Because specific plasma parameters dictate the relative amounts of radicals and ions

present in plasma, the nature of plasma-induced modifications can be controlled by the chosen parameters.[52,64-66] If ion bombardment was a major factor in silicone removal, higher-power/lower-pressure treatments would show consistently less Si transferred than low-power/high-pressure plasma. Comparison of results between treatments at 50 W, 980 mTorr and 300 W, 225 mTorr, which were expected to have distinctly different ion-to-radical ratios, shows no significant differences in transfer amounts, indicating that silicone removal may primarily depend on the presence of radical species and not ions.

In this respect, it is likely that oxygen plasma- and UV/ozone-treatments remove residual PDMS fragments by comparable mechanisms. Both UV/ozone- and oxygen plasma-treatments chemically modify PDMS stamp surfaces through the oxidation of Si atoms by reactive oxygen radicals to form silica-like surface layers. Additionally, both treatments have been shown to reduce Si transfer. Therefore, the implication is that the chemical reaction of oxygen radicals contained in both treatments is primarily responsible for the removal of silicone fragments. However, since physical modification by ion bombardment is a major characteristic of plasma-treatment, physical ablation of residual fragments may be occurring in our plasma systems. The relative ion concentration may not differ significantly enough over the range of powers and pressures studied for ion bombardment to be a bigger factor in fragment removal than the oxidation of fragments by radicals.

3.5.5 Other Possible Sources of Si Contamination

In addition to unremoved PDMS fragments pre-existing on the stamp surface, other possible sources of silicon-containing fragments exist to transfer Si during microcontact printing. It has been well established that oxygen plasma-treatment oxidizes the surface of PDMS into a brittle, silica-like (SiO_x) layer that is easily cracked by mechanical or thermal stresses.[46,48,49] Therefore, under extremely energetic plasma-treatment (i.e., high power treatments), this fragile surface may crack during treatment or handling, and particles originating from these cracks could be subsequently transferred during stamping. However, the data does not support this possibility because no correlation exists between power and Si transfer: high-power treatments did not show more transfer than lower powers. SEM results (Table 3-2) further illustrate the lack of correlation between extent of cracking and Si transfer. Some stamps exhibiting cracks did not show transfer, while some uncracked stamps did show transfer. In addition, Figure 3-5b shows that the positions of Si 2p peaks on PMMA substrates were consistent with untreated PDMS (102 eV), not plasma-treated PDMS (104 eV). Had this Si originated from the silica-like layer, the presence of highly oxidized silicon species would have been observed, as well as a correlation between cracking and Si transfer.

A second possible source of Si could be pre-existing oligomers diffusing from the PDMS bulk through the treated SiO_x layer of PDMS following plasma-treatment. Several studies on the hydrophobic recovery of discharge-exposed PDMS have demonstrated that following treatment, pre-existing low-molecular-weight PDMS fragments diffuse onto

the surface, causing a gradual decrease in surface hydrophilicity over time.[42,45,49] The rate of hydrophobic recovery has also been shown to increase by deliberately stressing treated PDMS surfaces, which induces cracking of the silica-like layer and facilitates the transport of unmodified fragments onto the surface.[43,46] Although this scenario would explain why the Si 2p binding energies of transferred fragments are consistent with untreated PDMS and not with plasma-treated PDMS, the lack of correlation between cracking and Si transfer is not supportive. Diffusion of low-molecular-weight silicon-containing fragments may not occur fast enough over the course of inking and stamping for this process to be a significant silicon source compared to residual fragments not removed by plasma-treatment.

A third possible Si source could be fragments/oligomers produced *in-situ* during plasma-treatment. Studies have demonstrated that discharge treatments form low-molecular-weight components in the bulk of PDMS and other silicone-containing polymers.[44,67,68] The fragments, which are formed by chain scission, would diffuse through the bulk onto the PDMS surface, just as the pre-existing oligomers diffuse (as previously described). A study by Kim et al. demonstrated that when PDMS elastomers are exposed to mild discharges, diffusion of preexisting silicone fluid in the elastomer plays an important role in its hydrophobic recovery.[68] However, the effect of preexisting silicone compounds was found to be less significant in the recovery mechanism than the migration of *in situ* produced low-molecular-weight species at severe discharge levels. As the discharge becomes more severe, the authors suggested that the dominant mechanism of hydrophobic recovery is the migration of the *in situ* produced low-molecular-weight

silicone species from the bulk.[68] These results indicate that more energetic discharge treatments (i.e., higher power) favor the formation of low-molecular-weight fragments within the PDMS bulk. Results from Figure 3-4 show examples in which PDMS stamps treated at 300 W showed little or no Si transfer, indicating that the formation and subsequent diffusion of low-molecular-weight PDMS fragments formed *in situ* is not a significant source of Si transferred to the PMMA substrates.

3.5.6 Significance of Results

The results contained in this study address some interesting issues regarding Si transfer during the μCP of aqueous-based inks. A primary goal of these experiments was to establish a single, optimized-plasma treatment that could consistently *eliminate* silicone fragments from the PDMS stamp surface without the need for additional pretreatments. However, on the basis of the results, it appears that no single set of plasma-treatment parameters reliably eliminates silicone transfer from PDMS stamps. Instead, it was found that many sets of treatment parameters significantly reduce transfer, and in some instances, reduce transfer to amounts below XPS detection limits. As there are numerous instances of using untreated PDMS stamps in the patterning of aqueous-based inks in the literature, the findings of this chapter illustrate an unknown advantage of plasma-treating stamps prior to use and will hopefully persuade others to reevaluate their stamping procedure. The results illustrate the common occurrence of Si transfer and the complexity of its elimination, a topic that has received surprisingly little attention in the literature and should be the focus of additional research. With the variability in Si

transfer, even among identically treated stamps, it is unlikely that Si transfer can be consistently eliminated *solely* using oxygen plasma; additional pretreatment methods may be necessary to completely eliminate Si transfer. In this respect, any of the plasma-treatments evaluated would complement the pretreatment procedure suggested by Graham et al.[55] to ensure maximum reduction in Si transfer. However, because no specific plasma system was significantly better at eliminating transfer, the "best" set of parameters can be based on which treatments damage the PDMS stamp surface the least. Severe topographical changes to PDMS stamp surfaces (i.e., cracking or pitting) may cause inhomogeneities on the stamp pattern that may negatively impact the quality of patterns transferred by μCP. Results from Table 3-2 demonstrate that only one treatment (200 W, 630 mTorr, 60 s) did not alter stamp topography, implying that this treatment may be better than the rest. Thus, these results should be used as a general guide for others who wish to reduce transfer of silicone fragments during μCP.

3.6 Conclusions

XPS was used to monitor Si amounts on plasma-activated PMMA that were stamped with unpatterned PDMS stamps treated with oxygen plasma under various plasma powers (50-300 W), chamber pressures (225-980 mTorr) and durations (10-120 s) to systematically evaluate their roles in the undesirable transfer of PDMS-related material that occurs during μCP. In addition, SEM was used to evaluate the topographical changes occurring to PDMS stamps due to plasma-treatment and stamping. The studies demonstrated all plasma-treatment methods evaluated significantly reduced the amount

of silicone-related material transferred during stamping as compared to untreated PDMS stamps. As no correlation exists between either plasma power or chamber pressure and transfer amounts, these results indicate that silicone fragments are removed from the PDMS stamp surface primarily by chemical means due to the interaction of radical species contained within oxygen plasma. Of the many possible sources of Si transferred onto PMMA surfaces, the predominant Si source is likely pre-existing silicone fragments not removed by plasma-treatment.

3.7 Acknowledgements

The author acknowledges Dr. Ted Madey for his helpful feedback during the preparation of this chapter as a manuscript, and financial assistance from DuPont and NIH (DE 13207-04).

3.8 References

(1) Kumar, A.; Whitesides, G. M. *Appl. Phys. Lett.* **1993**, *63*, 2002-2004.

(2) Xia, Y.; Whitesides, G. M. *Angew. Chem. Int. Ed.* **1998**, *37*, 550-575.

(3) Amro, N. A.; Xu, S.; Liu, G. *Langmuir* **2000**, *16*, 3006-3009.

(4) Ito, Y.; Nogawa, M. *Biomaterials* **2003**, *24*, 3021-3026.

(5) Kenseth, J. R.; Harnisch, J. A.; Jones, V. W.; Porter, M. D. *Langmuir* **2001**, *17*, 4105-4112.

(6) Wadu-Mesthrige, K.; Xu, S.; Amro, N. A.; Liu, G. *Langmuir* **1999**, *15*, 8580-8583.

(7) Ward, J. H.; Bashir, R.; Peppas, N. A. *J. Biomed. Mater. Res.* **2001**, *56*, 351-360.

(8) Schmalenberg, K. E.; Thompson, D. M.; Buettner, H. M.; Uhrich, K. E.; Garfias, L. F. *Langmuir* **2002**, *18*, 8593-8600.

(9) Shin, D.-S.; Lee, K.-N.; Jang, K.-H.; Kim, J.-K.; Chung, W.-J.; Kim, Y.-K.; Lee, Y.-S. *Biosens. Bioelectron.* **2003**, *19*, 485-494.

(10) Huck, W. T. S.; Yan, L.; Stroock, A.; Haag, R.; Whitesides, G. M. *Langmuir* **1999**, *15*, 6862-6867.

(11) Husemann, M.; Mecerreyes, D.; Hawker, C. J.; Hedrick, J. L.; Shah, R.; Abbott, N. L. *Angew. Chem. Int. Ed.* **1999**, *38*, 647-649.

(12) Larsen, N. B.; Biebuyck, H.; Delamarche, E.; Michel, B. *J. Am. Chem. Soc.* **1997**, *119*, 3017-3026.

(13) Jeon, N. L.; Choi, I. S.; Whitesides, G. M.; Kim, N. Y.; Laibinis, P. E.; Harada, Y.; Finnie, K. R.; Girolami, G. S.; Nuzzo, R. G. *Appl. Phys. Lett.* **1999**, *75*, 4201-4203.

(14) Csucs, G.; Künzler, T.; Feldman, K.; Robin, F.; Spencer, N. D. *Langmuir* **2003**, *19*, 6104-6109.

(15) Csucs, G.; Michel, R.; Lussi, J. W.; Textor, M.; Danuser, G. *Biomaterials* **2003**, *24*, 1713-1720.

(16) Lauer, L.; Klein, C.; Offenhäusser, A. *Biomaterials* **2001**, *22*, 1925-1932.

(17) Lee, K.; Kim, D. J.; Lee, Z.; Woo, S. I.; Choi, I. S. *Langmuir* **2004**, *20*, 2531-2535.

(18) McDevitt, T. C.; Angello, J. C.; Whitney, M. L.; Reinecke, H.; Hauschka, S. D.; Murry, C. E.; Stayton, P. S. *J. Biomed. Mater. Res.* **2002**, *60*, 472-479.

(19) Patel, N.; Bhandari, R.; Shakesheff, K. M.; Cannizzaro, S. M.; Davies, M. C.; Langer, R.; Roberts, C. J.; Tendler, S. B.; Williams, P. M. *J. Biomater. Sci. Polymer Edn.* **2000**, *11*, 319-331.

(20) Schmalenberg, K. E.; Buettner, H. M.; Uhrich, K. E. *Biomaterials* **2004**, *25*, 1851-1857.

(21) Vogt, A. K.; Lauer, L.; Knoll, W.; Offenhäusser, A. *Biotechnol. Prog.* **2003**, *19*, 1562-1568.

(22) Xu, C.; Taylor, P.; Ersoz, M.; Fletcher, P. D. I.; Paunov, V. N. *J. Mater. Chem.* **2003**, *13*, 3044-3048.

(23) Yang, Z.; Belu, A. M.; Liebmann-Vinson, A.; Sugg, H.; Chilkoti, A. *Langmuir* **2000**, *16*, 7482-7492.

(24) Yang, Z.; Chilkoti, A. *Adv. Mater.* **2000**, *12*, 413-417.

(25) Branch, D. W.; Wheeler, B. C.; Brewer, G. J.; Leckband, D. E. *IEEE Trans. Biomed. Eng.* **2000**, *47*, 290-300.

(26) Corey, J. M.; Feldman, E. L. *Experimental Neurology* **2003**, *184*, S89-S96.

(27) Garrison, M. D.; McDevitt, T. C.; Luginbühl, R.; Giachelli, C. M.; Stayton, P.; Ratner, B. D. *Ultramicroscopy* **2000**, *82*, 193-202.

(28) James, C. D.; Davis, R. C.; Kam, L.; Craighead, H. G.; Isaacson, M.; Turner, J. N.; Shain, W. *Langmuir* **1998**, *14*, 741-744.

(29) James, C. D.; Davis, R.; Meyer, M.; Turner, A.; Turner, S.; Withers, G.; Kam, L.; Banker, G.; Craighead, H.; Isaacson, M.; Turner, J.; Shain, W. *IEEE Trans. Biomed. Eng.* **2000**, *47*, 17-21.

(30) Kam, L.; Boxer, S. G. *J. Biomed. Mater. Res.* **2001**, *55*, 487-495.

(31) Howell, S. W.; Inerowicz, H. D.; Regnier, F. E.; Reifenberger, R. *Langmuir* **2003**, *19*, 436-439.

(32) Kaji, H.; Takii, Y.; Nishizawa, M.; Matsue, T. *Biomaterials* **2003**, *24*, 4239-4244.

(33) Kam, L.; Shain, W.; Turner, J. N.; Bizios, R. *Biomaterials* **2001**, *22*, 1049-1054.

(34) Runge, A. F.; Saavedra, S. S. *Langmuir* **2003**, *19*, 9418-9424.

(35) St. John, P. M.; Davis, R.; Cady, N.; Czajka, J.; Batt, C. A.; Craighead, H. G. *Anal. Chem.* **1998**, *70*, 1108-1111.

(36) Hyun, J.; Ma, H.; Zhang, Z.; Beebe, J., T. P.; Chilkoti, A. *Adv. Mater.* **2003**, *15*, 576-579.

(37) Lahiri, J.; Ostuni, E.; Whitesides, G. M. *Langmuir* **1999**, *15*, 2055-2060.

(38) Yan, L.; Huck, W. T. S.; Zhao, X.; Whitesides, G. M. *Langmuir* **1999**, *15*, 1208-1214.

(39) Donzel, C.; Geissler, M.; Bernard, A.; Wolf, H.; Michel, B.; Hilborn, J.; Delamarche, E. *Adv. Mater.* **2001**, *13*, 1164-1167.

(40) He, Q.; Liu, Z.; Xiao, P.; Liang, R.; He, N.; Lu, Z. *Langmuir* **2003**, *19*, 6982-6986.

(41) Liang, Z.; Li, K.; Wang, Q. *Langmuir* **2003**, *19*, 5555-5558.

(42) Tóth, A.; Bertóti, I.; Blazsó, M.; Bánhegyi, G.; Bognar, A.; Szaplonczay, P. *J. Appl. Polym. Sci.* **1994**, *52*, 1293-1307.

(43) Hillborg, H.; Gedde, U. W. *Polymer* **1998**, *39*, 1991-1998.

(44) Kim, J.; Chaudhury, M. K.; Owen, M. J. *IEEE Trans. Dielectrics Electr. Insul.* **1999**, *6*, 695-702.

(45) Hillborg, H.; Ankner, J. F.; Gedde, U. W.; Smith, G. D.; Yasuda, H. K.; Wikström, K. *Polymer* **2000**, *41*, 6851-6863.

(46) Hillborg, H.; Sandelin, M.; Gedde, U. W. *Polymer* **2001**, *42*, 7349-7362.

(47) Glasmästar, K.; Gold, J.; Andersson, A. S.; Sutherland, D. S.; Kasemo, B. *Langmuir* **2003**, *19*, 5475-5483.

(48) Owen, M. J.; Smith, P. J. *J. Adhesion Sci. Technol.* **1994**, *8*, 1063-1075.

(49) Fritz, J. L.; Owen, M. J. *J. Adhesion* **1995**, *54*, 33-45.

(50) Olander, B.; Wirsén, A.; Albertsson, A. *J. Appl. Polym. Sci.* **2003**, *90*, 1378-1383.

(51) Liston, E. M. *J. Adhesion* **1989**, *30*, 199-218.

(52) Chan, C. M.; Ko, T. M.; Hiraoka, H. *Surf. Sci. Rep.* **1996**, *24*, 1-54.

(53) Hyun, J.; Zhu, Y.; Liebmann-Vinson, A.; Beebe, J., T. P.; Chilkoti, A. *Langmuir* **2001**, *17*, 6358-6367.

(54) Langowski, B. A.; Uhrich, K. E. *Polymeric Materials: Science & Engineering* **2002**, *87*, 132-133.

(55) Graham, D. J.; Price, D. D.; Ratner, B. D. *Langmuir* **2002**, *18*, 1518-1527.

(56) Dukovic, G. In *Department of Chemistry and Chemical Biology*; Rutgers University: New Brunswick, 2001**;** p 49.

(57) Morra, M.; Occhiello, E.; Marola, R.; Garbassi, F.; Humphrey, P.; Johnson, D. *J. Coll. Int. Sci.* **1990**, *137*, 11-24.

(58) Murakami, T.; Kuroda, S.; Osawa, Z. *J. Coll. Int. Sci.* **1998**, *202*, 37-44.

(59) Bar, G.; Delineau, L.; Häfele, A.; Whangbo, M. H. *Polymer* **2001**, *42*, 3527-3632.

(60) Hettlich, H. J.; Otterbach, F.; Mittermayer, C.; Kaufmann, R.; Klee, D. *Biomaterials* **1991**, *12*, 521-524.

(61) Chua, D. B. H.; Ng, H. T.; Li, S. F. Y. *Appl. Phys. Lett.* **2000**, *76*, 721-723.

(62) Wheale, S. H.; Badyal, J. P. S. In *Interfacial Science*; Roberts, M. W., Ed.; Blackwell Science Ltd: Oxford, 1997; pp 237-255.

(63) Kersten, H. In *Low temperature plasma physics*; Hippler, R.; Pfau, S.; Schmidt, M.; Schoenbach, K. H., Eds.; Wiley-VCH: Berlin, 2001; pp 113-130.

(64) Martinu, L.; Wertheimer, M. R.; Klemberg-Sapieha, J. E. In *Plasma deposition and treatment of polymers*; Lee, W. W.; d'Agostino, R.; Wertheimer, M. R., Eds.; Materials Research Society: Warrendale, 1999; Vol. 544, pp 251-255.

(65) Weikart, C. M.; Yasuda, H. K. *J. Polym. Sci. A Polym. Chem.* **2000**, *38*, 3028-3042.

(66) Hegemann, D.; Brunner, H.; Oehr, C. *Nucl. Instr. and Meth. in Phys. Res. B* **2003**, *208*, 281-286.

(67) Kim, J.; Chaudhury, M. K.; Owen, M. J. *J. Coll. Int. Sci.* **2000**, *226*, 231-236.

(68) Kim, J.; Chaudhury, M. K.; Owen, M. J.; Orbeck, T. *J. Coll. Int. Sci.* **2001**, *244*, 200-207.

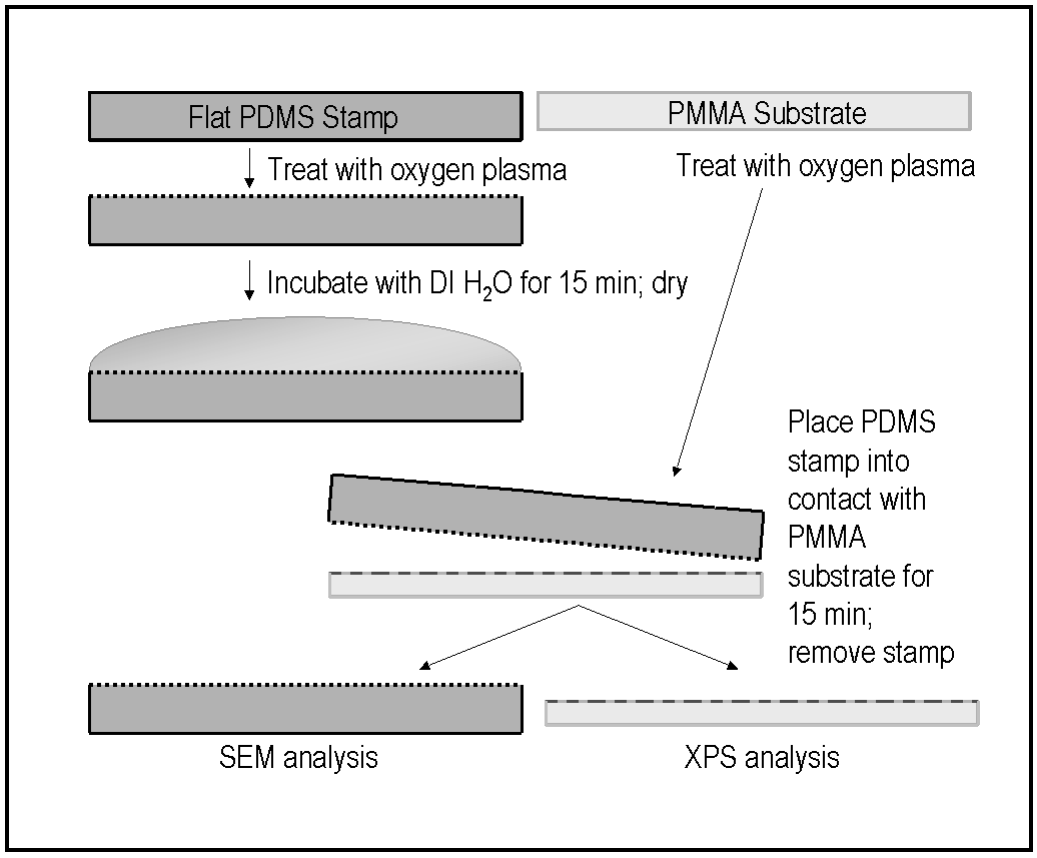

Figure 3-1: Schematic of the μCP procedure.

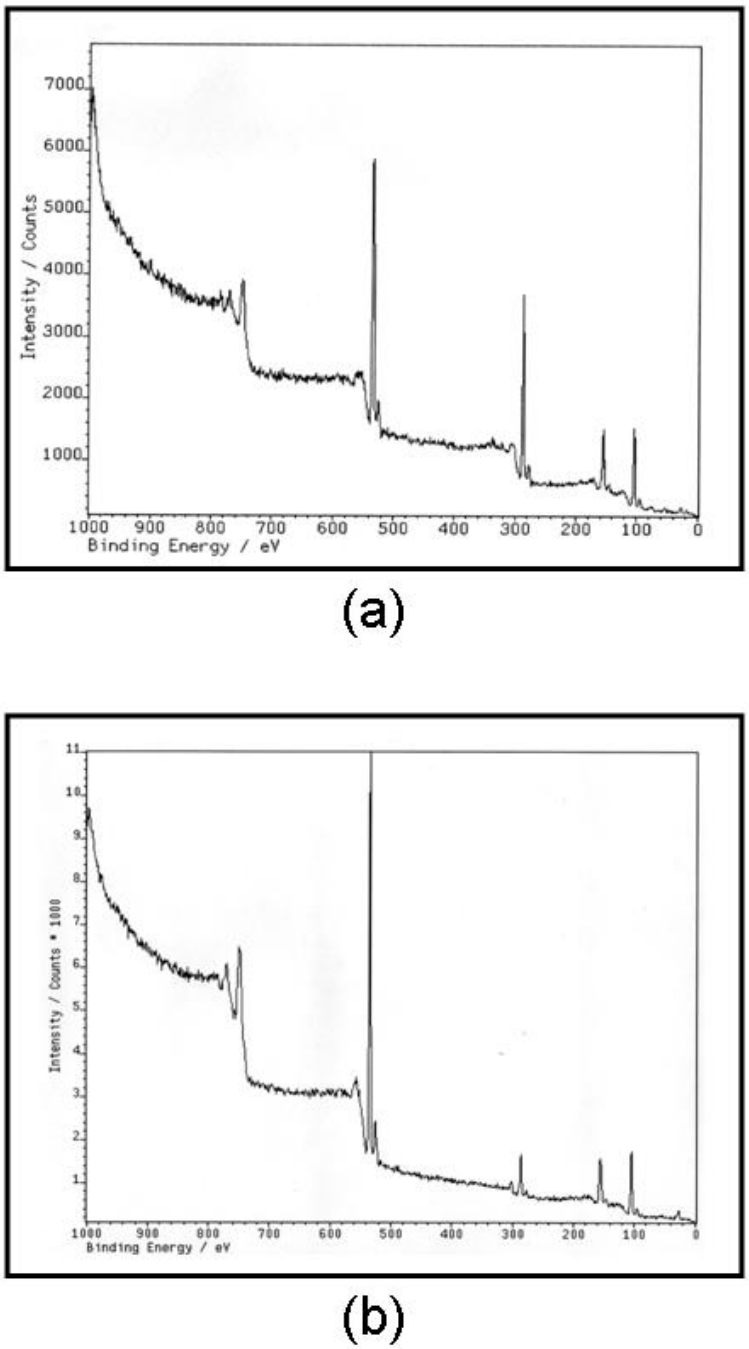

Figure 3-2: Representative XPS survey spectra of PDMS: (a) untreated and (b) oxygen plasma-treated at 50 W and 660 mTorr for 300 s.

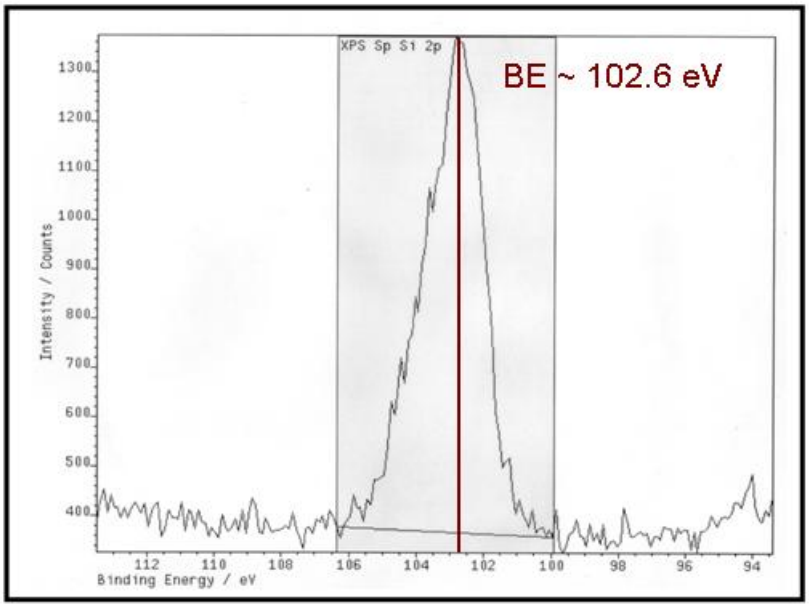

(a)

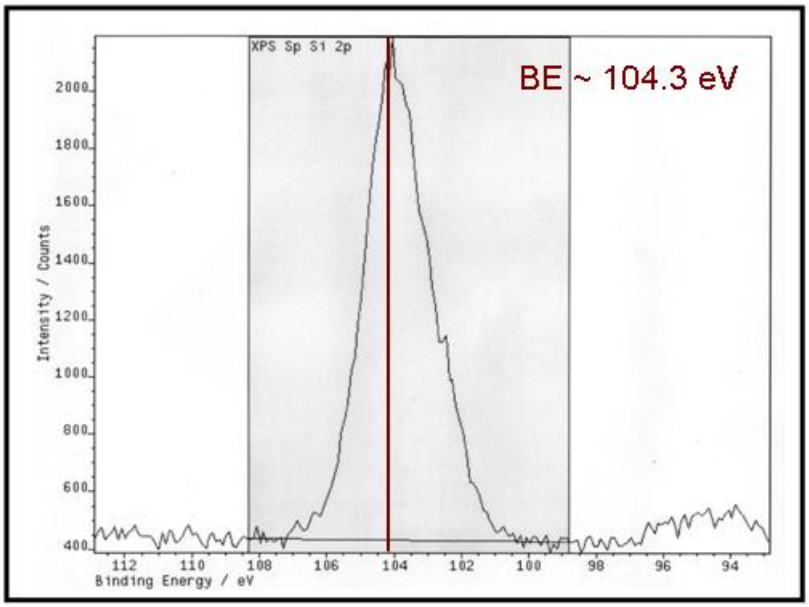

(b)

Figure 3-3: Representative Si 2p XPS spectra of PDMS: (a) untreated and (b) oxygen plasma-treated at 50 W, 660 mTorr for 300 s.

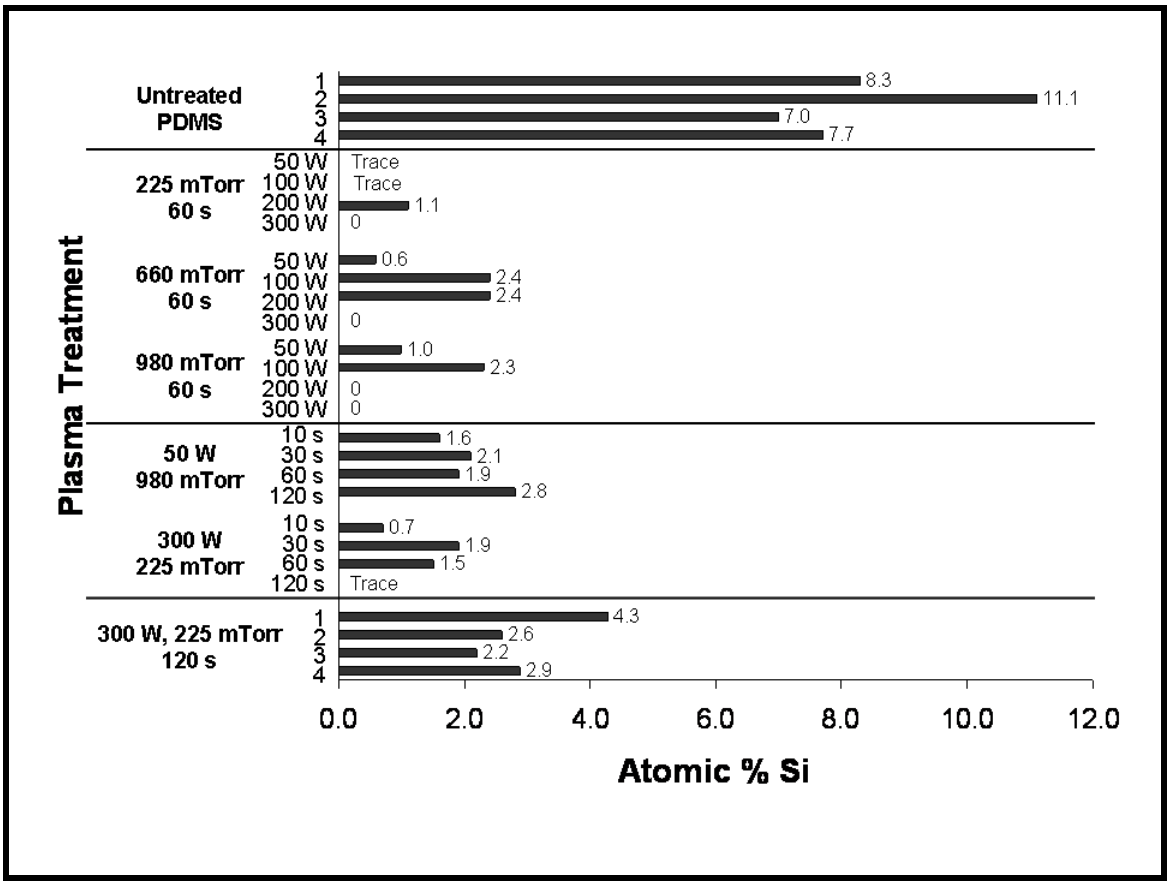

Figure 3-4: % Si measured by XPS for PMMA stamped with PDMS stamps that were oxygen plasma-treated under various conditions: (i) untreated PDMS; (ii) varied power and chamber pressure at 60 s; (iii) varied duration at 50 W, 980 mTorr and 300 W, 225 mTorr; and (iv) identically treated stamps at 300 W, 225 mTorr, and 120 s. % Si indicates the extent of transfer of PDMS-related material during μCP. In all instances of transfer, the binding energies of the Si 2p peaks were consistent with untreated PDMS (~102.6 eV). Samples with "trace" amounts of Si showed protrusions in the background signal in the Si 2s and Si 2p regions; however, signal intensities were too low for reliable quantification. Labels "1-4" denote the four distinct stamps treated under the stated conditions. Typical standard deviation for XPS measurements was ± 0.7.

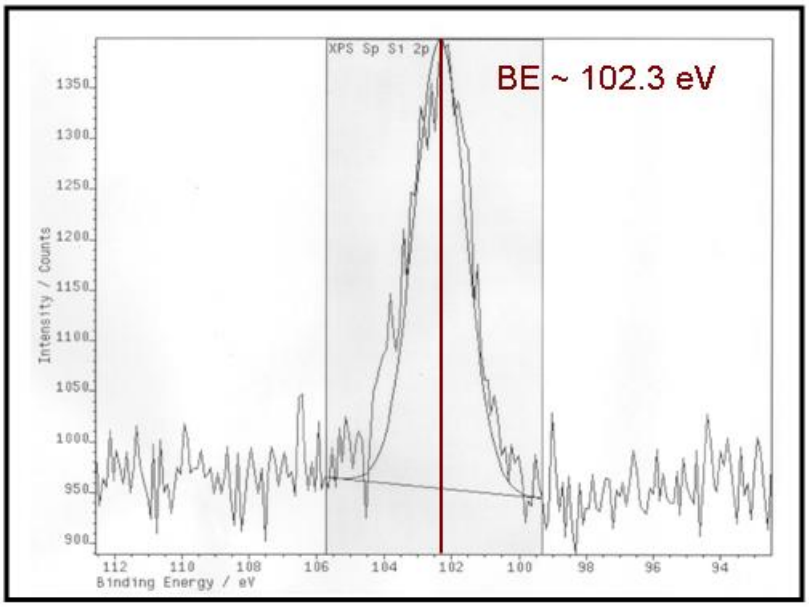

(a)

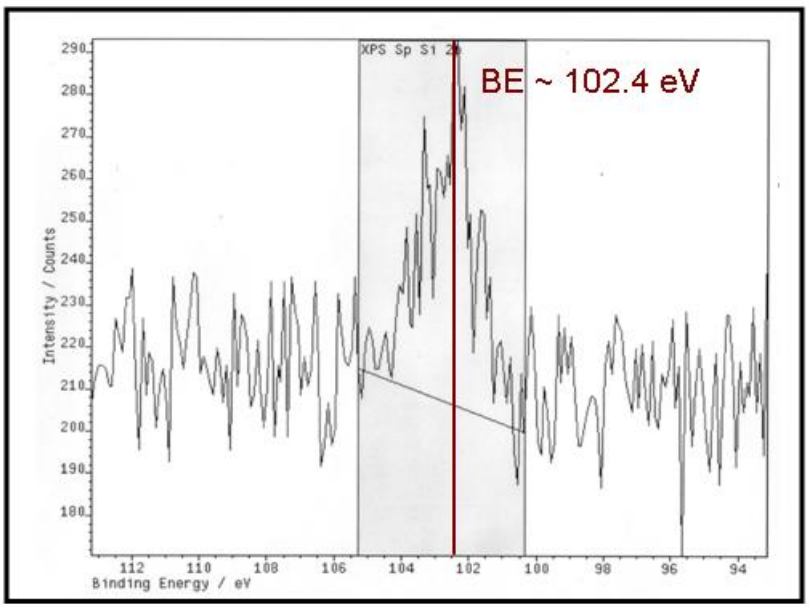

(b)

Figure 3-5: Representative Si 2p XPS spectra of PMMA stamped with: (a) an untreated PDMS stamp and (b) an oxygen plasma-treated PDMS stamp.

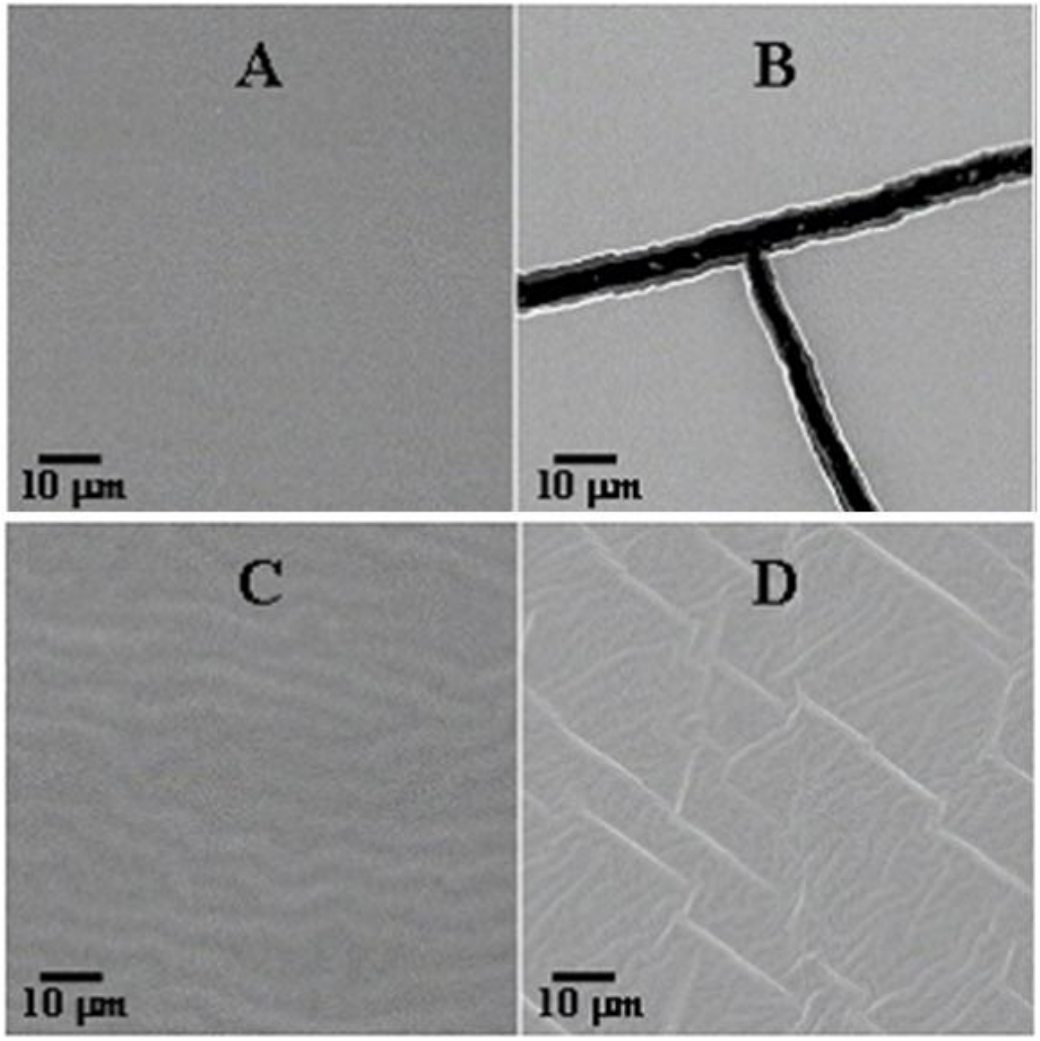

Figure 3-6: Representative SEM micrographs (1000 × magnification) of used PDMS stamps illustrating commonly encountered topographies: (a) smooth and devoid of topographical features; (b) smooth with micrometer-sized cracks; (c) rippled; and (d) rippled with sub-micrometer-sized cracks.

	% C	% O	% Si	Si 2p (eV)
Untreated PMMA	72.1	27.9	0.0	-
Oxygen plasma-treated PMMA	65.0	35.0	0.0	-
Untreated PDMS	47.2	29.5	23.3	102.6
Oxygen plasma-treated PDMS	24.5	50.9	24.6	104.3

Table 3-1: XPS compositional data and Si 2p binding energies for PMMA and PDMS (untreated vs. oxygen plasma-treated at 50 W, 660 mTorr, for 300 s). Typical standard deviation for XPS measurements was ± 0.7.

	Treatment (60 s)	Topography at 1000 × Magnification
Measurable Si Transfer	untreated	A
	225 mTorr, 200 W	C,D
	630 mTorr, 50 W	A,C,D
	630 mTorr, 100 W	A,B
	630 mTorr, 200 W	A
	980 mTorr, 50 W	A,B
	980 mTorr, 100 W	A,B
No Measurable Si Transfer	225 mTorr, 50 W	D
	225 mTorr, 100 W	C,D
	225 mTorr, 300 W	A,C
	630 mTorr, 300 W	D
	980 mTorr, 200 W	D
	980 mTorr, 300 W	D

***A:** Smooth **B:** Smooth/Deep Cracks **C:** Rippled **D:** Rippled/Shallow Cracks*

Table 3-2: Surface topographies of used PDMS stamps that generated XPS data in Figure 3-4(ii).

CHAPTER 4: MICROSCALE PLASMA-INITIATED PATTERNING (μPIP)

4.1 Abstract

A novel technique to create biomolecular micropatterns of varying complexity on several types of polymer substrates, termed microscale plasma-initiated patterning (μPIP), is presented. This method uses a patterned poly(dimethylsiloxane) (PDMS) stamp to preferentially expose or protect areas of an underlying polymer substrate from oxygen plasma. Following plasma-treatment, the substrate is immersed in a biomolecular ink, whereby molecules preferentially adsorb to either the plasma-exposed or plasma-protected substrate regions, depending on the particular substrate/ink combination. Using this method, polyethylene, polystyrene, poly(methyl methacrylate), PDMS, and poly(hydroxybutyrate/hydroxyvalerate) were micropatterned with different aqueous-based biomolecular inks (i.e., goat anti-rabbit immunoglobulin G, poly-L-lysine, and bovine serum albumin). Water contact angle measurements performed on substrates after oxygen plasma exposure showed that the hydrophilicity of substrate areas exposed to plasma was significantly greater than areas protected from plasma by the PDMS stamp. In addition, scanning electron microscopy results demonstrated that substrate areas exposed to plasma were physically modified (e.g., roughened) as compared to adjacent, protected areas. Areas in contact with a patterned PDMS stamp during plasma exposure were found to be physically unaffected by plasma-treatment, and exhibited spatial features/dimensions consistent with the corresponding features of the patterned stamp.

Lastly, protein patterns of bovine serum albumin on the polymer substrates were stable and distinct after four weeks of incubation at 37 °C.

4.2 Introduction

Microscale patterning of biomolecules is used in a wide range of biological and medical applications including biosensors, DNA microarrays, tissue engineering, and immunoassays.[1-6] Methods to micropattern biomolecules onto both organic and inorganic surfaces include photolithography,[1,3,7] microcontact printing,[1,2,5,6,8-12] micromolding in capillaries (MIMIC)/microfluidic networks,[1,13-16] and micromolding.[1,17] Each technique has relative advantages and limitations in terms of cost-efficiency, ease, reproducibility and applicability to specific ink/substrate combinations. For example, protein patterns by microcontact printing requires that the protein molecules interact with the final substrate more strongly than with the micropatterned stamp that is first inked with the biomolecules.[11] The difference in wettability between the surfaces of the stamp and substrate appears to be the dominant parameter that determines success with this method.[11] As another example, a cited critical drawback of MIMIC/microfluidic network patterning is the intrinsic slowness in pattern formation, which strongly limits its use for large area applications, and requires additional steps to pattern viscous liquids.[18] More detailed descriptions of microcontact printing and microfluidic network patterning are given in Chapter 1 of this thesis.

Presented herein is a simplified micropatterning technique that immobilizes aqueous-based biomolecular inks into microscale patterns on organic, biocompatible substrates. The method, termed microscale plasma-initiated patterning (μPIP), uses a patterned poly(dimethylsiloxane) (PDMS) stamp to selectively expose or protect underlying substrate regions from the chemical and physical effects of oxygen plasma exposure, thereby, forming distinct microscale domains with relatively different hydrophilicities on the substrate. These chemically different areas exhibit varying affinities for a given biomolecule, allowing microscale pattern formation based on the preferential adsorption of ink molecules onto either the plasma-exposed or plasma-protected regions of a particular substrate. The inks evaluated include fluorescein isothiocyanate (FITC)-conjugated goat anti-rabbit immunogobulin G, FITC-conjugated poly-L-lysine, and Texas Red-conjugated bovine serum albumin. The micropatterned substrates include non-biodegradable polymers such as polyethylene, polystyrene, poly(methyl methacrylate, poly(dimethylsiloxane), and a biodegradable polymer, poly(hydroxybutyrate/hydroxyvalerate) (PHBV).

The goals of this chapter are to illustrate the versatility of ink/substrate combinations successfully patterned, and to demonstrate the more complex patterns that can be formed with this method. In addition, this chapter demonstrates the stability, under physiologically relevant conditions, of bovine serum albumin patterns formed by μPIP. Lastly, to show the plasma induced chemical and physical modifications, respectively, occurring on the substrate surfaces when exposed to oxygen plasma while in contact with

a patterned PDMS stamp, results from contact angle analysis and scanning electron microscopy are presented.

4.3 Materials and Methods

4.3.1 Substrates

Sheets of polyethylene (PE), polystyrene (PS), poly(methyl methacrylate) (PMMA), and poly(hydroxybutyrate/hydroxyvalerate) (PHBV) were obtained from Goodfellow (Huntingdon, England) and cut into squares (1 cm^2) using a razor blade. Poly(dimethylsiloxane) (PDMS) substrates were made using Sylgard 184 silicone elastomer kit (Dow Corning, Midland, MI). Elastomer base and curing agent were combined in a 10:1 ratio (w\w), after which prepolymer was placed under vacuum to remove entrapped air. Thin layers of uncured elastomer (~ 5 mm) were poured into petri dishes (150 mm × 10 mm) and allowed to cure for 24 h under vacuum (-0.98 bar, room temperature). Once cured, PDMS sheets were cut with a razor blade into squares (1 cm^2). All substrates were rinsed with HPLC grade ethanol (Sigma-Aldrich, St. Louis, MO) prior to patterning.

4.3.2 Biomolecular Inks

Fluorescein isothiocyanate (FITC)-conjugated poly-L-lysine (Sigma, St. Louis, MO), FITC-conjugated goat anti-rabbit immunoglobulin G (α-rabbit IgG, Sigma), and Texas Red-conjugated bovine serum albumin (BSA, Molecular Probes, Eugene, OR) were

diluted with phosphate buffered saline (PBS, pH 7.4, MP Biomedicals, Aurora, OH) to concentrations of 1 mg/mL, 34 μg/mL, and 100 μg/mL, respectively.

4.3.3 Patterned PDMS Stamps

PDMS stamps were prepared by pouring Sylgard 184 silicone elastomer kit (10:1 w\w base to crosslinker) over lithographically created masters, previously described in detail.[12] In brief, masters were created by exposing photoresist-coated silicon wafers through a photomask producing a relief pattern on the silicon surface. The relief pattern consists of a series of raised, parallel lanes (20 μm wide) separated by 20 μm spaces, over which the silicone elastomer was poured. Upon curing, the PDMS was peeled off the master, and the patterned regions were cut using a razor blade into stamps (8 mm × 8 mm). To ensure that the ends of the channels would be unobstructed during plasma-treatment, the stamps were further trimmed on all sides to remove the outer portions of the patterned regions.

4.3.4 Simple-Pattern Formation

PE, PMMA, PS, PDMS, and PHBV were patterned with biomolecular inks (poly-L-lysine, α-rabbit IgG, and BSA) using the procedure outlined in Figure 4-1. This method utilizes a striped, patterned PDMS stamp to preferentially expose and protect areas of the underlying substrate to oxygen plasma. The patterned PDMS stamp, consisting of parallel lanes (20 μm) separated by 20 μm spaces, was placed into contact with the substrate, and the entire unit exposed to oxygen plasma (March Plasma, Concord, CA) for 300 s at 50 W and 660 mTorr (Fig. 4-1ii). Once plasma treated, the stamp was

removed and the substrate immersed, treated side down, in a few drops of the biomolecular ink for no more than 60 s at room temperature (Fig. 4-1iii). Typically, substrates were immersed in ink within 60 s after plasma-treatment to allow for the biomolecules to adsorb onto either the hydrophobic or hydrophilic regions of the substrate, depending on the specific substrate/ink combination (Fig. 4-1iv). Following immersion, the substrates were gently swirled in a beaker of deionized water (~ 20 mL) for approximately 10 s to remove non-adsorbed biomolecules, then allowed to air-dry. The biomolecular patterns, consisting of 20 μm stripes separated by 20 μm spaces, were visualized using confocal laser scanning microscopy (CLSM).

4.3.5 Complex-Pattern Formation

To illustrate the ability of μPIP to create more complex micropatterns consisting of distinct regions with differing ink concentrations, PDMS, PMMA, PE, PS, and PHBV substrates were patterned with poly-L-lysine, α-rabbit IgG, or BSA following the method outlined in Figure 4-2. The patterned stamp is placed into contact with the substrate and is exposed to oxygen plasma (50 W, 660 mTorr, 150 s). The stamp is removed, rotated 90°, placed back into contact with the substrate, and exposed to plasma a second time (50 W, 660 mTorr, 60 s, Fig. 4-2i). Completion of the second step forms four distinct substrate regions: areas exposed to plasma twice, areas first exposed to plasma and then protected in the second step, areas first protected from plasma and then exposed in the second step, and areas protected from the two subsequent plasma-treatments. Following the second plasma-treatment, the stamp was removed and the substrate immersed, treated side down, in a few drops of the specific ink for no more than 60 s at room temperature

(Fig. 4-2ii). Following immersion (Fig. 4-2iii), the substrates were gently swirled in a beaker of deionized water (~ 20 mL) for approximately 10 s to remove non-adsorbed biomolecules and allowed to air-dry. The patterns, ideally consisting of 10 × 10 μm boxes with different fluorescent intensities, were visualized with CLSM.

To illustrate the effect of different plasma-treatments after stamp rotation on pattern formation, PDMS was patterned with poly-L-lysine as follows: the stamp/substrate unit was first exposed to a relatively mild oxygen plasma-treatment (50 W, 660 mTorr, 60 s), and then to a more energetic treatment (300 W, 660 mTorr, 120 s) following stamp rotation. The substrate was immersed in ink, rinsed, dried and analyzed as described above.

4.3.6 Dual Ink-Pattern Formation

To demonstrate the ability of μPIP to create micropatterns consisting of distinct, alternating regions of different biomolecules, PMMA was simultaneously patterned with BSA and poly-L-lysine following the method outlined in Figure 4-1. However, instead of immersing the plasma-treated substrate in a single ink, the PMMA was immersed in a mixture of BSA and poly-L-lysine (equal parts by volume) for 60 s at room temperature. The substrate was rinsed, dried and analyzed as described above.

4.3.7 Pattern Imaging by CLSM

Simple- and complex-pattern formation was confirmed using a Zeiss LSM 410 CLSM with a computer-controlled laser scanning assembly attached to the microscope. An

Omnichrome 3 line Ar/Kr laser operating at 488, 568, and 647 nm was used as the excitation source. The images were processed with Zeiss LSM control software.

4.3.8 Static Contact Angle Measurements

Wettability of substrate areas exposed to or protected from oxygen plasma during treatment was established by contact angle measurements recorded at room temperature using an NRL contact angle goniometer (Rame-Hart). Measurements were taken separately on substrates exposed to oxygen plasma at 50 W and 660 mTorr for 300 s (i.e., "plasma treated *exposed*"), and substrates that were plasma-treated while in contact with a flat, *unpatterned* PDMS stamp (i.e., "plasma treated *protected*"). In each experiment, a drop of deionized, doubly distilled water was placed on the sample, and two contact angle measurements per drop were taken by direct reading. Reported values are an average of at least 6 measurements per sample type.

4.3.9 Evaluation of Substrate and Stamp Topography by Scanning Electron Microscopy (SEM)

The surfaces of the substrates following exposure to oxygen plasma (50 W, 660 mTorr, 300 s) while in contact with *patterned* PDMS stamps, *in addition to the PDMS stamps*, were imaged with an Amray 1830I scanning electron microscope, using an acceleration potential of 10 kV. Prior to imaging, substrates and patterned stamps were sputter-coated with gold and palladium using a Balzers SCD004 sputter coater (working pressure, 0.05 mbar; working distance, 50 mm; current, 30 mA; time, 120 s).

4.3.10 Evaluation of Pattern Stability

Substrates were micropatterned with BSA following the procedure described in Figure 4-1 and imaged with CLSM. Substrates were subsequently immersed in PBS, wrapped in foil, and stored in an incubator at 37 °C for a period of 14 days. The samples were removed from PBS and directly imaged again with CLSM. The samples were stored an additional 14 days under PBS at 37 °C, upon which they were imaged with CLSM again, after a total storage time of 28 days.

4.4 Results and Discussion

The concept of selective plasma-treatment by employing a patterned PDMS stamp has been scantily covered in the literature.[19-21] The focus of the previous studies has been to preferentially treat the PDMS *stamp* surface rather than the underlying substrate surface.[19-21] In this work, it was observed that simultaneously plasma-treating a substrate while in physical contact with a patterned PDMS stamp preferentially increases the hydrophilicity of the exposed substrate regions to produce distinct patterns on the substrate with different relative hydrophilicities determined by the *stamp* patterns. Once formed, the hypothesis was that these distinct regions would exhibit varying affinities for biomolecules, thereby creating patterns by the preferential attachment of ink molecules to either the plasma-exposed or plasma-protected substrate regions.

4.4.1 Simple Micropatterns Generated by μPIP

Figure 4-3 displays representative fluorescence micrographs of biomolecular inks on polymeric surfaces formed by μPIP, illustrating the applicability of this technique to a varied range of polymers and inks. Generally, the striped patterns were well resolved from the underlying substrate, exhibited uniform ink distribution within the pattern, and had lateral dimensions in good agreement with stamp features. Although the striped patterns shown in Figure 4-3 were formed after immersion in ink for 60 s, pattern formation was observed even after 5 s of immersion. However, the quality and uniformity of the resulting patterns were, at times, not as consistent at short immersion relative to longer immersion times. Immersion times significantly longer than 60 s (e.g., 60 min), periodically resulted in patterns with poorer resolution due to significant ink adsorption in both plasma-protected and plasma-exposed regions. Thus, immersion time, as well as plasma-treatment parameters (e.g., feed gas, power, duration, chamber pressure), may be two key variables that can be optimized for highly resolved patterns for a given ink/substrate combination.

One significant advantage of this technique is that pattern formation is widespread, occurring wherever the stamp is in good contact with the substrate, as illustrated in Figure 4-4a (BSA on PS) and Figure 4-4b (α-rabbit IgG on PS). Another benefit of this method is the ability to easily produce more complex patterns than simple stripes. Figure 4-5 illustrates the effect of dual plasma-treatments/stamp orientations on ink adsorption and resulting complex-pattern formation.

4.4.2 Complex Micropatterns Generated by μPIP

Plasma-treating the substrates as outlined in Figure 4-2 creates four distinct zones: areas exposed to plasma twice, areas first exposed to plasma and then protected in the second step, areas first protected from plasma and then exposed in the second step, and areas protected from the two subsequent plasma-treatments. However, as the same plasma-treatment is used after stamp rotation, regions that are exposed to plasma only once are chemically modified to the same extent and should exhibit similar affinities for a given ink compared to each other, but different affinities as compared to regions exposed to plasma twice or protected from plasma twice. As shown in Figures 4-5a-c, substrates with three distinct concentrations of the ink were formed. The relative orientations of these regions change depending on the ink/substrate combination and/or with the plasma-treatment parameters used. For example, the effect of ink/substrate combination can be shown by comparing the fluorescent micrographs of Figures 4-5. The substrates in Figures 4-5a-c were treated using the same oxygen plasma-treatment (50 W, 660 mTorr, 150 s, rotate 90° , 50 W, 660 mTorr, 150 s), yet the resulting patterns on PMMA (Figure 4-5a) appear strikingly different from those on PDMS (Figure 4-5b) and PS (Figure 4-5c). Rather than patterns consisting of lines with the weakest fluorescence alternating with lines that exhibit intermediate and strongest fluorescence (Figures 4-5b-c), a "plaid" pattern is formed on PMMA (Figure 4-5a). Figure 4-5d shows the effect of employing two different plasma-treatments on pattern formation. The substrate was exposed to a mild treatment (50 W, 660 mTorr, 60 s), and then with a relatively more energetic treatment (300 W, 660 mTorr, 120 s) after stamp rotation. In contrast to the patterns in

Figures 4-5a-c, stripes with uniform fluorescence are created, rather than forming alternating boxes of differing fluorescence. This result indicates that the second, more energetic plasma-treatment modified the exposed regions to the same extent, regardless of the initial modifications introduced by the first treatment.

Figures 4-3 through 4-5 illustrate the versatility of this technique and also highlight the many factors that may contribute to pattern formation; treatment parameters can be optimized based on the ink/substrate combination, as a given ink cannot be expected to behave the same way on two different substrates. For example, BSA molecules attach to the plasma-*exposed* regions of PHBV, whereas BSA attaches to the plasma-*protected* regions of PS; the specific molecular interactions at the BSA/PHBV interface are obviously different than the BSA/PS interface. The specific molecular interactions at the various ink/substrate must still be investigated, and are beyond the scope of this chapter. Yet, preliminary information on these interactions is obtained from the stability of BSA-patterned substrates upon storage.

4.4.3 Micropattern Stability

The micrographs in Figure 4-6 highlight the stability of BSA on substrates following four weeks of storage in PBS at 37 °C. Images for PS (Figures 4-6a-b) were taken from the same area of the substrate, whereas images for PDMS (Figures 4-6c-d) were taken from different areas of the same substrate. The BSA patterns on PS remained intact and exhibited no changes in stripe width, indicating good stability at physiologically relevant

conditions for at least four weeks (Figure 4-6b). In fact, pattern resolution was actually improved upon storage: the faint fluorescence between the BSA stripes shown in Figure 4-6a disappeared, indicating that longer incubation removed weakly adsorbed ink molecules on the "unpatterned" regions. The encircled area of Figure 4-6b is not a result of pattern loss on storage, as this region was originally present (encircled area, Figure 4-6a), and is likely a result of an anomaly on the PDMS stamp surface. BSA patterns on PE, PMMA, and PHBV (not shown) were equally stable after four weeks; these substrates displayed well resolved, distinct striped patterns that exhibited improved pattern resolution upon long term storage. In contrast, BSA patterns on PDMS, although present and intact, exhibited significant pattern-widening and diffusion after four weeks. This loss of pattern resolution was not observed after two weeks of storage, indicating that these patterns are stable for a period of somewhere between two and four weeks. As stated previously, the difference in pattern stability is likely due to differences in molecular interactions at the ink/substrate interface.

4.4.4 Relative Hydrophilicity: Plasma-Protected vs. Plasma-Exposed

Comparison of "plasma treated *protected*" and "plasma treated *exposed*" contact angles in Table 4-1 shows that exposure to oxygen plasma significantly increased the hydrophilicity of each polymer substrate, with PDMS exhibiting the largest change in contact angle (~ 76°) and PE showing the smallest decrease (~ 36°). It is well established that oxygen plasma-treatments increase the hydrophilicity of a polymer surface by chemically incorporating polar, oxygen-containing functionalities.[22-26] Clearly, plasma-

treatment of polymer substrates in the fashion outlined in Figure 4-1 creates distinct regions with significantly different hydrophilicities that enable distinct patterns on various polymer substrates (as shown in Figures 4-3 through 4-5).

To further verify that distinct regions with significantly different hydrophilicities are formed on polymer substrates by the method in Figure 4-1, dual ink patterns were formed on PMMA by immersion of the substrate in a mixture of poly-L-lysine and BSA (equal parts by volume). As shown in Figure 4-7, the biomolecules spontaneously segregated and preferentially adsorbed to either the plasma-exposed (i.e., relatively hydrophilic) or plasma-protected (i.e., relatively hydrophobic) regions of the substrate.

4.4.5 Plasma-Induced Surface Roughening

Exposure to oxygen plasma physically modifies the polymer surfaces, in addition to increasing hydrophilicity. SEM micrographs (Figures 4-8a-c) show two distinct regions where plasma-treating polymer substrates in contact with a patterned PDMS stamp. Areas exposed to plasma, which appear lightened in Figures 4-8a-c, were rougher compared to adjacent, plasma-protected regions, which are the darker regions (encircled areas in Figures 4-8a-c). The resulting topographies of PMMA, PS, PE, and PHBV are consistent with those of Figures 4-8a and 4-8c, which show clear delineation of the differently exposed surfaces. In contrast, the delineation was more subtle in the case of PDMS (Figure 4-8b). Instead of increased roughening relative to the plasma-protected regions, the plasma-exposed regions of PDMS exhibited a relatively smooth surface

interspersed with numerous cracks. This cracking has been well documented and is consistent with prior studies of PDMS surfaces exposed to plasma.[27-32] The ability to physically modify polymer surface topography by oxygen plasma is well documented, and has been attributed to the chemical and physical etching by radical reactions and ion bombardment, respectively.[22,24,26,33-37]

Figures 4-8c and 4-8d show the topography of the bottom-left region of a PHBV substrate and the corresponding bottom-right region of the patterned PDMS stamp in contact with the substrate during plasma-treatment, respectively. The micrographs, which are mirror images of each other, illustrate the excellent agreement between the spatial dimensions/features of the PDMS stamp pattern and the resulting pattern on the substrate. These results support the contention that the underlying substrate surface is effectively shielded from the oxidative effects of plasma in the regions that make sufficient contact with the PDMS stamp.

4.4.6 Comparison to Other Micropatterning Methods

Previously published methods to generate micropatterns on polymer surfaces by using plasma or photochemical methods differ in several respects from the method presented herein. For example, Feng et al. utilize plasma-treatment to selectively expose recessed regions of a patterned PDMS stamp,[19] which is incubated in protein solution such that the protein ink fills the recessed regions. The protein ink is then transferred from the recessed regions of the PDMS stamp upon physical contact with the substrate. Because

the method relies on the PDMS stamp to transfer patterns to the substrate rather than on simple adsorption from solution, the relative affinities of the ink for the PDMS stamp and the final substrate hampers homogeneous pattern transfer. Furthermore, complex patterns as shown in Figure 4-5 cannot be generated by this method. In another example, Lhoest et al. developed a photolithographic technique to produce hydrophilic/hydrophobic regions on polystyrene to promote cell adhesion.[38] As with any microlithography approach, photoresist patterns must first be produced to protect areas of the underlying substrate from plasma, making this procedure much more labor-intensive than μPIP. A related method by Goessl et al. utilizes plasma lithography to pattern polymeric substrates with a hydrophobic fluorocarbon plasma polymer.[39] This method requires multiple steps and the use of photoresist to define the different pattern regions. Three recent, non-plasma patterning methods have utilized a photomask or contact mask to selectively expose polymers to UV radiation, thereby only modifying the underlying substrate surfaces that were exposed to radiation.[40-42] Hozumi et al. patterned BSA onto PMMA by preferentially exposing the polymer to vacuum ultraviolet light through a photomask.[40] The exposed regions, after being chemisorbed with aminosilane by chemical vapor deposition, were used to immobilize BSA. A similar technique by Kim et al., which also used a photomask to selectively expose a polymer substrate to UV radiation, produced patterns of contrasted hydrophilicity on non-porous thin-films of polymethylsilsesquioxane.[41] A third method by McCarley et al. formed patterns of carboxylic acids on PMMA and poly(carbonate) by irradiating the substrates with UV light through a simple contact mask.[42] The patterns, after exposure to poly(*N*-isopropylacrylamide), were subsequently used to immobilize proteins from solution. The

three aforementioned techniques differ from μPIP in that they do not use plasma-treatment, have not been shown to produce complex patterns, and in the case of Kim et al., was not used to pattern a wide range of substrates with various biomolecular inks.

4.5 Conclusions

μPIP *consistently and reproducibly* generates well resolved, high quality microscale patterns of biomolecules quickly (~ 8 minutes), cost-effectively, while producing little waste. As this technique does not depend on transfer from the PDMS stamp to the substrate, as in microcontact printing, the relative ink affinities for the PDMS stamp relative to the substrate no longer hampers successful patterning. Furthermore, because the PDMS stamp is not in contact with the substrate during ink immersion, issues regarding leakage, channel blockage or ink viscosity are not applicable. Simple and complex biomolecular patterns were generated, demonstrating the enhanced versatility of μPIP as compared to other techniques used to pattern biomolecular inks. Contact angle measurements and SEM results confirmed that substrates can be preferentially modified, both chemically and physically, simply by contact with a patterned PDMS stamp during plasma exposure. Following plasma-treatments, the substrates exhibited preferential adsorption of ink molecules such as poly-L-lysine, BSA and goat anti-rabbit IgG, to create micron-sized patterns that showed excellent stability after four weeks of incubation. The inherent simplicity of μPIP makes it an attractive and reliable alternative to other patterning methods currently used to micropattern biomolecules on organic substrates.

4.6 Acknowledgements

The author acknowledges the New Jersey Commission on Spinal Cord Research (03-3028-SCR-E-O) for financial support.

4.7 References

(1) Xia, Y.; Whitesides, G. M. *Angew. Chem. Int. Ed.* **1998**, *37*, 550-575.

(2) St. John, P. M.; Davis, R.; Cady, N.; Czajka, J.; Batt, C. A.; Craighead, H. G. *Anal. Chem.* **1998**, *70*, 1108-1111.

(3) Blawas, A. S.; Reichert, W. M. *Biomaterials* **1998**, *19*, 595-609.

(4) Orth, R. N.; Clark, T. G.; Craighead, H. G. *Biomedical Microdevices* **2003**, *5*, 29-34.

(5) Xu, C.; Taylor, P.; Ersoz, M.; Fletcher, P. D. I.; Paunov, V. N. *J. Mater. Chem.* **2003**, *13*, 3044-3048.

(6) Howell, S. W.; Inerowicz, H. D.; Regnier, F. E.; Reifenberger, R. *Langmuir* **2003**, *19*, 436-439.

(7) Schmalenberg, K. E.; Thompson, D. M.; Buettner, H. M.; Uhrich, K. E.; Garfias, L. F. *Langmuir* **2002**, *18*, 8593-8600.

(8) James, C. D.; Davis, R. C.; Kam, L.; Craighead, H. G.; Isaacson, M.; Turner, J. N.; Shain, W. *Langmuir* **1998**, *14*, 741-744.

(9) Bernard, A.; Renault, J. P.; Michel, B.; Bosshard, H. R.; Delamarche, E. *Adv. Mater.* **2000**, *12*, 1067-1070.

(10) Yang, Z.; Chilkoti, A. *Adv. Mater.* **2000**, *12*, 413-417.

(11) Tan, J. L.; Tien, J.; Chen, C. S. *Langmuir* **2002**, *18*, 519-523.

(12) Schmalenberg, K. E.; Buettner, H. M.; Uhrich, K. E. *Biomaterials* **2004**, *25*, 1851-1857.

(13) Delamarche, E.; Bernard, A.; Schmid, H.; Bietsch, A.; Michel, B.; Biebuyck, H. *J. Am. Chem. Soc.* **1998**, *120*, 500-508.

(14) Folch, A.; Toner, M. *Biotechnol. Prog.* **1998**, *14*, 388-392.

(15) Patel, N.; Sanders, G. H. W.; Shakesheff, K. M.; Cannizzaro, S. M.; Davies, M. C.; Langer, R.; Roberts, C. J.; Tendler, S. J. B.; Williams, P. M. *Langmuir* **1999**, *15*, 7252-7257.

(16) Papra, A.; Bernard, A.; Juncker, D.; Larsen, N. B.; Michel, B.; Delamarche, E. *Langmuir* **2001**, *17*, 4090-4095.

(17) Suh, K. Y.; Khademhosseini, A.; Yang, J. M.; Eng, G.; Langer, R. *Adv. Mater.* **2004**, *16*, 584-588.

(18) Pisignano, D.; Di Benedetto, F.; Persano, L.; Gigli, G.; Cingolani, R. *Langmuir* **2004**, *20*, 4802-4804.

(19) Feng, X.; Roberts, C. J.; Armitage, D. A.; Davies, M. C.; Tendler, S. J. B.; Allen, S.; Williams, P. M. *Analyst* **2001**, *126*, 1100-1104.

(20) Su, Y.-C.; Lin, L. In *12th International Conference on Solid-State Sensors, Actuators and Microsystems, Transducers '03*; Institute of Electrical and Electronics Engineers: Boston, MA, 2003; Vol. 2, pp 1812-1815.

(21) Khademhosseini, A.; Suh, K. Y.; Jon, S.; Eng, G.; Yeh, J.; Chen, G.; Langer, R. *Anal. Chem.* **2004**, *76*, 3675-3681.

(22) Liston, E. M. *J. Adhesion* **1989**, *30*, 199-218.

(23) Hegemann, D.; Brunner, H.; Oehr, C. *Nucl. Instr. and Meth. in Phys. Res. B* **2003**, *208*, 281-286.

(24) Weikart, C. M.; Yasuda, H. K. *J. Polym. Sci. A Polym. Chem.* **2000**, *38*, 3028-3042.

(25) Wheale, S. H.; Badyal, J. P. S. In *Interfacial Science*; Roberts, M. W., Ed.; Blackwell Science Ltd: Oxford, 1997; pp 237-255.

(26) Inagaki, N. *Plasma surface modification and plasma polymerization*; Technomic Publishing Co., Inc.: Lancaster, 1996.

(27) Langowski, B. A.; Uhrich, K. E. *Langmuir* **2005**, *21*, 6366-6372.

(28) Hettlich, H. J.; Otterbach, F.; Mittermayer, C.; Kaufmann, R.; Klee, D. *Biomaterials* **1991**, *12*, 521-524.

(29) Owen, M. J.; Smith, P. J. *J. Adhesion Sci. Technol.* **1994**, *8*, 1063-1075.

(30) Fritz, J. L.; Owen, M. J. *J. Adhesion* **1995**, *54*, 33-45.

(31) Hillborg, H.; Ankner, J. F.; Gedde, U. W.; Smith, G. D.; Yasuda, H. K.; Wikström, K. *Polymer* **2000**, *41*, 6851-6863.

(32) Hillborg, H.; Sandelin, M.; Gedde, U. W. *Polymer* **2001**, *42*, 7349-7362.

(33) Taylor, G. N.; Wolf, T. M. *Polym. Eng. Sci.* **1980**, *20*, 1087-1092.

(34) Lieberman, M. A.; Lichtenberg, A. J. *Principles of plasma discharges and materials processing*; John Wiley & Sons, Inc.: New York, 1994.

(35) Chan, C. M.; Ko, T. M.; Hiraoka, H. *Surf. Sci. Rep.* **1996**, *24*, 1-54.

(36) Kersten, H. In *Low temperature plasma physics*; Hippler, R.; Pfau, S.; Schmidt, M.; Schoenbach, K. H., Eds.; Wiley-VCH: Berlin, 2001; pp 113-130.

(37) Collaud Coen, M.; Lehmann, R.; Groening, P.; Schlapbach, L. *Appl. Surf. Sci.* **2003**, *207*, 276-286.

(38) Lhoest, J.-B.; Detrait, E.; Dewez, J.-L.; van den Bosch de Aguilar, P. *J. Biomater. Sci. Polymer Edn.* **1996**, *7*, 1039-1054.

(39) Goessl, A.; Garrison, M. D.; Lhoest, J.-B.; Hoffman, A. S. *J. Biomater. Sci. Polymer Edn.* **2001**, *12*, 721-738.

(40) Hozumi, A.; Saito, T.; Shirahata, N.; Yokogawa, Y.; Kameyama, T. *J. Vac. Sci. Technol. A* **2004**, *22*, 1836-1841.

(41) Kim, H.-C.; Wallraff, G.; Kreller, C. R.; Angelos, S.; Lee, V. Y.; Volksen, W.; Miller, R. D. *Nano Lett.* **2004**, *4*, 1169-1174.

(42) McCarley, R. L.; Vaidya, B.; Wei, S.; Smith, A. F.; Patel, A. B.; Feng, J.; Murphy, M. C.; Soper, S. A. *J. Am. Chem. Soc.* **2005**, *127*, 842-843.

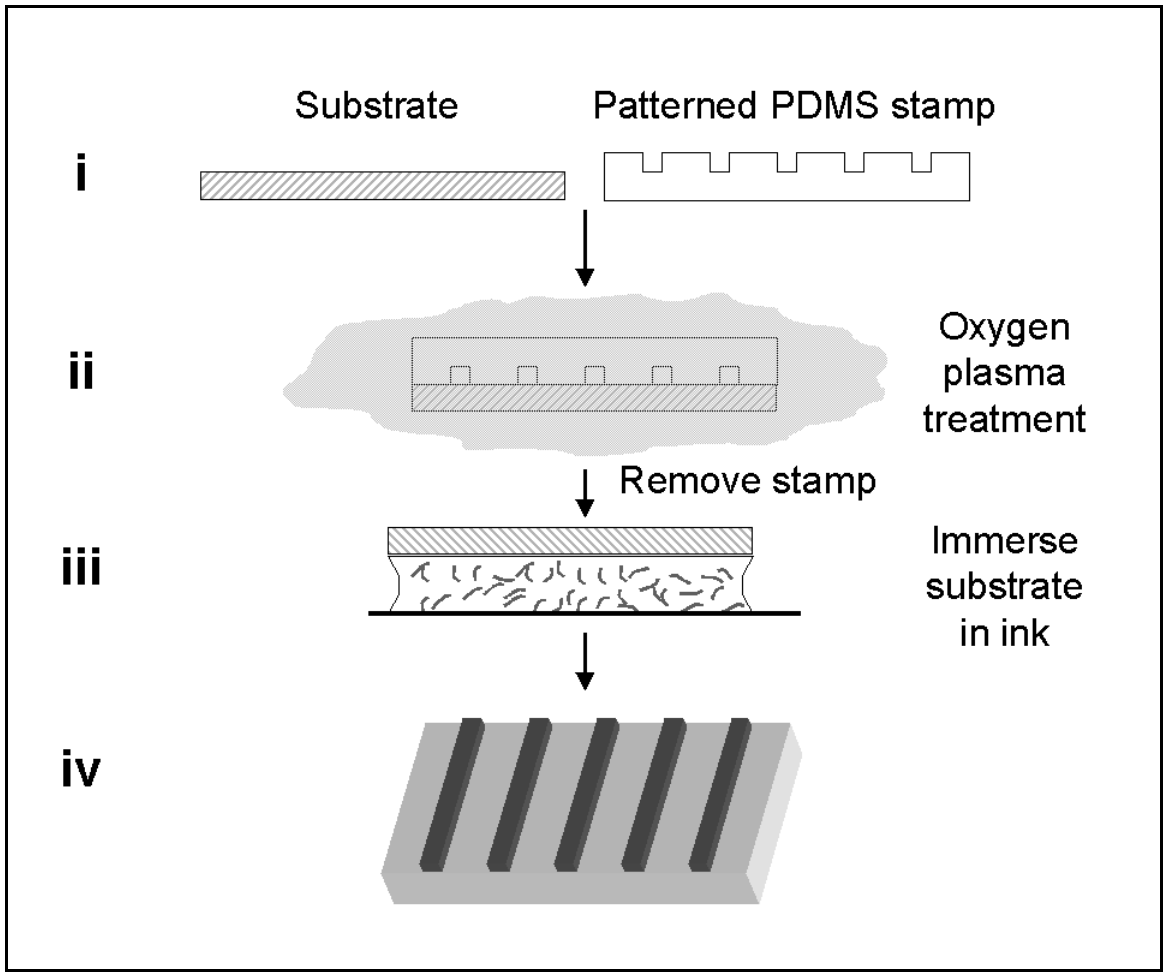

Figure 4-1: Schematic of patterning procedure used to generate simple biomolecular micropatterns.

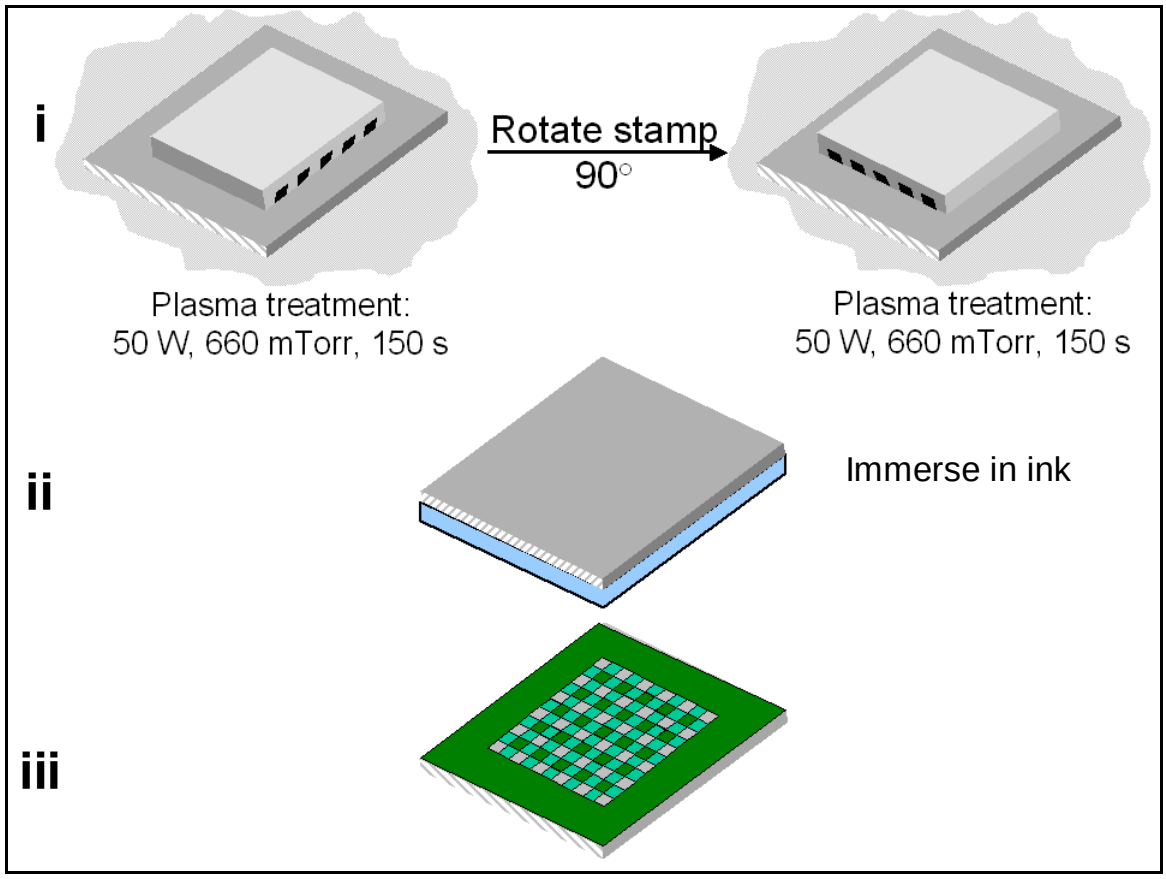

Figure 4-2: Schematic of patterning procedure used to generate complex biomolecular micropatterns.

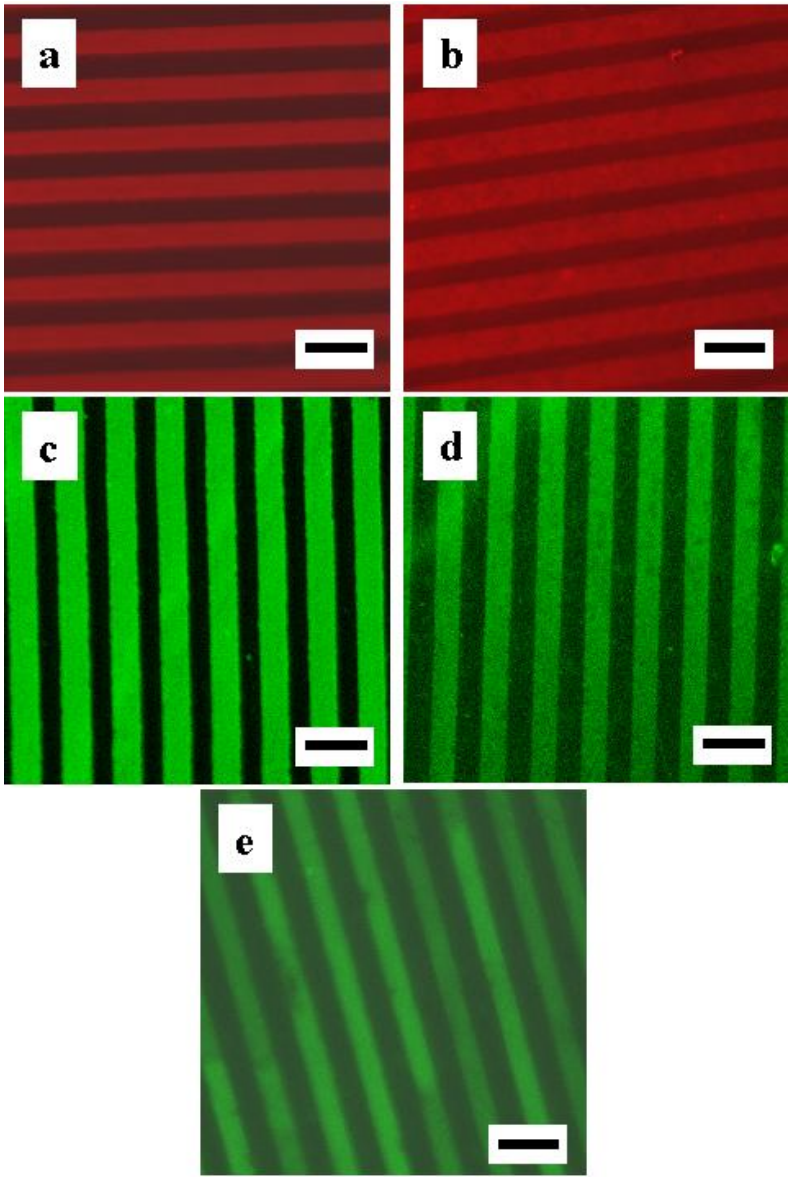

Figure 4-3: Fluorescent micrographs of simple patterns generated by the method outlined in Figure 4-1: (a) BSA on PDMS, (b) BSA on PHBV, (c) poly-L-lysine on PMMA, (d) poly-L-lysine on PE, and (e) α-rabbit IgG on PS. Scale bars indicate 50 μm.

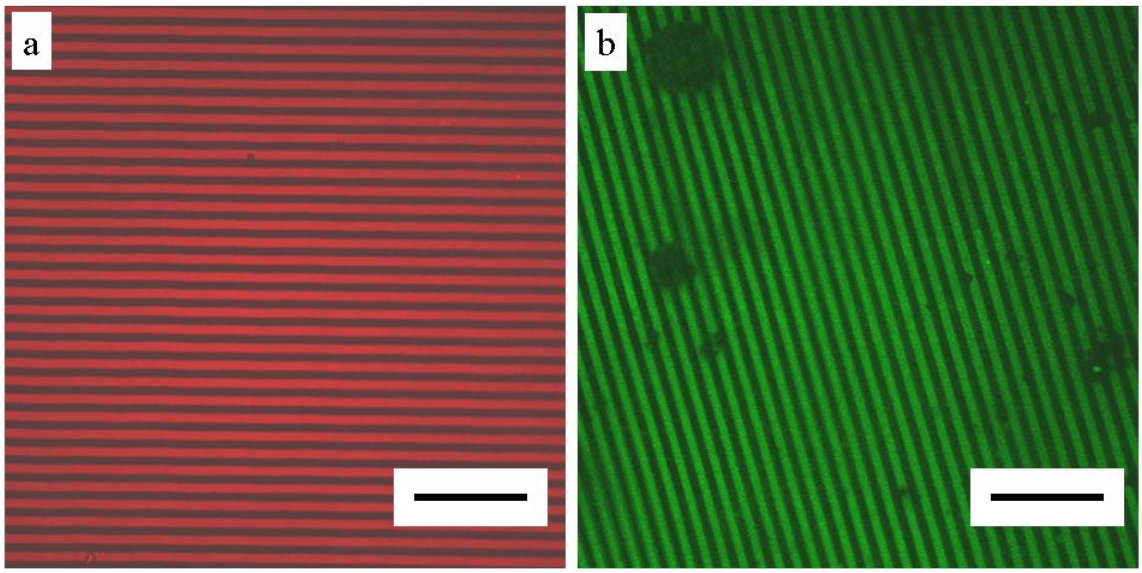

Figure 4-4: Fluorescent micrograph illustrating extent of pattern formation by the method outlined in Figure 4-1: (a) BSA on PS and (b) α-rabbit IgG on PS. Scale bars indicate 250 μm.

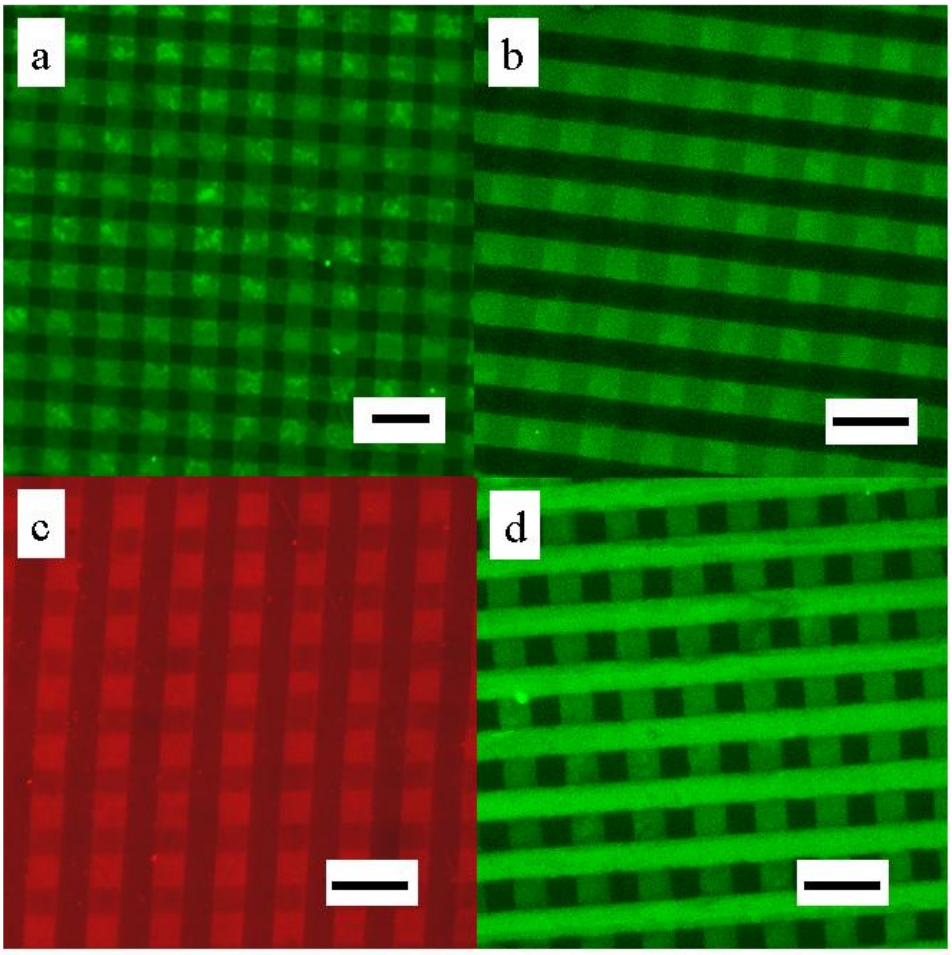

Figure 4-5: Fluorescent micrographs of complex patterns generated by the method outlined in Figure 4-2: (a) poly-L-lysine on PMMA, (b) α-rabbit IgG on PDMS, (c) BSA on PS, and (d) poly-L-lysine on PDMS. Scale bars indicate 50 μm.

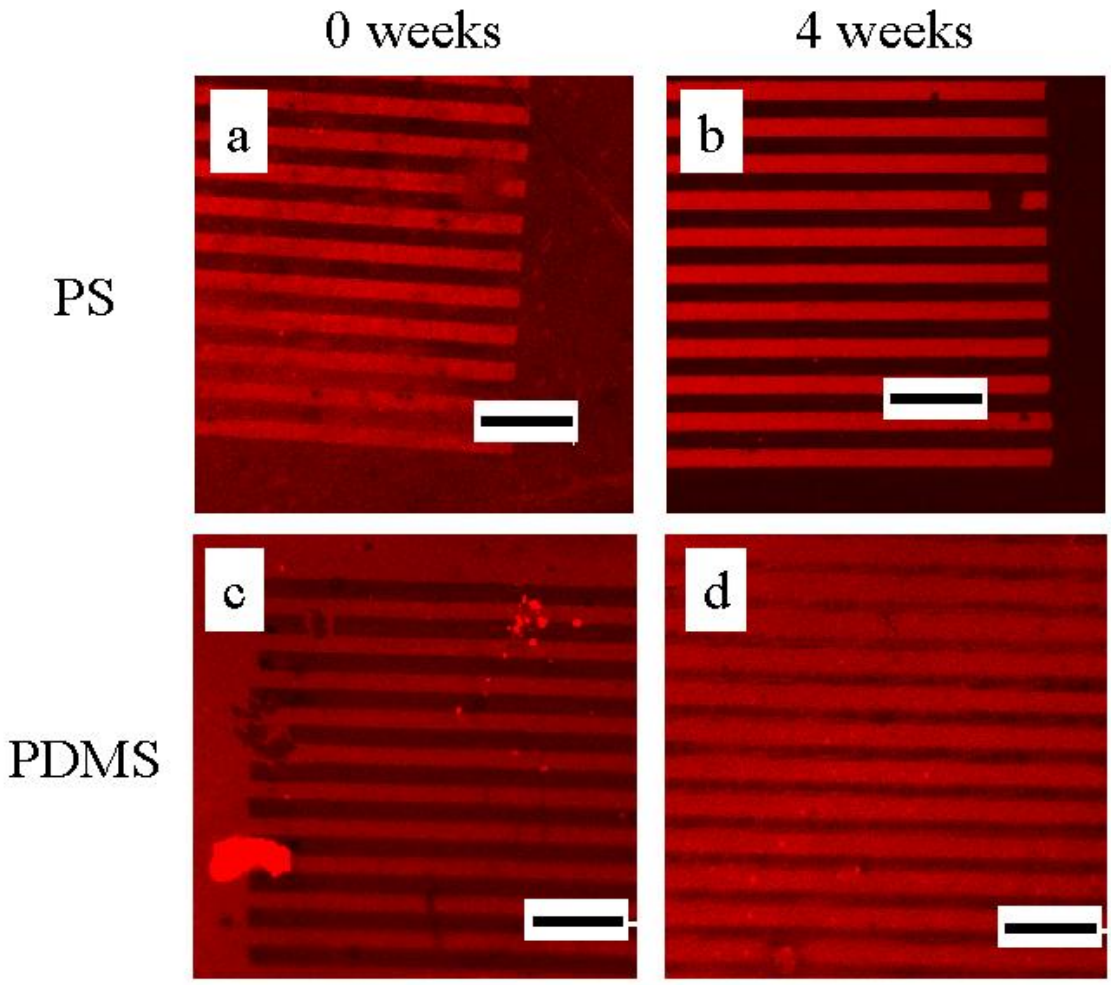

Figure 4-6: Fluorescent micrographs of BSA patterns on PS (*a* & *b*) and PDMS (*c* & *d*). Images *a* and *c* were taken immediately after patterning, whereas images *b* and *d* were taken following four weeks of storage in PBS at 37 °C. Images *a* and *b* are from the same area on the same sample, whereas images *c* and *d* are from different areas on the same sample. Scale bars indicate 100 μm.

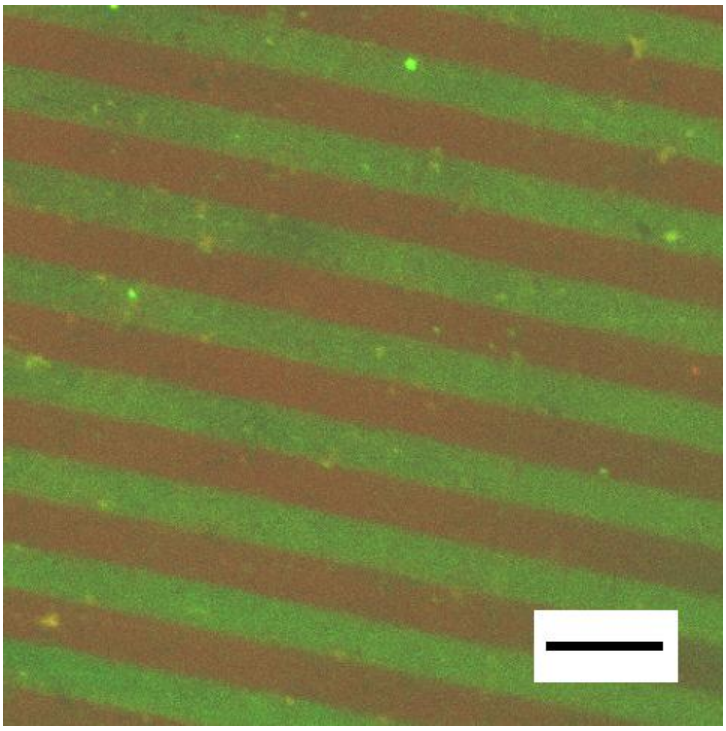

Figure 4-7: Fluorescent micrograph of PMMA patterned with poly-L-lysine (green) and BSA (red) by immersion in a mixture of both inks. Scale bar indicates 50 μm.

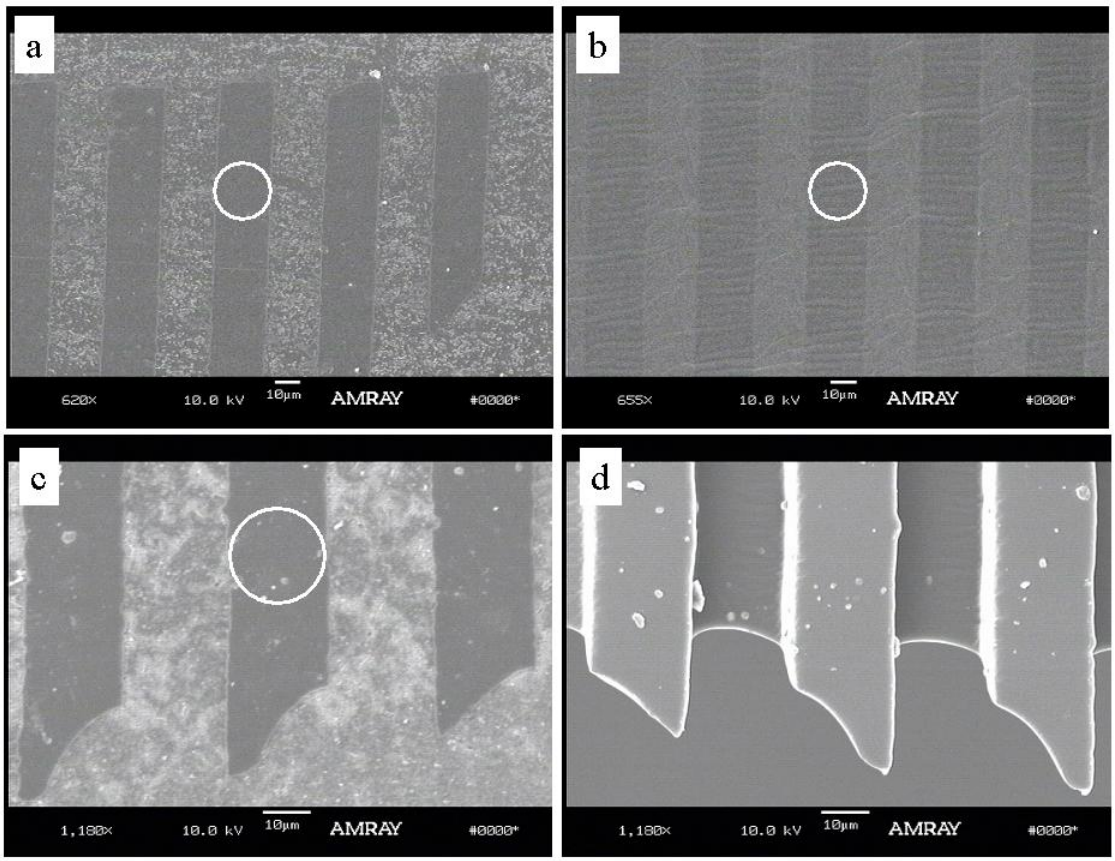

Figure 4-8: SEM micrographs of various substrates following exposure to oxygen plasma while in contact with a patterned PDMS stamp: (a) PMMA (620 ×), (b) PDMS (655 ×), and (c) PHBV (1180 ×). Encircled regions denote areas that were protected from plasma. SEM micrograph (d) of the patterned PDMS stamp (1180 ×) in contact with PHBV (c) during oxygen plasma-treatment.

	Plasma treated *Protected*	**Plasma treated** *Exposed*	**Differential**
PDMS	111.4 ± 3.7°	35.4 ± 5.4°	76.0°
PMMA	83.4 ± 9.8°	38.8 ± 4.4°	44.6°
PS	91.0 ± 4.2°	21.0 ± 2.1°	70.0°
PE	81.1 ± 9.8°	45.0 ± 2.6°	36.1°
PHBV	81.5 ± 2.8°	31.4 ± 2.8°	50.1°

Table 4-1: Water contact angles (deg) of polymer substrates after oxygen plasma-treatment (50 W, 660 mTorr, 300 s): protected vs. exposed.

CHAPTER 5: BIOACTIVITY EVALUATION OF μPIP-GENERATED LAMININ MICROPATTERNS TO DIRECT NEURAL STEM CELL ATTACHMENT AND OUTGROWTH

5.1 Abstract

Microscale plasma-initiated patterning (μPIP) was used to create laminin stripes on glass and poly(methyl methacrylate) (PMMA) substrates for directed nerve cell growth. Pattern bioactivity (i.e., the ability to direct cell attachment and activities) was evaluated by the response of neural stem cells (NL2.3) to laminin micropatterns on glass and polymer substrates. Cell attachment only occurred when laminin was present on the substrate surfaces, indicating that cell attachment was independent of the underlying substrate topology. Although cell attachment occurred on laminin monolayers, *directed* attachment, outgrowth, and cellular process extension was *not observed* on these monolayered surfaces. Cells attached onto laminin micropatterned substrates exhibited significant directionality in process extension and outgrowth. The morphology of the NL2.3 cells further indicated that the laminin was bioactive following μPIP pattern formation. In addition, lower laminin ink concentration resulted in decreased cellular attachment and poor cell morphology.

5.2 Introduction

Several methods currently exist to micropattern biomolecules[1-7] for use in biological and medical applications including biosensors, DNA microarrays, immunoassays, and tissue engineering.[1-3,6-13] In tissue engineering, biomolecular micropatterns are commonly used

to control the placement and function of several cell types[2,4,12,14,15] with the potential to aid in the functional restoration of damaged tissues and organs.[12,14,16-21] For example, the ability of biomolecular micropatterns to direct cell attachment and outgrowth may be critical to the restoration of cellular function[4,14,16,19,20,22-25] and, in the case of nerve regeneration, aid in the design of nerve guides to replace or enhance current nerve injury treatments.[5,19,26,27] Laminin, an extracellular matrix protein well known as a ligand for cell adhesion molecules that promote axonal and neurite outgrowth, is a popular candidate for micropatterns on organic and inorganic substrates.[16-18,20-25,28-31] In addition to nerve cells, laminin micropatterns have been used to control the behavior of multiple cell types.[16-25,27,29,32] As denaturation and conformational changes may adversely affect biomolecular function,[1,33-35] retention of bioactivity is imperative in biomolecular micropatterning. As such, it is crucial that the biological function of micropatterns formed by newly emerging patterning techniques is appropriately evaluated.

Microscale plasma-initiated patterning (μPIP) is a recently developed technique[36] that uses a patterned PDMS stamp to selectively expose or protect underlying substrate regions from the chemical and physical effects of gaseous plasma exposure, thereby, forming distinct microscale domains with relatively different hydrophilicities on the substrate surface. These chemically different areas exhibit distinct differential affinities for biomolecules, allowing microscale pattern formation based on the preferential adsorption of ink molecules onto either the plasma-exposed or plasma-protected regions of a substrate. Because pattern formation relies on the biomolecule adsorption from solution, and not on molecule-transfer from a PDMS stamp to substrate, μPIP does not

suffer from the drawbacks of inadequate ink transfer and inhomogeneous micropattern formation commonly experienced with microcontact printing.[37] Furthermore, micropattern-generation via μPIP is quick (~ 6 min), requires only small volumes of biomolecule-based ink, is cost-effective, and is technically easy to perform. Taken together, these attributes make μPIP an attractive alternative to some of the better-established methods currently used for biomolecular micropatterning.

Although μPIP has been used to pattern a wide range of biologically relevant inks onto different polymer substrates,[36] it has not yet been applied to an inorganic substrate such as glass. More importantly, the bioactivity of micropatterns generated by μPIP has not been demonstrated. In this study, μPIP was used to form laminin stripes on glass and poly(methyl methacrylate) (PMMA). The laminin-micropatterned surfaces were then seeded with NL2.3 cells to determine if laminin retained its bioactivity based on the micropatterns' ability to spatially control nerve cell attachment and outgrowth. NL2.3 cells are derived from radial glial/neural stem cell clones L2.3 by over expressing the activated form of Notch protein.[38,39] Notch signaling has been shown to promote radial glial phenotype in rodent forebrain during development.[40] The enhanced radial glial phenotypes of NL2.3 cells, including their elongated bipolar radial morphology and adhesive cell membrane properties, make them an excellent candidate cell type for facilitating neuronal regeneration in spinal cord injury[39] and suitable for evaluating cell behavior on the laminin-micropatterned substrates. In addition, this chapter demonstrates the impact of ink concentration on pattern formation during μPIP and the resulting cellular response.

5.3 Materials and Methods

5.3.1 Materials

Sheets of PMMA were obtained from Goodfellow (Huntingdon, England) and cut into squares (1 cm^2) using a razor blade. Circular microscope cover glasses (12 mm diameter) were purchased from Fisher Scientific (Pittsburgh, PA). All substrates were rinsed with HPLC-grade ethanol (Sigma-Aldrich, St. Louis, MO) prior to patterning. Laminin from Engelbreth-Holm-Swarm murine sarcoma (Sigma) was serially diluted with phosphate buffered saline (PBS, pH 7.4, MP Biomedicals, Aurora, OH) to concentrations of 100, 50, 10, and 1 μg/mL, and used immediately after preparation.

5.3.2 Patterned PDMS Stamps

PDMS stamps were prepared by pouring Sylgard 184 silicone elastomer kit (Dow Corning, Midland, MI; 10:1 w/w base to crosslinker) over lithographically created masters, previously described in detail.[32] In brief, masters were created by exposing photoresist-coated silicon wafers through a photomask producing a relief pattern on the silicon surface. The relief pattern consists of a series of raised, parallel lanes (20 μm wide) separated by 20 μm spaces, over which the silicone elastomer was poured. Upon curing, the PDMS was peeled off the master, and the patterned regions were cut using a razor blade into stamps (8 mm × 8 mm).

5.3.3 Micropattern Formation

Glass and PMMA substrates were patterned with laminin using the procedure outlined in previous chapters (Figure 4-1). The patterned PDMS stamp, consisting of parallel lanes (20 μm) separated by 20 μm spaces, was placed into contact with the substrate, and the entire unit exposed to oxygen plasma (March Plasma, Concord, CA) for 300 s at 300 W and 660 mTorr (Figure 4-1-ii). Once plasma-treated, the stamp was removed and the substrate immersed, treated side down, in 50 μL of laminin solution for 5 s at room temperature (Figure 4-1-iii). Following immersion, the substrates were gently swirled in a beaker of PBS (~ 20 mL) for approximately 20 s to remove weakly adhered laminin.

5.3.4 Pattern Imaging by Fluorescence Microscopy

An aliquot of laminin (starting concentration of 1.2 mg/mL) was conjugated with rhodamine red using a FluoReporter Rhodamine Red -X Protein Labeling Kit (Invitrogen, Carlsbad, CA) following the conjugation protocol provided with the kit. Using the rhodamine-conjugated laminin, micropatterns on glass and PMMA were formed following the procedure outlined in Figure 4-1. The rhodamine-labeled laminin was only used to confirm pattern formation on the glass and PMMA substrates. Fluorescence imaging was performed with an Axiovert 200 deconvolution microscope (Zeiss, Thornwood, NY); the absorption and emission wavelengths for rhodamine red are 580 and 590 nm, respectively.

5.3.5 Cell Culture

Generation and culturing conditions of radial glial clones L2.3 have been previously described[38] and used for the NL2.3 clones. Briefly, the serum-free culture medium contained DMEM/F12 (Invitrogen, Carlsbad, CA) and was supplemented with 25 mM glucose (Sigma), 2 mM glutamine (Invitrogen), penicillin/streptomycin (Invitrogen), 10 ng/ml FGF2 (BD Biosciences, San Jose, CA), 2 μg/ml heparin (Sigma) and 1x B27 (Invitrogen). Cells were propagated as neurospheres and passaged by mild trypsinization (Invitrogen, 0.025 % for 5 min at 37 °C) every 3 days.

5.3.6 Evaluation of Micropattern Bioactivity and Ink Concentration by Cell Response

Glass and PMMA substrates were patterned with laminin following the procedure outlined in Figure 4-1 using four different laminin concentrations: 100, 50, 10 and 1 μg/mL. The micropatterned substrates were then transferred to a 24-well tissue culture plate (BD Falcon, Franklin Lakes, NJ) and seeded with NL2.3 cells ($4x10^4$ cells/well). Cells were incubated overnight at 37 °C and 10 % CO_2 in serum-free medium. The substrates were imaged approximately 12-18 h after seeding with phase contrast microscopy (described below). The response of cells on laminin-patterned substrates was compared with cell responses to bare substrates (i.e., laminin-free substrates), as well as substrates completely coated with a laminin monolayer. Laminin monolayers were formed by exposing uncovered substrates (i.e., substrates *not* in contact with a PDMS stamp) to oxygen plasma (300 W, 300 s, 660 mTorr) and immersing them in 50 μL laminin solution (100 μg/mL) for 5 s, followed by a rinse in PBS for 20 s.

5.3.7 Cell Imaging by Phase Contrast Microscopy

Representative fields were digitally captured from each culture using a phase contrast microscope (Nikon Diaphot, Diagnostic Instruments, Sterling Heights, MI) and a digital Spot camera. Time-lapse images on live cultures showing NL2.3 responses to laminin micropatterns on glass were taken with a Zeiss Axiovert 200 deconvolution microscope every 10 min for a total of 140 min. Attached cells were kept at 37 °C and 10 % CO_2 in serum-free medium during all imaging experiments.

5.4 Results and Discussion

Although μPIP has been shown to be a consistent, reliable method for generating well-defined, stable biomolecular micropatterns on polymeric substrates,[36] the utility of these patterns to elicit biological responses from cells has not been clarified. The quality of the laminin micropatterns was confirmed using rhodamine-conjugated laminin on PMMA and glass substrates (Figure 5-1). The striped laminin patterns (shown in red) were well resolved from the underlying substrate (shown as black), exhibited uniform laminin distribution throughout, and maintained lateral dimensions in good agreement with the PDMS stamp features (20 μm stripes, 20 μm spaces). As the diameters of NL2.3 cells are approximately 10 μm, the 20 μm/20 μm pattern dimensions were chosen to provide ample, but not excessive, regions for cell attachment. Laminin patterns on PMMA substrates (data not shown) were of comparable quality to glass substrates.

5.4.1 Cell Response to Laminin Stripes

To evaluate the bioactivity of laminin stripes formed by μPIP, NL2.3 cells were seeded onto bare substrates with no laminin on the surface, substrates coated with a monolayer of laminin (Figure 5-2a & 5-2c), and substrates micropatterned with laminin stripes (Figure 5-2b & 5-2d). Cell attachment did not occur on bare glass and bare PMMA, and cells were observed floating in the surrounding media. In addition, the cells did not exhibit flattened cell bodies or extended processes. Glass (Figure 5-2a) and PMMA (Figure 5-2c) substrates coated with laminin monolayers showed significant cellular attachment, illustrating the necessity of laminin for attachment of this special cell line. Based on our previous experiences,[39] NL2.3 cells are sensitive to the underlying surface environment of the culturing substrate and will not strongly attach to or significantly proliferate on protein-free substrates. Figures 5-2a and 5-2c exhibit cell flattening and process extension; both are positive morphological responses for this cell line and indicate suitable surface environments.[39,41] Because laminin is imperative for attachment of NL 2.3 cells onto a substrate, this cell line is an appropriate biological indicator for the presence of laminin. Although cells attached to and proliferated on the continuous laminin layers (Figure 5-2a & 5-2c), they did not exhibit directed orientation, process extension or motility. In contrast, cellular response to laminin micropatterns on glass (Figure 5-2b) and PMMA (Figure 5-2d) substrates showed striking directionality in cell body attachment, process alignment (Figure 5-3) and motility (Figure 5-4). These results clearly indicate that laminin is not significantly denatured during the μPIP process and

remains bioactive, further demonstrating μPIP as a reliable method for generating biologically relevant micropatterns.

5.4.2 Impact of Ink Concentration on Cell Response

The results outlined in Figures 5-2 through 5-4 utilized laminin micropatterns created using an ink concentration of 100 μg/mL. To assess the impact of ink concentration on pattern quality and cellular response, laminin micropatterns on glass and PMMA substrates were generated at four different laminin ink concentrations: 100, 50, 10, and 1 μg/mL. Figure 5-5 shows representative images for micropatterns generated from various laminin ink concentrations: 100 μg/mL (Figure 5-5a & 5-5e), 50 μg/mL (Figure 5-5b & 5-5f), 10 μg/mL (Figure 5-5c & 5-5g) and 1 μg/mL (Figure 5-5d & 5-5h). Within a given substrate type, manual cell counts revealed that more cells attached to substrates patterned at either 100 or 50 μg/mL compared to 10 or 1 μg/mL. However, no appreciable differences in cell number were noted between 100 and 50 μg/mL or between 10 and 1 μg/mL. Both 100 and 50 μg/mL laminin solutions produced patterns of sufficient concentrations of adsorbed laminin.

In addition to decreased cell attachment, substrates with 10 and 1 μg/mL laminin ink concentrations also displayed different cell morphologies. Figure 5-6 compares glass substrates micropatterned with laminin solutions at various concentrations, where cell bodies and cell processes are respectively indicated by circles and arrows. At higher concentrations (Figure 5-6a & b), the attached cells displayed numerous processes that

were significantly longer than cells on lower-concentration substrates (Figure 5-6c & d). Although low concentration laminin inks produced patterns with sufficient localized laminin to support *some* cell attachment, insufficient laminin is present to promote normal process extension. As illustrated in Figures 5-5 and 5-6, ink concentration is an important, controllable parameter of μPIP that significantly impacts cell attachment and morphology.

5.5 Conclusions

The bioactivity of laminin micropatterns generated by μPIP was evaluated by NL2.3 cell response. As cell attachment occurred only when laminin was present on the substrate surfaces, this cell line was appropriate as a biological indicator for laminin bioactivity following micropatterning. Although cell attachment was observed on laminin monolayers, *directed* attachment, outgrowth, and cellular process extension was *not observed*. In contrast, cells attached to laminin micropatterns exhibited significant directionality in process extension and outgrowth, and appropriate cell morphology. Lower concentrations of the laminin ink resulted in decreased cellular attachment and decreased process extension, confirming that ink concentration is an important controllable variable in μPIP. The results presented herein illustrate the ease and time efficiency (~ 6 min) by which bioactive biomolecular micropatterns can be generated by μPIP, demonstrating the method as a reliable approach to create bioactive micropatterns multiple substrates.

5.6 Acknowledgements

The author acknowledges Dr. Hedong Li (W.M. Keck Center for Collaborative Neuroscience, Rutgers University) for performing the cell studies (culturing and seeding), the New Jersey Commission on Spinal Cord Research (03-3028-SCR-E-O) and NIH (DE 13205) for financial support, and Chris Ricupero for supplying the rhodamine red-conjugated laminin.

5.7 References

(1) Blawas, A. S.; Reichert, W. M. *Biomaterials* **1998**, *19*, 595-609.

(2) Folch, A.; Toner, M. *Biotechnol. Prog.* **1998**, *14*, 388-392.

(3) Xia, Y.; Whitesides, G. M. *Angew. Chem. Int. Ed.* **1998**, *37*, 550-575.

(4) Ito, Y. *Biomaterials* **1999**, *20*, 2333-2342.

(5) Corey, J. M.; Feldman, E. L. *Experimental Neurology* **2003**, *184*, S89-S96.

(6) Park, T. H.; Shuler, M. L. *Biotechnol. Prog.* **2003**, *19*, 243-253.

(7) Falconnet, D.; Csucs, G.; Grandin, H. M.; Textor, M. *Biomaterials* **2006**, *27*, 3044-3063.

(8) St. John, P. M.; Davis, R.; Cady, N.; Czajka, J.; Batt, C. A.; Craighead, H. G. *Anal. Chem.* **1998**, *70*, 1108-1111.

(9) Orth, R. N.; Clark, T. G.; Craighead, H. G. *Biomedical Microdevices* **2003**, *5*, 29-34.

(10) Xu, C.; Taylor, P.; Ersoz, M.; Fletcher, P. D. I.; Paunov, V. N. *J. Mater. Chem.* **2003**, *13*, 3044-3048.

(11) Howell, S. W.; Inerowicz, H. D.; Regnier, F. E.; Reifenberger, R. *Langmuir* **2003**, *19*, 436-439.

(12) Desai, T. A. *Med. Eng. Phys.* **2000**, *22*, 595-606.

(13) Delamarche, E.; Bernard, A.; Schmid, H.; Bietsch, A.; Michel, B.; Biebuyck, H. *J. Am. Chem. Soc.* **1998**, *120*, 500-508.

(14) Smith, J. T.; Tomfohr, J. K.; Wells, M. C.; Beebe, J., T. P.; Kepler, T. B.; Reichert, W. M. *Langmuir* **2004**, *20*, 8279-8286.

(15) Chen, G.; Ito, Y. *Biomaterials* **2001**, *22*, 2453-2457.

(16) Tai, H.; Buettner, H. M. *Biotechnol. Prog.* **1998**, *14*, 364-370.

(17) Recknor, J. B.; Recknor, J. C.; Sakaguchi, D. S.; Mallapragada, S. K. *Biomaterials* **2004**, *25*, 2753-2767.

(18) McDevitt, T. C.; Woodhouse, K. A.; Hauschka, S. D.; Murry, C. E.; Stayton, P. S. *J. Biomed. Mater. Res.* **2003**, *66A*, 586-595.

(19) Recknor, J. B.; Sakaguchi, D. S.; Mallapragada, S. K. *Biomaterials* **2006**, *27*, 4098-4108.

(20) Schmalenberg, K. E.; Uhrich, K. E. *Biomaterials* **2005**, *26*, 1423-1430.

(21) Lam, M. T.; Sim, S.; Zhu, X.; Takayama, S. *Biomaterials* **2006**, *27*, 4340-4347.

(22) Li, B.; Ma, Y.; Wang, S.; Moran, P. M. *Biomaterials* **2005**, *26*, 1487-1495.

(23) Kam, L.; Shain, W.; Turner, J. N.; Bizios, R. *Biomaterials* **2001**, *22*, 1049-1054.

(24) Clark, P.; Dunn, G. A.; Knibbs, A.; Peckham, M. *Int. J. Biochem. Cell Biol.* **2002**, *34*, 816-825.

(25) Turcu, F.; Tratsk-Nitz, K.; Thanos, S.; Schuhmann, W.; Heiduschka, P. *J. Neurosci. Methods* **2003**, *131*, 141-148.

(26) Kannan, R. Y.; Salacinski, H. J.; Butler, P. E. M.; Seifalian, A. M. *Biotechnol. Appl. Biochem.* **2005**, *41*, 193-200.

(27) Vogt, A. K.; Lauer, L.; Knoll, W.; Offenhäusser, A. *Biotechnol. Prog.* **2003**, *19*, 1562-1568.

(28) Sgarbi, N.; Pisignano, D.; Di Benedetto, F.; Gigli, G.; Cingolani, R.; Rinaldi, R. *Biomaterials* **2004**, *25*, 1349-1353.

(29) McDevitt, T. C.; Angello, J. C.; Whitney, M. L.; Reinecke, H.; Hauschka, S. D.; Murry, C. E.; Stayton, P. S. *J. Biomed. Mater. Res.* **2002**, *60*, 472-479.

(30) Schmalenberg, K. E.; Thompson, D. M.; Buettner, H. M.; Uhrich, K. E.; Garfias, L. F. *Langmuir* **2002**, *18*, 8593-8600.

(31) Song, H. K.; Toste, B.; Ahmann, K.; Hoffman-Kim, D.; Palmore, G. T. R. *Biomaterials* **2006**, *27*, 473-484.

(32) Schmalenberg, K. E.; Buettner, H. M.; Uhrich, K. E. *Biomaterials* **2004**, *25*, 1851-1857.

(33) Mrksich, M. *Chem. Soc. Rev.* **2000**, *29*, 267-273.

(34) Mrksich, M.; Whitesides, G. M. *Annu. Rev. Biophys. Biomol. Struct.* **1996**, *25*, 55-78.

(35) Biasco, A.; Pisignano, D.; Krebs, B.; Pompa, P. P.; Persano, L.; Cingolani, R.; Rinaldi, R. *Langmuir* **2005**, *21*, 5154-5158.

(36) Langowski, B. A.; Uhrich, K. E. *Langmuir* **2005**, *21*, 10509-10514.

(37) Tan, J. L.; Tien, J.; Chen, C. S. *Langmuir* **2002**, *18*, 519-523.

(38) Li, H.; Babiarz, J.; Woodbury, J.; Kane-Goldsmith, N.; Grumet, M. *Dev. Biol.* **2004**, *271*, 225-238.

(39) Grumet, M.; Chang, Y.; Ricupero, C. L.; Mohan, K.; Su, Y.; Gaiano, N. R.; Hart, R. P.; Li, H. In *Neuroscience 2006*; Society for Neuroscience: Atlanta, GA, 2006.

(40) Gaiano, N. R.; Nye, J. S.; Fishell, G. *Neuron* **2000**, *26*, 395-404.

(41) Li, H.; Berlin, Y.; Hart, R. P.; Grumet, M. *Glia* **2003**, *44*, 37-46.

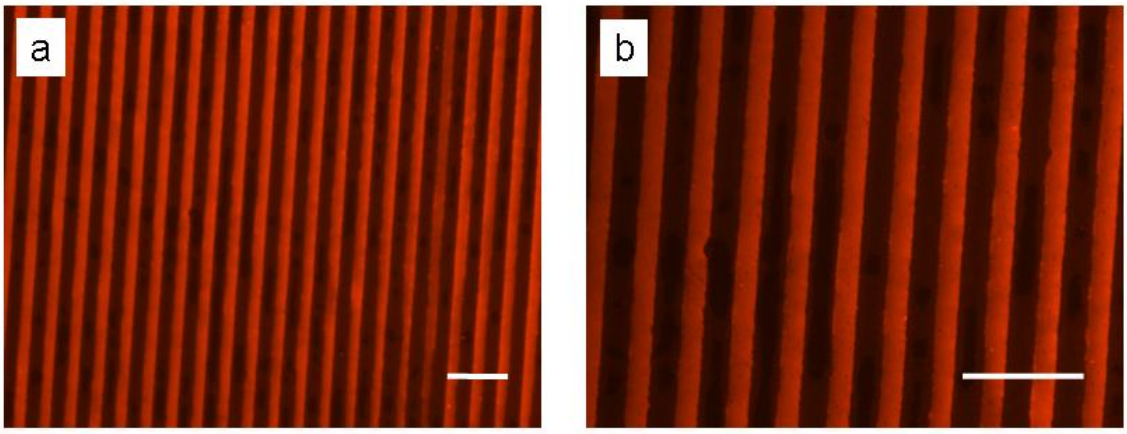

Figure 5-1: Fluorescent micrographs of rhodamine red-conjugated laminin micropatterns on glass generated by μPIP: (a) 10 × magnification and (b) 20 × magnification. Scale bars indicate 100 μm.

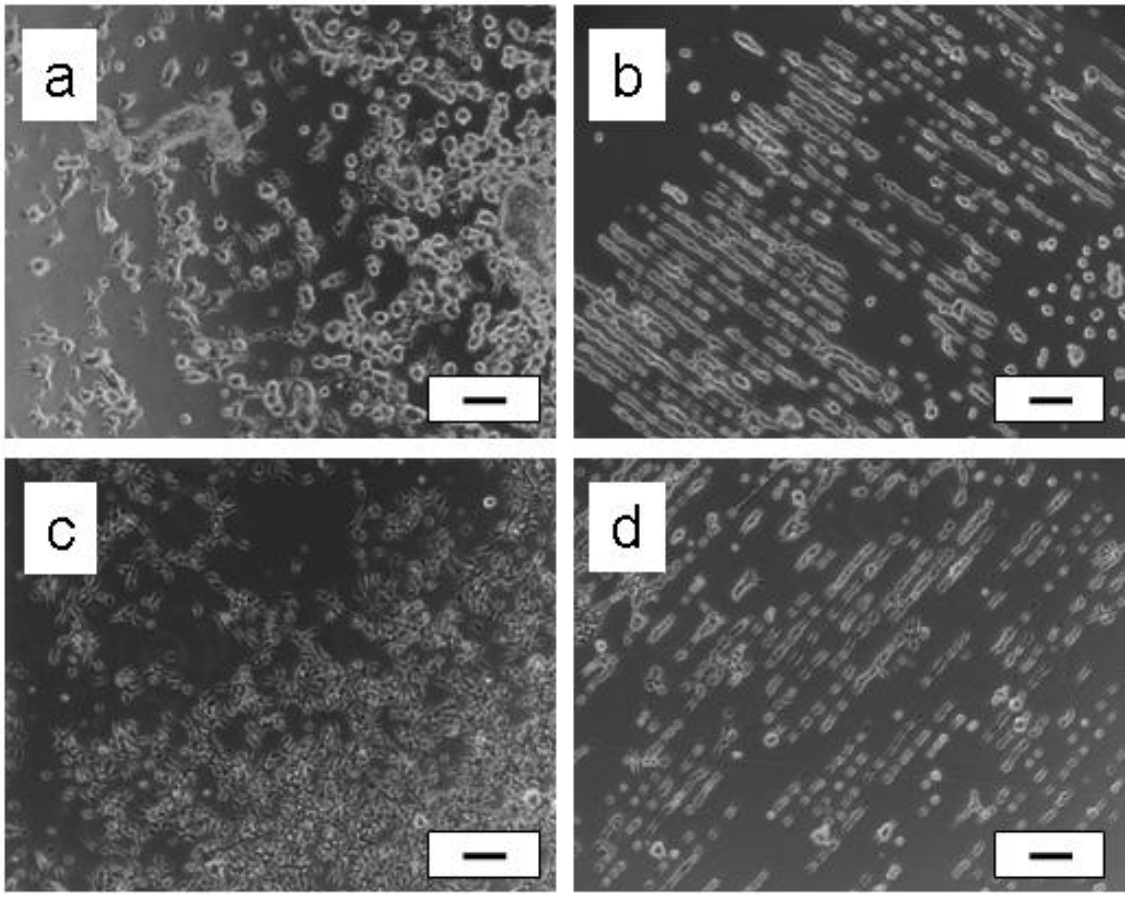

Figure 5-2: Phase contrast micrographs of NL2.3 cellular response to: (a) glass covered with laminin monolayer, (b) laminin-micropatterned glass, (c) PMMA covered with laminin monolayer, and (d) laminin-micropatterned PMMA. Scale bars indicate 100 μm.

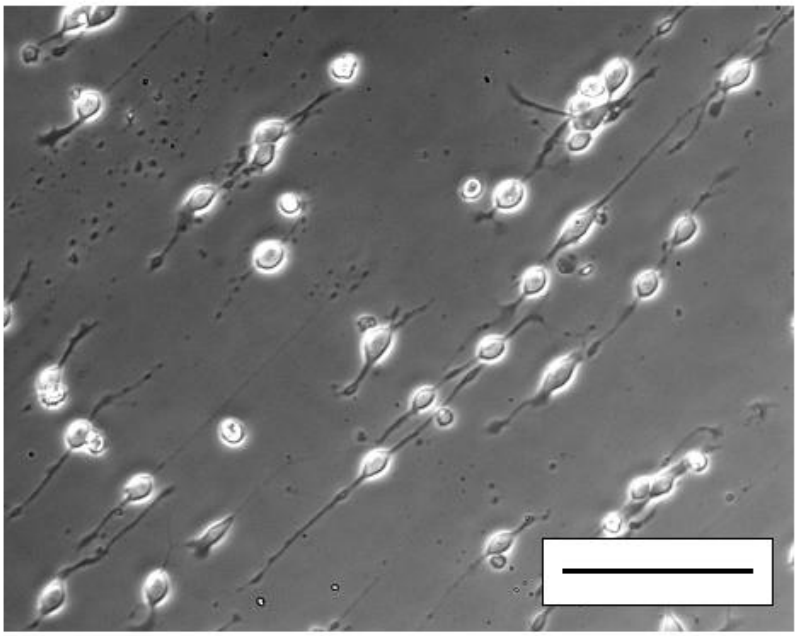

Figure 5-3: Phase contrast micrograph of NL2.3 cellular alignment and morphology on laminin-micropatterned glass. Scale bar indicates 100 μm.

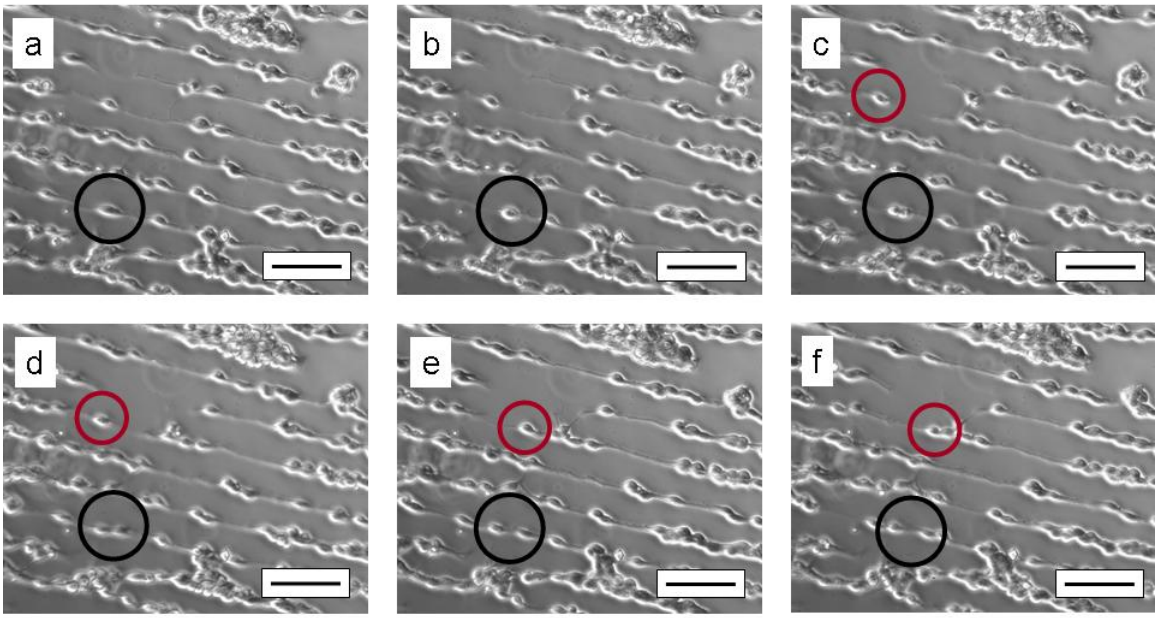

Figure 5-4: Time lapse phase contrast micrographs of NL2.3 cell behavior on laminin-micropatterned glass. The black encircled areas show evidence of cell division in progress and the red encircled areas show directed cell motility. Scale bars indicate 100 μm.

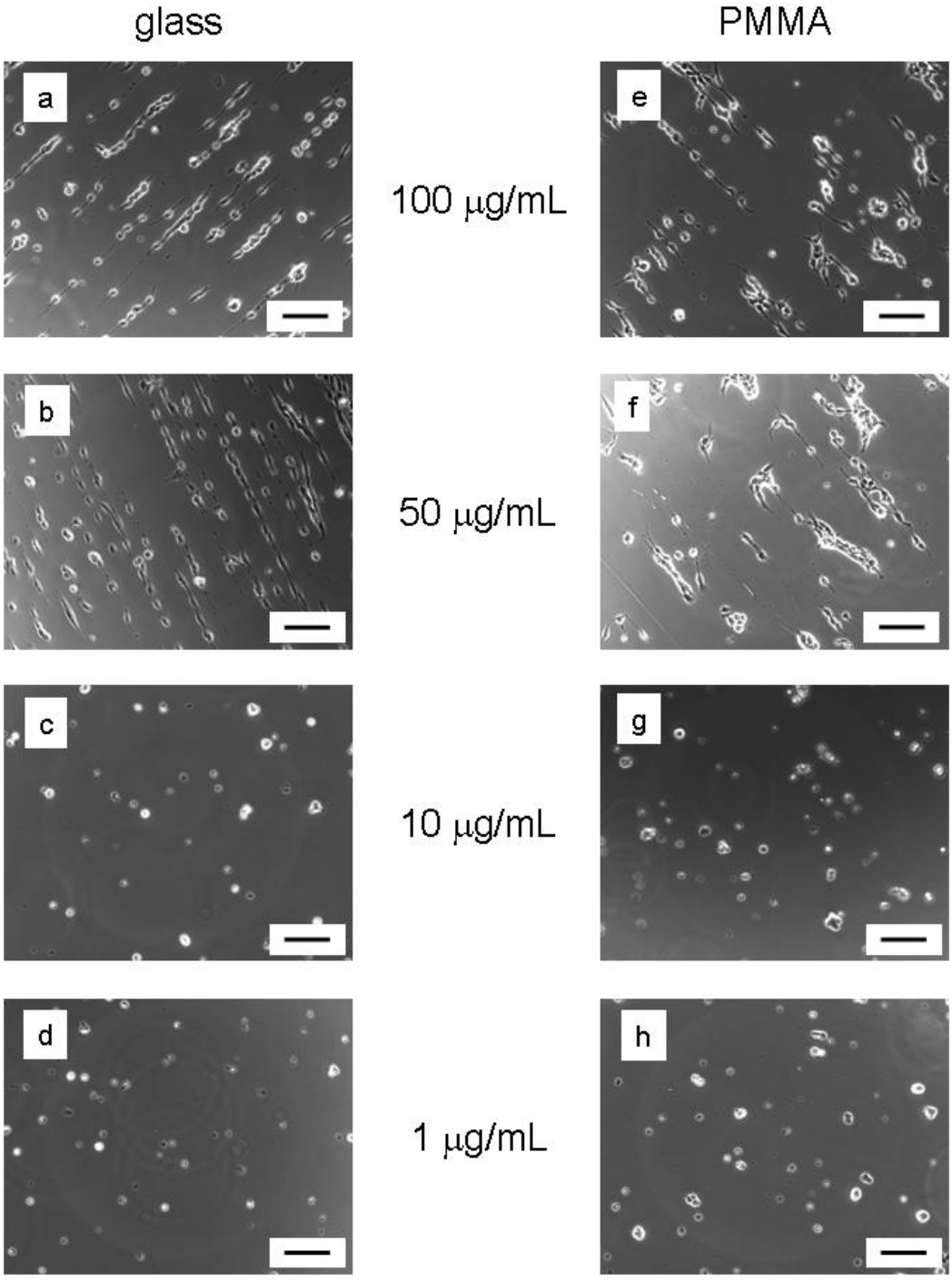

Figure 5-5: Phase contrast micrographs of NL2.3 cellular response to laminin micropatterns on glass (a-d) and PMMA (e-h) patterned from various ink concentrations: (a) & (e) 100 μg/mL, (b) & (f) 50 μg/mL, (c) & (g) 10 μg/mL, and (d) & (h) 1 μg/mL. Scale bars indicate 100 μm.

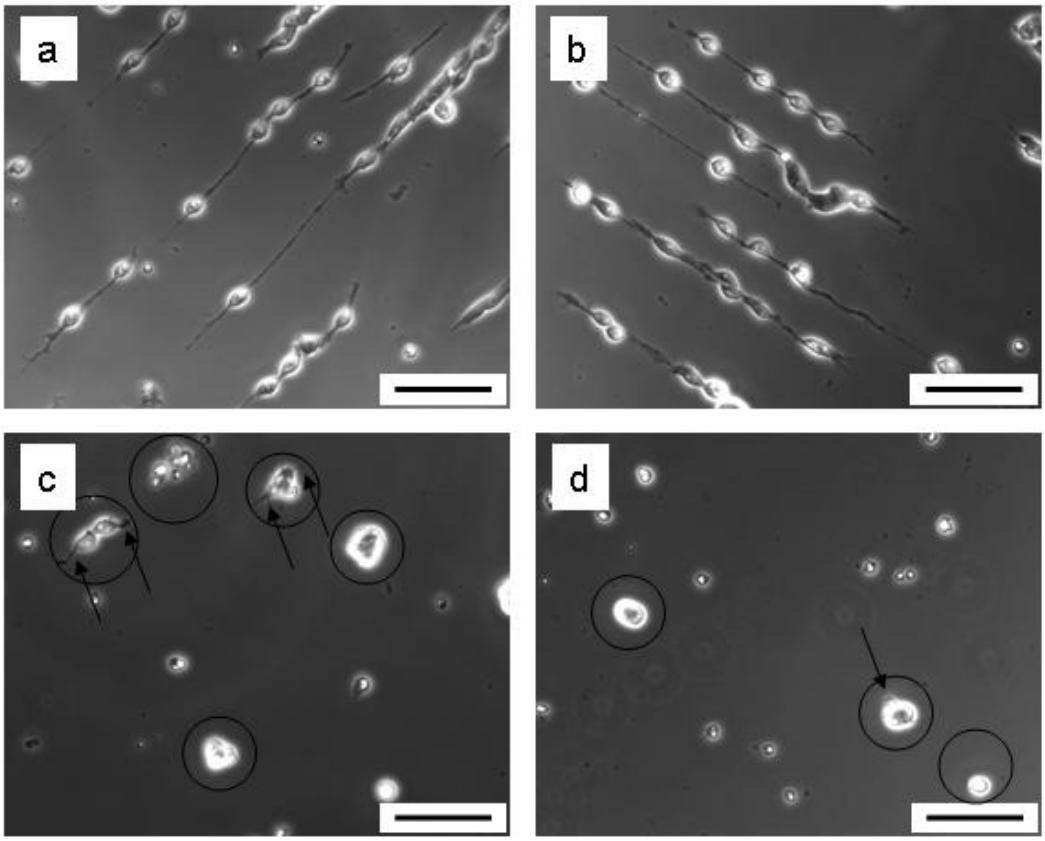

Figure 5-6: Phase contrast micrographs of NL2.3 cellular response to laminin micropatterns on glass patterned with different ink concentrations: (a) 100 μg/mL, (b) 50 μg/mL, (c) 10 μg/mL, and (d) 1 μg/mL. Cell bodies in (c) and (d) are circled whereas cell processes are marked by arrows. Scale bars indicate 100 μm.

CHAPTER 6: FACILE GENERATION OF MICROPATTERNED BIOMOLECULAR GRADIENTS BY MICROSCALE PLASMA-INITIATED PATTERNING (μPIP)

6.1 Abstract

Microscale plasma-initiated patterning (μPIP) utilizing a patterned polydimethylsiloxane (PDMS) stamp was used to generate microscale biomolecular gradients on polymer substrates. The stamp pattern, which consisted of a series of raised parallel lanes (20 μm wide) separated by 20 μm spaces, forms channels when the stamp is contacting the underlying substrate. Upon plasma exposure, these channels allow plasma to chemically modify the exposed substrate. By using modified stamps having channel openings on only one end of the stamp (i.e., "mono-portal" PDMS stamps), plasma flow is restricted to one direction. As exposed substrate regions closer to the channel opening are chemically modified more than interior regions, a plasma induced chemical gradient is formed that ultimately produces a biomolecular gradient. Using this method, gradients of FITC-conjugated poly-L-lysine were generated on poly(methyl methacrylate) (PMMA) and PDMS. In addition, the effect of plasma-treatment duration on gradient length was investigated. Although increased duration extended the overall length of the micropatterns, the lengths of the gradient portions of the micropatterns decreased.

6.2 Introduction

Several methods currently exist to micropattern biomolecules onto inorganic and organic surfaces for use in biological and medical applications.[1-18] However, relatively few

techniques have been used to successfully generate gradient micropatterns of chemicals/biomolecules.[19-29] As biomolecular gradients are naturally occurring and direct cell behavior *in vivo*[20-22,24,25,27,30,31], biomolecular gradients on polymeric substrates will permit easier *in vitro*-investigation of cell responses to elucidate the mechanisms by which cell behavior is controlled *in vivo*. Early attempts to generate micropatterned biomolecular gradients relied on photochemical means that required the conjugation of biomolecules to photoreactive molecules and subsequent UV or laser exposure.[19,20,23] More recently, after covalently immobilizing proteins onto surfaces using a photosensitive polysaccharide-based polymer, Caelen et al. generated gradients by varying the dose of light during the photoimmobilization.[25] A related technique by Li et al. used photochemical methods to generate gradients of poly(acrylic acid) (PAA) on polymeric substrates. Protein gradients were subsequently formed by covalently linking the proteins to the carboxyl groups on the PAA chains.[27] Non-photochemical methods (e.g. microstamping[22,26,28,29] and microfluidics[21,24]) have also been employed to generate biomolecular[22,26] and non-biomolecular gradients[21,24,28] with varying success. Although these techniques have advantages, they can be time consuming and require multiple processing steps and specialized equipment to successfully generate microscale biomolecular gradients. For example, electrophoretic microstamping[22] takes over 60 minutes and requires that the stamp be carefully soaked in solution so as not to disturb the gradient, making this method susceptible to failure based on operator ability. Furthermore, some photochemical methods[19,20,23,25] expose the proteins to UV irradiation, which could potentially denature the proteins.

In contrast, this chapter demonstrates facile generation of poly-L-lysine gradients on polymeric substrates using microscale plasma-initiated patterning (μPIP).[32] μPIP is a recently developed technique that uses a patterned PDMS stamp to selectively expose and protect underlying substrate regions from chemical modification via plasma exposure. Upon subsequent immersion in biomolecular solution, micropatterns are formed by the preferential adsorption of biomolecules onto either the plasma-exposed or plasma-protected regions of the substrate, depending upon the specific ink/substrate combination.[32] In this paper, poly(methyl methacrylate) (PMMA) and PDMS substrates were contacted with patterned PDMS stamps and exposed to oxygen plasma for a short duration. The stamp pattern, which consists of a series of raised parallel lanes (20 μm wide) separated by 20 μm spaces, forms channels when the stamp is contacted with an underlying substrate. Upon plasma exposure, these channels allow plasma diffusion and chemical modification of the plasma-exposed regions. Normally, plasma flows through both channel openings of the stamp; this type of PDMS stamp is hereafter referred to as a "bi-portal" stamp. However, by using modified stamps having channel openings on only one end of the stamp (i.e., "mono-portal" stamps), plasma flow is restricted to one direction. As plasma-exposed substrate regions closer to the channel opening are chemically modified more so than interior regions, a plasma-induced chemical gradient is formed upon ink immersion and adsorption. The goals of this chapter are to demonstrate the ease and speed with which biomolecular gradients can be generated by this method, as well as to illustrate the impact of plasma-treatment duration.

6.3 Materials and Methods

6.3.1 Materials

Materials. Sheets of poly(methyl methacrylate) (Goodfellow, Huntingdon, England, 0.7 mm thick, CQ grade) were cut into squares (1 cm^2) using a razor blade. Polydimethylsiloxane (PDMS) substrates were made using Sylgard 184 silicone elastomer kit (Dow Corning, Midland, MI). Elastomer base and curing agent were combined in a 10:1 ratio (w\w), after which prepolymer was placed under vacuum for 30 min. at room temperature to remove entrapped air. Thin layers of uncured elastomer (~ 5 mm) were poured into petri dishes (150 mm × 10 mm) and allowed to cure for 24 h under vacuum (-0.98 bar, room temperature). Once cured, PDMS sheets were cut with a razor blade into squares (1 cm^2). All substrates were rinsed with HPLC grade ethanol (Sigma-Aldrich, St. Louis, MO) prior to patterning. Fluorescein isothiocyanate (FITC)-conjugated poly-L-lysine (Sigma, St. Louis, MO) was diluted with phosphate buffered saline (PBS, pH 7.4, MP Biomedicals, Aurora, OH) to a concentration of 50 μg/mL.

6.3.2 Patterned PDMS Stamps

6.3.2.1 Bi-portal Stamps

PDMS stamps were prepared by pouring Sylgard 184 silicone elastomer kit (10:1 w\w base to crosslinker) over lithographically created masters, previously described in detail.[17] In brief, masters were created by exposing photoresist-coated silicon wafers through a photomask producing a relief pattern on the silicon surface. The silicone elastomer was poured over the master whose relief pattern consists of numerous 8 mm ×

8 mm areas comprised of a series of raised, parallel lanes (20 μm wide) separated by 20 μm spaces. Upon curing, the PDMS sheet was peeled off the master. The sheet of bi-portal stamps was cut into individual stamps (8 mm × 8 mm) using a razor blade or used to make mono-portal stamps (as described below).

6.3.2.2 Mono-portal Stamps

Figure 6-1a is a cartoon representation of a patterned PDMS stamp typically generated from the photolithographically fashioned master previously discussed. As shown, the stamp consists of raised patterned lanes separated by recessed spaces and surrounded by a recessed border (Figure 6-1a). A sheet of bi-portal stamps was made (as previously described), covered with a layer of uncured PDMS (Figure 6-1b), and allowed to cure for 24 h under vacuum (-0.98 bar, room temperature). Upon curing, the PDMS stamps were removed (Figure 6-1c) and trimmed with a razor blade to produce mono-portal stamps (Figure 6-1d).

6.3.3 Gradient Formation

PDMS and PMMA substrates were patterned with poly-L-lysine using the procedure outlined in Figure 6-2. A patterned PDMS stamp was placed into contact with the substrate, and the entire unit exposed to oxygen plasma (March Plasma, Concord, CA) for 15 s at 50 W and 660 mTorr (Figure 6-2-ii). Both bi-portal (Figure 6-1a) and mono-portal (Figure 6-1d) PDMS stamps were used. Once plasma-treated, the stamp was removed and the substrate immersed, treated side down, in a drop of the biomolecular ink (~ 50 μL at 50 μg/mL) for approximately 2 s at room temperature (Figure 6-2-iii).

Typically, substrates were immersed in ink within 30 s after plasma-treatment. Following immersion, the substrates were gently swirled in a beaker of deionized water (~ 20 mL) for approximately 20 s to remove non-adsorbed biomolecules, then allowed to air-dry. The poly-L-lysine gradients were visualized using confocal laser scanning microscopy (CLSM, described below).

6.3.4 Pattern Imaging by CLSM

Gradient formation was confirmed using a Zeiss LSM 410 CLSM with a computer-controlled laser scanning assembly attached to the microscope. An Omnichrome 3 line Ar/Kr laser operating at 488 nm was used as the excitation source. The images were processed with Zeiss LSM control software.

6.3.5 Evaluation of Stamp Topography by Scanning Electron Microscopy (SEM)

Bi-portal (Figure 6-1a) and pre-trimmed mono-portal PDMS stamps (Figure 6-1c) were imaged with an Amray 1830I scanning electron microscope, using acceleration potentials of 10-20 kV. Prior to imaging, stamps were sputter-coated with gold and palladium using a Balzers SCD004 sputter coater (working pressure: 0.05 mbar, working distance: 50 mm, current: 30 mA, time: 120 s).

6.3.6 Evaluation of Plasma Duration on Gradient Formation

PMMA substrates were micropatterned with poly-L-lysine following the procedure described in Figure 6-2 using oxygen plasma at 50 W and 660 mTorr. Samples were exposed to plasma for 15, 60, 420, or 900 s. Following patterning, substrates were

imaged with CLSM. The same mono-portal PDMS stamp was used throughout the experiment and the corresponding areas on each PMMA substrates were monitored and imaged. Images were analyzed with Image-Pro® Plus software to establish micropattern lengths.

6.4 Results and Discussion

Microscale plasma-initiated patterning (μPIP) has been shown to produce a range of simple and complex biomolecular micropatterns quickly (~ 6 min), consistently, and cost-effectively.[32] As the process consists solely of plasma-treatment, ink-immersion and rinsing, the procedure is easy to perform and amenable to environmentally sensitive biomolecules, such as proteins. During μPIP, the stamp/substrate complex is plasma-treated to ensure homogeneous chemical modification of the underlying, exposed substrate regions. Early observations showed that short treatment times (i.e., < 60 s) consistently formed micropatterns with varying levels of fluorescence depending on where the micropatterns were located on the substrate (e.g., substrate center vs. periphery; results not published). As a result, plasma-treatment duration is an important parameter that impacts micropattern homogeneity, with longer plasma-treatment times producing more homogeneous patterns than shorter treatment times. However, short duration plasma-treatments can be exploited to form *gradient* micropatterns, especially when plasma flow is unidirectional (i.e., restricted to a single direction across the substrate).

6.4.1 SEM Evaluation of PDMS Stamps

As shown in Figures 6-3a and 6-3b, bi-portal PDMS stamps have a series of raised lanes (20 μm-wide) separated by recessed spaces (20 μm), and at the stamp ends, recessed borders. When in contact with a substrate, the raised lanes form the channel walls with openings at either end for plasma flow (Figure 6-4a). However, when bi-portal stamps are used as a master (as shown in Figure 6-1b), the resulting PDMS stamp features are the negative of bi-portal stamps. Figures 6-3c and 6-3d are scanning electron micrographs of mono-portal stamps prior to cutting (see also Figure 6-1c). As shown, the pattern consists of a series of recessed 20 μm spaces (the darker regions in Figures 6-3c and 6-3d). By cutting one end of the stamp, the stamp will have only one set of channel openings for plasma flow when contacted with a substrate (Figure 6-4b), and thus will direct plasma flow in a single direction. As plasma would be assumed to diffuse along the PDMS channels at a constant rate, substrate regions closer to the channel openings would be more chemically modified than interior regions such that a gradient may result upon varying plasma-exposure time.

Figure 6-4 depicts schematically the hypothesized plasma flow through bi-portal (Figure 6-4a) and mono-portal (Figure 6-4b) PDMS stamps and the resulting increases in hydrophilicity of the underlying substrates. Because FITC-conjugated poly-L-lysine adsorbs to the plasma-exposed regions of PMMA and PDMS upon ink immersion, a poly-L-lysine gradient forms. As cell behavior can be directed by poly-L-lysine

micropatterns[30,33-43], it is a commonly used biomolecule and therefore, was employed as the ink for gradient generation.

6.4.2 CLSM Evaluation of Patterned Substrates

Figure 6-5 is a series of fluorescent micrographs of FITC-conjugated poly-L-lysine micropatterns on PDMS formed following the procedure outlined in Figure 6-2 using a mono-portal stamp. As decreased fluorescence indicates decreased poly-L-lysine adsorption, the amount of localized poly-L-lysine decreases as the micropatterned stripes extend towards the substrate center. The pattern fluorescence in Figure 6-5a, located at the edge of the substrate near the PDMS stamp openings, gradually decreases as the patterns extend away from the substrate periphery. The colored circles within Figure 6-5 enclose distinctive areas that were used as "landmarks" to ensure sequential capture of features. Figure 6-5f, taken farther inwards from the area shown in Figure 6-5e, illustrates that pattern fluorescence eventually decreases below detection as the surface was insufficiently modified to promote poly-L-lysine adsorption. When PMMA was utilized as a substrate, similar results were observed (data not shown). According to Figure 6-5, the mono-portal PDMS stamp effectively directed plasma flow through the channels so that substrate areas were chemically modified to different extents based on their location, with areas closer to the channel openings adsorbing more poly-L-lysine than substrate areas away from the periphery. When bi-portal PDMS stamps were plasma-treated for only 15 s, poly-L-lysine patterns were also generated (Figure 6-6) where fluorescent intensities are highest at the channel openings and lowest in the

interior. Fluorescent micrographs of poly-L-lysine micropatterns on PMMA represent substrate areas at the channel openings (Figure 6-6a & c) and at the center (Figure 6-6b). As illustrated, a double-gradient was formed when using a bi-portal PDMS stamps and short (i.e., 15-30 s) plasma-treatments.

6.4.3 Impact of Plasma-Treatment Duration

The micropatterns in Figures 6-5 and 6-6 were formed following plasma exposures of 15-30 s. As plasma exposure was increased, *qualitative* changes in micropattern fluorescence intensity were observed. Generally, increased plasma duration increased the overall length of the micropatterns, but decreased the length of the gradient portions of the micropatterns. In other words, increased plasma duration formed micropatterns with longer regions exhibiting homogeneous fluorescence than micropatterns formed after shorter plasma exposures. When using bi-portal stamps, plasma duration was eventually increased to the point where the micropatterns no longer exhibited gradual decreases in fluorescence as a function of location on the substrate. As the optimum plasma duration for gradient generation should depend on the dimensions of the stamp pattern (e.g., channel length and width), plasma conditions (e.g., feed gas, power, chamber pressure), and substrate characteristics (e.g., susceptibility to plasma modification), it is not possible to state a single set of conditions that should be employed for gradient generation.

The results described thus far can be explained by the nature of plasma, its interaction with polymer surfaces, and the relative amounts of reactive plasma species along the channels formed by the PDMS stamp. Oxygen plasma, an energetic mixture of many

reactive species, including ions and oxygen-containing radicals, [44,45] increases polymer hydrophilicity by incorporating polar, oxygen-containing functionalities onto the surface.[45-51] Based on the results, plasma diffuses along the channels to chemically modify interior substrate regions; thus regions closer to the channel openings encounter a greater number of reactive species than regions further into the substrate interior. Consequently, interior substrate areas will be chemically modified to a lesser degree and will exhibit different amounts of poly-L-lysine adsorption than areas at the periphery, provided that plasma duration is relatively short. Peripheral areas will continue to be chemically modified until equilibrium is reached where the rate of chemical incorporation equals the rate of chemical ablation/removal, after which no additional increase in oxygen incorporation will take place. This steady-state phenomena has been documented by studies that evaluated the effect of plasma exposure on polymer surfaces.[44,45,52-55] As plasma exposure is increased, a larger fraction of the overall micropattern will be composed of homogeneously fluorescent areas that were chemically modified to the same extent, with only the ends of the micropatterns at the substrate interior exhibiting any gradient effect. Therefore, the results indicate that relatively short plasma exposure times are needed to produce gradient micropatterns.

6.4.4 Comparison to Other Gradient-Generation Methods

The technique presented herein differs from previous methods used to generate biomolecular gradients. Although μPIP utilizes patterned stamps similar to those used in microcontact printing[22,26,28,29] (μCP) and microfluidic patterning[21,24] (μFP), the stamp is

selectively used to protect the underlying substrate regions from the effects of plasma during μPIP; the gradient is a result of plasma exposure, not on transfer from stamp to substrate, as in μCP, or on the ability to force solution through channels without leakage, as in μFP.

The concept of forming chemical gradients via plasma exposure has been previously investigated. For example, Pitt formed wettability gradients on polyethylene, polystyrene, poly(tetrafluoroethylene), and PDMS with ammonia, oxygen or sulfur dioxide by exposing the polymers to plasma at a constant velocity.[53] This process formed polymer surfaces with a continuous spectrum of surface energies on one sample. Similarly, Lee et al., produced hydroxyl gradients on polymer surfaces by utilizing water vapor plasma and a moveable glass mask that gradually exposed the polymers to plasma.[56] A third study by Spijker et al. formed chemical gradients with a stationary aluminum cover placed above and halfway over polyethylene samples to partly shield the polymers from plasma.[57] However, the chemical gradients formed by the three aforementioned techniques were not micron-sized, nor were the gradients directly composed of biomolecules as the ones produced by μPIP. In addition, the methods by Pitt and Lee et al. require specialized mechanical apparatuses to generate gradients, whereas μPIP uses a PDMS stamp commonly used for soft lithographic patterning. A review by Ruardy et al.[58] and other published studies[30,59-62] detail several methods used to generate chemical gradients on various surfaces, however, none of the methods cited could generate micro-sized gradients.

6.5 Conclusions

Using mono-portal and bi-portal PDMS stamps and relatively short plasma durations (e.g., 15-30 s), biomolecular gradient micropatterns on polymer substrates were readily produced. As μPIP is extremely quick (~ 2 min), and requires very little specialized equipment, it is easier to perform than most methods currently used to generate biomolecular gradients. Numerous plasma systems, other than oxygen, can be employed in μPIP, giving this method more potential versatility than current photochemical methods with regards to the chemical functionalities that can be introduced onto polymer surfaces for gradient micropatterning. Additionally, as this technique does not depend on transfer from the PDMS stamp to the substrate, as in microcontact printing, the relative ink affinities for the PDMS stamp relative to the substrate no longer hampers successful micropatterning. Furthermore, because the PDMS stamp is not in contact with the substrate during ink immersion, as in microfluidic patterning, issues regarding leakage, channel blockage or ink viscosity are not applicable. The inherent simplicity of μPIP makes it an attractive and reliable alternative to other patterning methods currently used to micropattern biomolecular gradients onto organic substrates.

6.6 Acknowledgements

The author acknowledges the New Jersey Commission on Spinal Cord Research (03-3028-SCR-E-O) and NIH (DE 13205) for financial support.

6.7 References

(1) Blawas, A. S.; Reichert, W. M. *Biomaterials* **1998**, *19*, 595-609.

(2) Dewez, J.-L.; Lhoest, J.-B.; Detrait, E.; Berger, V.; Dupont-Gillain, C. C.; Vincent, L.-M.; Schneider, Y.-J.; Bertrand, P.; Rouxhet, P. G. *Biomaterials* **1998**, *19*, 1441-1445.

(3) Xia, Y.; Whitesides, G. M. *Angew. Chem. Int. Ed.* **1998**, *37*, 550-575.

(4) Folch, A.; Toner, M. *Biotechnol. Prog.* **1998**, *14*, 388-392.

(5) Delamarche, E.; Bernard, A.; Schmid, H.; Bietsch, A.; Michel, B.; Biebuyck, H. *J. Am. Chem. Soc.* **1998**, *120*, 500-508.

(6) Tai, H.; Buettner, H. M. *Biotechnol. Prog.* **1998**, *14*, 364-370.

(7) DeFife, K. M.; Colton, E.; Nakayama, Y.; Matsuda, T.; Anderson, J. M. *J. Biomed. Mater. Res.* **1999**, *45*, 148-154.

(8) Ito, Y. *Biomaterials* **1999**, *20*, 2333-2342.

(9) Yang, Z.; Chilkoti, A. *Adv. Mater.* **2000**, *12*, 413-417.

(10) Hyun, J.; Chilkoti, A. *J. Am. Chem. Soc.* **2001**, *123*, 6943-6944.

(11) Whitesides, G. M.; Ostuni, E.; Takayama, S.; Jiang, X.; Ingber, D. E. *Annu. Rev. Biomed. Eng.* **2001**, *3*, 335-373.

(12) Park, T. H.; Shuler, M. L. *Biotechnol. Prog.* **2003**, *19*, 243-253.

(13) Turcu, F.; Tratsk-Nitz, K.; Thanos, S.; Schuhmann, W.; Heiduschka, P. *J. Neurosci. Method* **2003**, *131*, 141-148.

(14) Corey, J. M.; Feldman, E. L. *Experimental Neurology* **2003**, *184*, S89-S96.

(15) Hozumi, A.; Saito, T.; Shirahata, N.; Yokogawa, Y.; Kameyama, T. *J. Vac. Sci. Technol. A* **2004**, *22*, 1836-1841.

(16) Recknor, J. B.; Recknor, J. C.; Sakaguchi, D. S.; Mallapragada, S. K. *Biomaterials* **2004**, *25*, 2753-2767.

(17) Schmalenberg, K. E.; Buettner, H. M.; Uhrich, K. E. *Biomaterials* **2004**, *25*, 1851-1857.

(18) Falconnet, D.; Csucs, G.; Grandin, H. M.; Textor, M. *Biomaterials* **2006**, *27*, 3044-3063.

(19) Herbert, C. B.; McLernon, T. L.; Hypolite, C. L.; Adams, D. N.; Pikus, L.; Huang, C. C.; Fields, G. B.; Letourneau, P. C.; Distefano, M. D.; Hu, W. *Chem. Biol.* **1997**, *4*, 731-737.

(20) Hypolite, C. L.; McLernon, T. L.; Adams, D. N.; Chapman, K. E.; Herbert, C. B.; Huang, C. C.; Distefano, M. D.; Hu, W. *Bioconjugate Chem.* **1997**, *8*, 658-663.

(21) Jeon, N. L.; Dertinger, S. K. W.; Chiu, D. T.; Choi, I. S.; Stroock, A. D.; Whitesides, G. M. *Langmuir* **2000**, *16*, 8311-8316.

(22) Venkateswar, R. A.; Branch, D. W.; Wheeler, B. C. *Biomedical Microdevices* **2000**, *2*, 255-264.

(23) Chen, G.; Ito, Y. *Biomaterials* **2001**, *22*, 2453-2457.

(24) Dertinger, S. K. W.; Chiu, D. T.; Jeon, N. L.; Whitesides, G. M. *Anal. Chem.* **2001**, *73*, 1240-1246.

(25) Caelen, I.; Gao, H.; Sigrist, H. *Langmuir* **2002**, *18*, 2463-2467.

(26) Mayer, M.; Yang, J.; Gitlin, I.; Gracias, D. H.; Whitesides, G. M. *Proteomics* **2004**, *4*, 2366-2376.

(27) Li, B.; Ma, Y.; Wang, S.; Moran, P. M. *Biomaterials* **2005**, *26*, 1487-1495.

(28) Kraus, T.; Stutz, R.; Balmer, T. E.; Schmid, H.; Malaquin, L.; Spencer, N. D.; Wolf, H. *Langmuir* **2005**, *21*, 7796-7804.

(29) von Philipsborn, A. C.; Lang, S.; Loeschinger, J.; Bernard, A.; David, C.; Lehnert, D.; Bonhoeffer, F.; Bastmeyer, M. *Development* **2006**, *133*, 2487-2495.

(30) Halfter, W. *J. Neurosci.* **1996**, *16*, 4389-4401.

(31) Rosentreter, S. M.; Davenport, R. W.; Löschinger, J.; Huf, J.; Jung, J.; Bonhoeffer, F. *J. Neurobiol* **1998**, *37*, 541-562.

(32) Langowski, B. A.; Uhrich, K. E. *Langmuir* **2005**, *21*, 10509-10514.

(33) Wheeler, B. C.; Corey, J. M.; Brewer, G. J.; Branch, D. W. *J. Biomech. Eng.* **1999**, *121*, 73-78.

(34) James, C. D.; Davis, R.; Meyer, M.; Turner, A.; Turner, S.; Withers, G.; Kam, L.; Banker, G.; Craighead, H.; Isaacson, M.; Turner, J.; Shain, W. *IEEE Trans. Biomed. Eng.* **2000**, *47*, 17-21.

(35) Branch, D. W.; Wheeler, B. C.; Brewer, G. J.; Leckband, D. E. *IEEE Trans. Biomed. Eng.* **2000**, *47*, 290-300.

(36) Kam, L.; Shain, W.; Turner, J. N.; Bizios, R. *Biomaterials* **2001**, *22*, 1049-1054.

(37) Branch, D. W.; Wheeler, B. C.; Brewer, G. J.; Leckband, D. E. *Biomaterials* **2001**, *22*, 1035-1047.

(38) Chang, J. C.; Brewer, G. J.; Wheeler, B. C. *Biosens. Bioelectron.* **2001**, *16*, 527-533.

(39) Chang, J. C.; Brewer, G. J.; Wheeler, B. C. *Biomaterials* **2003**, *24*, 2863-2870.

(40) Vogt, A. K.; Lauer, L.; Knoll, W.; Offenhäusser, A. *Biotechnol. Prog.* **2003**, *19*, 1562-1568.

(41) Recknor, J. B.; Sakaguchi, D. S.; Mallapragada, S. K. *Biomaterials* **2006**, *27*, 4098-4108.

(42) Goldner, J. S.; Bruder, J. M.; Li, G.; Gazzola, D.; Hoffman-Kim, D. *Biomaterials* **2006**, *27*, 460-472.

(43) Moore, K.; MacSween, M.; Shoichet, M. *Tissue Eng.* **2006**, *12*, 267-278.

(44) Liston, E. M. *J. Adhesion* **1989**, *30*, 199-218.

(45) Wheale, S. H.; Badyal, J. P. S. In *Interfacial Science*; Roberts, M. W., Ed.; Blackwell Science Ltd: Oxford, 1997; pp 237-255.

(46) Gerenser, L. J. *J. Adhesion Sci. Technol.* **1987**, *1*, 303-318.

(47) Gerenser, L. J. *J. Adhesion Sci. Technol.* **1993**, *7*, 1019-1040.

(48) Süzer, S.; Özden, N.; Akaltan, F.; Akovali, G. *Appl. Spectroscopy* **1997**, *51*, 1741-1744.

(49) Owen, M. J.; Smith, P. J. *J. Adhesion Sci. Technol.* **1994**, *8*, 1063-1075.

(50) Fritz, J. L.; Owen, M. J. *J. Adhesion* **1995**, *54*, 33-45.

(51) Hillborg, H.; Ankner, J. F.; Gedde, U. W.; Smith, G. D.; Yasuda, H. K.; Wikström, K. *Polymer* **2000**, *41*, 6851-6863.

(52) Olde Riekerink, M. B.; Terlingen, J. G. A.; Engbers, G. H. M.; Feijen, J. *Langmuir* **1999**, *15*, 4847-4856.

(53) Pitt, W. G. *J. Coll. Int. Sci.* **1989**, *133*, 223-227.

(54) Øiseth, S. K.; Krozer, A.; Kasemo, B.; Lausmaa, J. *Appl. Surf. Sci.* **2002**, *202*, 92-103.

(55) Oehr, C. *Nucl. Instr. and Meth. in Phys. Res. B* **2003**, *208*, 40-47.

(56) Lee, J. H.; Park, J. W.; Lee, H. B. *Polymer (Korea)* **1990**, *14*, 646-652.

(57) Spijker, H. T.; Bos, R.; Busscher, H. J.; van Kooten, T. G.; van Oeveren, W. *Biomaterials* **2002**, *23*, 757-766.

(58) Ruardy, T. G.; Schakenraad, J. M.; van der Mei, H. C.; Busscher, H. J. *Surf. Sci. Rep.* **1997**, *29*, 1-30.

(59) Murnane, A. C.; Brown, K.; Keith, C. H. *J. Neurosci. Res.* **2002**, *67*, 321-328.

(60) Liedberg, B.; Tengvall, P. *Langmuir* **1995**, *11*, 3821-3827.

(61) Terrill, R. H.; Balss, K. M.; Zhang, Y.; Bohn, P. W. *J. Am. Chem. Soc.* **2000**, *122*, 988-989.

(62) Smith, J. T.; Tomfohr, J. K.; Wells, M. C.; Beebe, J., T. P.; Kepler, T. B.; Reichert, W. M. *Langmuir* **2004**, *20*, 8279-8286.

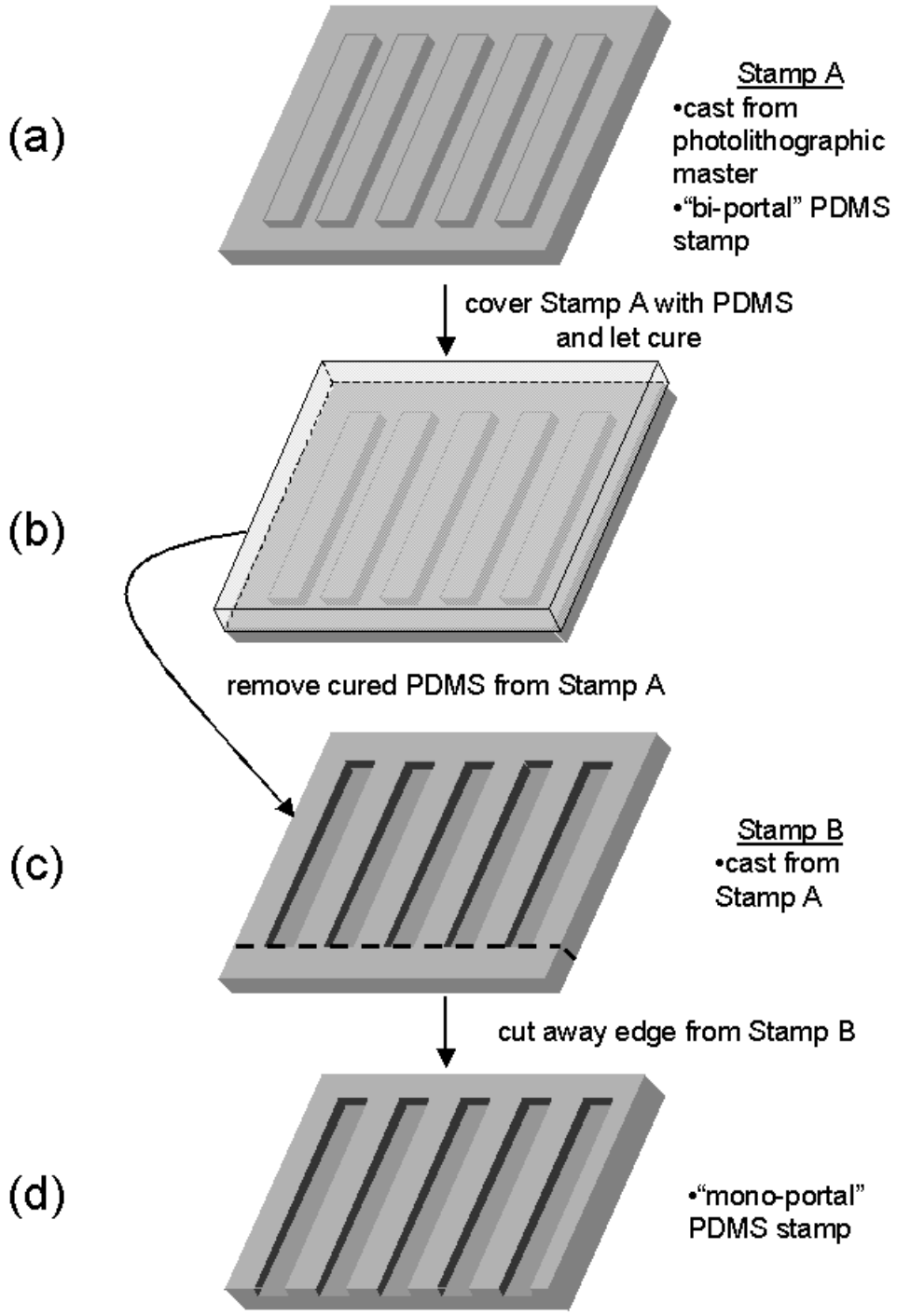

Figure 6-1: Schematic of procedure used to generate mono-portal PDMS stamps: (a) a bi-portal stamp, cast from a photolithographic master is (b) covered with uncured PDMS. Once cured, the PDMS is (c) removed from the bi-portal stamp and (d) trimmed to form a mono-portal stamp.

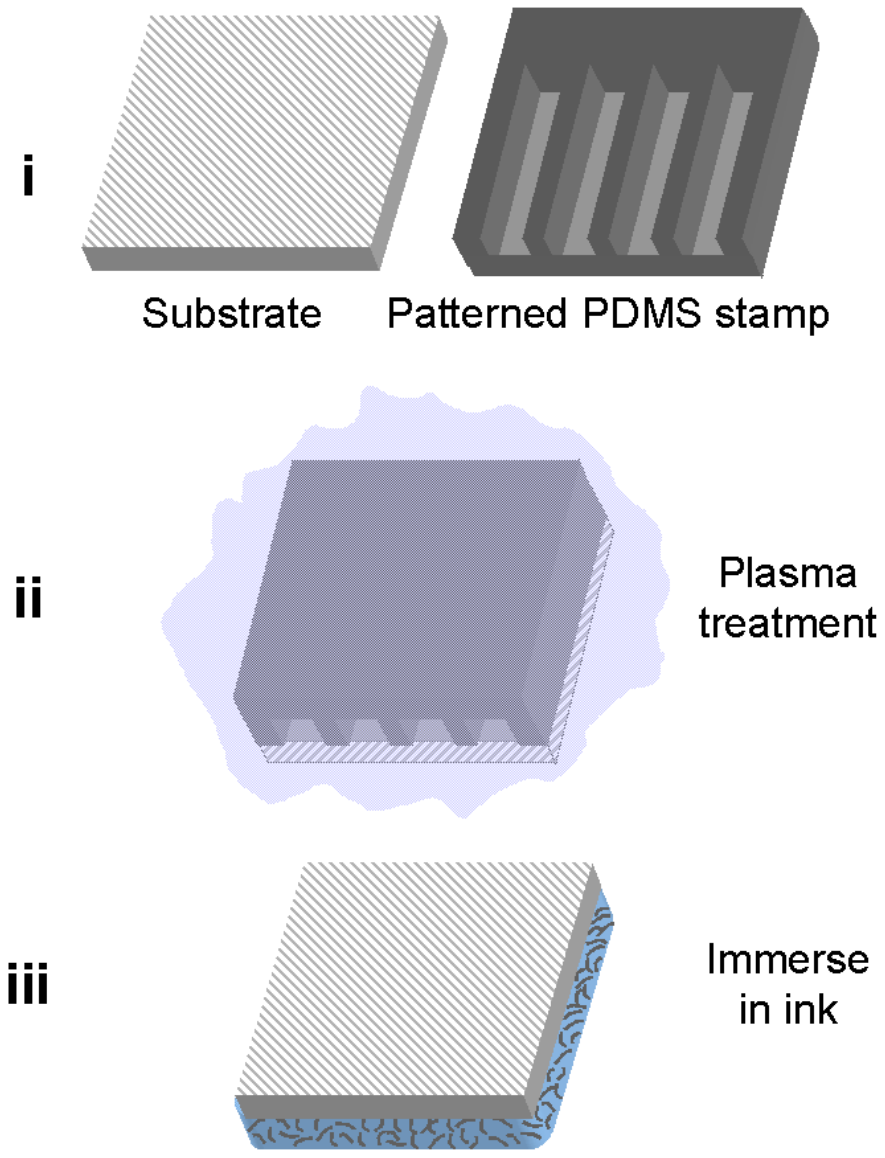

Figure 6-2: Schematic of patterning procedure used to generate biomolecular gradients.

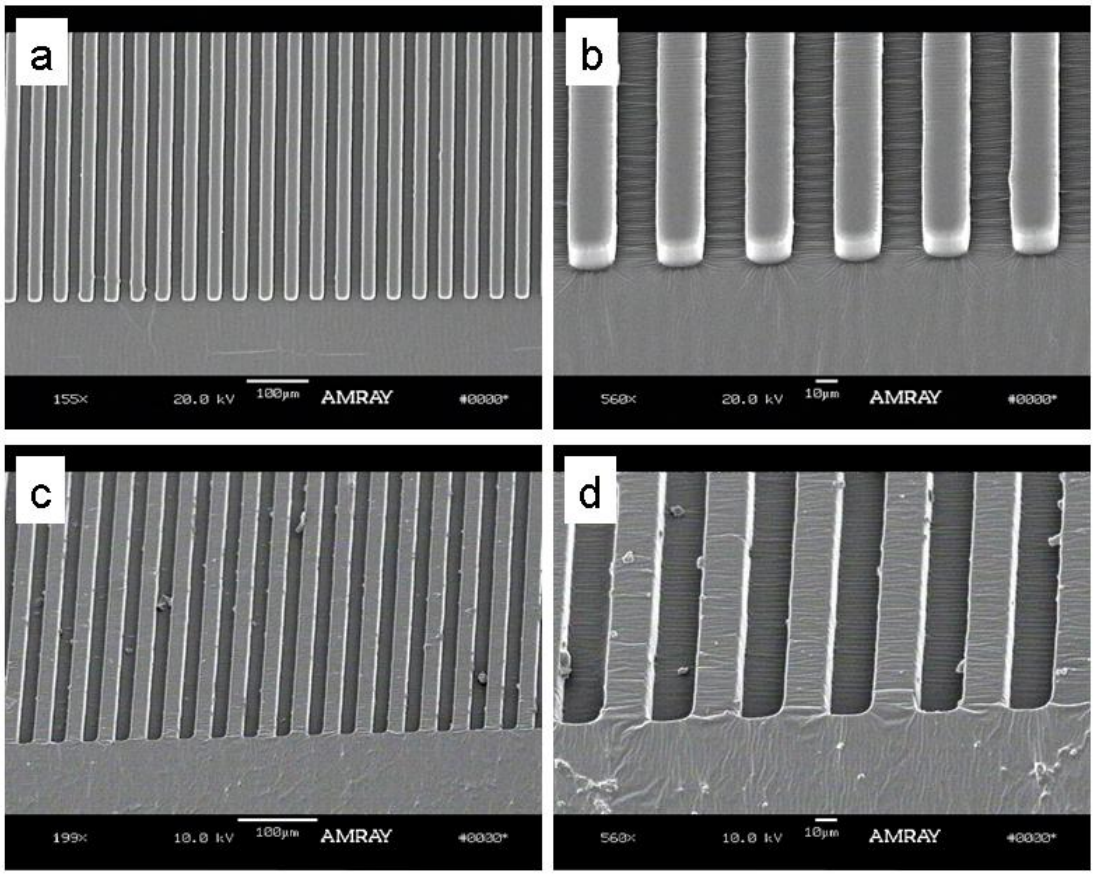

Figure 6-3: Scanning electron micrographs of bi-portal PDMS stamps (a & b) and pre-trimmed mono-portal PDMS stamps used for gradient generation (c & d). (a) 155 × magnification, (c) 199 × magnification, and (b) and (d) 560 × magnification.

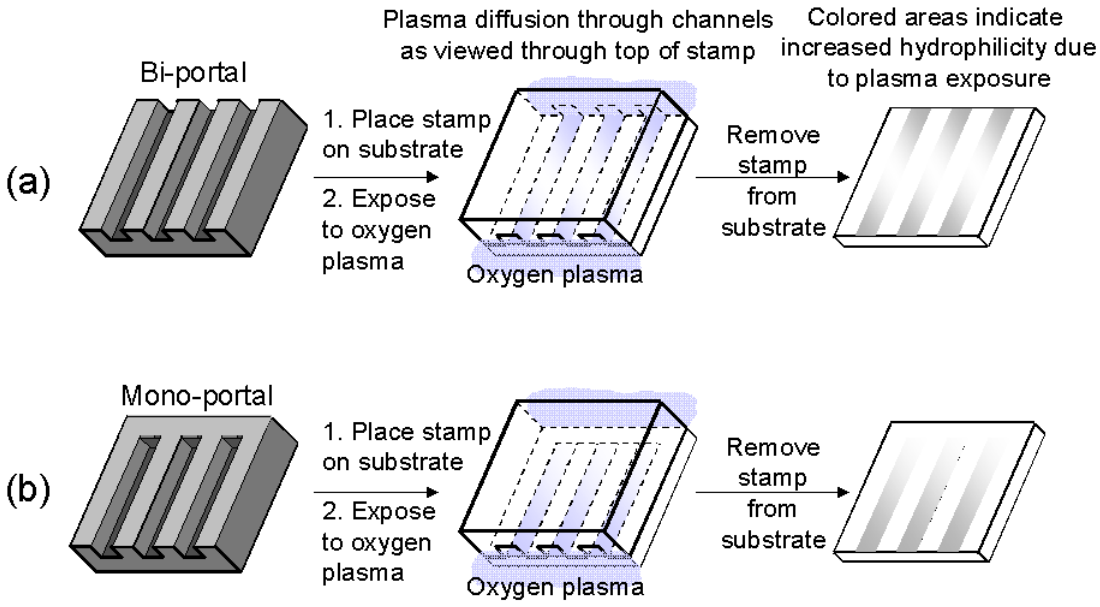

Figure 6-4: Schematic representations of plasma flow through patterned PDMS stamps and resulting hydrophilicity increases of substrate surfaces: (a) bi-portal PDMS stamps, and (b) mono-portal PDMS stamps.

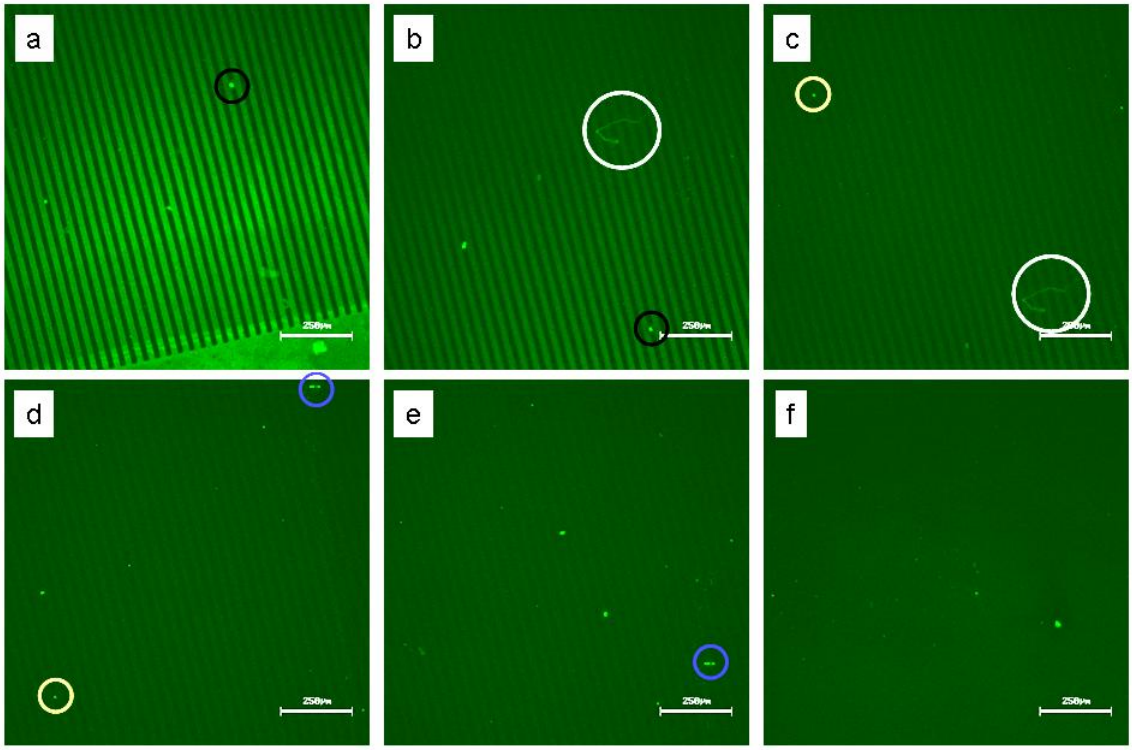

Figure 6-5: A series of fluorescent micrographs of FITC-conjugated poly-L-lysine micropatterns on PDMS. (a) – (e) were sequentially taken to monitor the change in fluorescence as the micropatterns extended towards the center of the substrate. The colored circles mark distinctive areas on the pattern present in the preceding or proceeding images to illustrate the change in fluorescence as a function of location. (f) was taken at a location farther inwards than (e), but not directly above. Scale bars indicate 250 μm.

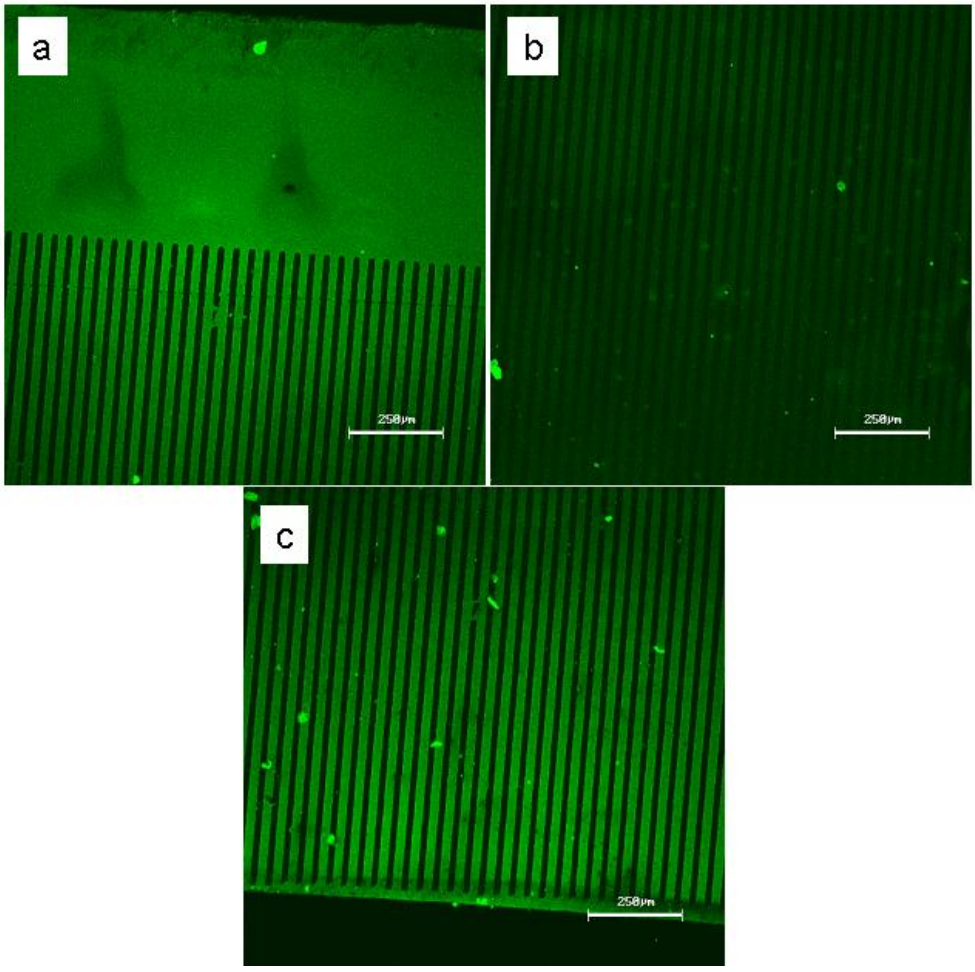

Figure 6-6: Fluorescent micrographs of poly-L-lysine micropatterns on PMMA captured at different locations on the substrate: (a) and (c) at opposite ends near the channel openings, and (b) at the approximate center. The large fluorescent particles shown in (a)-(c) are debris not removed from the substrate during rinsing. Scale bars indicate 250 μm.

CHAPTER 7: FUTURE DIRECTIONS

This dissertation documents the invention and preliminary development of microscale plasma-initiated patterning (μPIP) as a reliable technique for biomolecular micropatterning of polymeric substrates. However, as μPIP is relatively new, several issues should be addressed to realize its full versatility and potential.

7.1 Systematic Evaluation of μPIP Parameters on Pattern Formation

Although μPIP involves relatively few processing steps compared to other, more established micropatterning methods, many variables exist within those steps which may affect the extent and quality of the resulting patterns. For example, the ink concentration in which the substrate is immersed may control the amount of biomolecular adsorption, with more concentrated inks producing patterns with greater amounts of biomolecules than dilute inks. Although the effect of ink concentration was addressed in Chapter 5, the amounts of adsorbed biomolecules were evaluated indirectly by cell response, and not directly quantified. Another example is immersion time (i.e., the amount of time the substrate is in contact with the ink). While it is conceivable that longer immersion times could allow greater biomolecular adsorption on the patterns than shorter immersion times, longer immersion may also result in poorer delineation between "patterned" and "unpatterned" regions due to significant ink adsorption over the whole substrate. Therefore, to better understand μPIP pattern formation and improve pattern homogeneity and resolution, it is necessary to systematically and *quantitatively* evaluate the roles of the different processing parameters on pattern quality.

Figure 7-1 shows the effect of ink concentration on patterns formed where immersion time and plasma-treatment conditions were held constant. FITC-conjugated poly-L-lysine solution and PMMA were the biomolecular ink and substrate, respectively. At relatively low concentrations (e.g., 1 μg/mL, Figure 7-1a), the resulting patterns were ill-formed, with spatial dimensions in poor agreement with the PDMS stamp features and bare spots within the stripes. In addition, patterns were not widespread, with several bare substrate areas exhibiting no fluorescence. When ink concentration was increased to 10 μg/mL (Figure 7-1b), pattern formation was widespread with patterns exhibiting more homogeneous fluorescence along a given stripe. The resulting stripes had spatial dimensions in good agreement with the PMDS stamp, and showed complete ink coverage. Patterns formed with 100 μg/mL (Figure 7-1c) were similar in quality and patterning extent to those with 10 μg/mL. However, *qualitative* comparison of Fig. 7-1b and 7-1c shows that the fluorescence intensity of 100 μg/mL was noticeably stronger than 10 μg/mL, thus indicating more biomolecular adsorption at the higher ink concentration. Interestingly, further increase in concentration to 1000 μg/mL (Figure 7-1d) did not produce patterns with greater fluorescence intensity, indicating that biomolecular adsorption had not significantly increased when using a concentration higher than 100 μg/mL. The stepwise increases in ink concentration from 1 μg/mL (Figure 7-1a) to 10 μg/mL (Figure 7-1b) to 100 μg/mL (Figure 7-1c) successively improved pattern coverage and fluorescence intensity, indicating both 1 and 10 μg/mL were too dilute for maximum coverage of the plasma-exposed substrate regions. The increase in pattern fluorescence when going from 10 μg/mL to 100 μg/mL shows that although both sets of patterns

appeared well formed (i.e., good resolution from surrounding unpatterned region, lack of bare spots within the stripes, dimensions consistent with PDMS stamp features), the latter patterns had a higher density of biomolecules. Because pattern quality and fluorescence were not further improved by increasing ink concentration to 1000 μg/mL (Figure 7-1d), the optimal concentration for full coverage of plasma-exposed substrate regions is between 10 and 100 μg/mL and concentrations higher than 100 μg/mL serve no useful purpose.

Figure 7-2 shows the effect of ink immersion time (5 vs. 600 s) on patterns using two different ink concentrations: 1 μg/mL (Figure 7-2a, b) and 1000 μg/mL (Figure 7-2c, d). Figures 7-2a and 7-2c, formed after 5 s ink-immersion, illustrate that biomolecule adsorption is almost immediate. The patterns in Figures 7-2b and 7-2d were formed after 600 s ink-immersion. The differences in fluorescence intensity between Fig. 7-2a and 7-2c and between Fig. 7-2b and 7-2d are consistent with the results of Figure 7-1. As before, the lowest concentration patterns were ill-formed and had numerous bare spots within the stripes (Figure 7-2a, b), whereas higher ink concentrations produced more homogeneous patterns (Figure 7-2c, d). However, as shown in Figure 7-2b and 7-2d, patterns were not improved by increasing immersion times to 600 s. For example, the stripes of Figure 7-2b are of the same poor quality as those from Figure 7-2a, even though Figure 7-2b was immersed in ink significantly longer. *Qualitative* comparison of Figure 7-2c with Figure 7-2d illustrates that the same result was found at significantly higher ink concentrations. The preliminary, non-quantitative results from Figure 7-2 indicate that the amount of time a treated substrate contacts an ink (i.e., immersion time)

has no effect on the resulting pattern. As poly-L-lysine adsorption at room temperature is essentially immediate, controlling its adsorption rate by reducing the immersion time is not realistic.

While these initial results indicate that ink concentration is a controllable micropatterning parameter (Figure 7-1), and immersion time is not (Figure 7-2), the findings are based on qualitative comparisons of fluorescence intensities. To more accurately monitor changes in the amount of adsorbed biomolecule, fluorescence intensity must be quantified. The effect of other processing parameters (e.g., plasma-treatment feed gas, plasma power, plasma duration, PBS-rinse duration) could also be monitored quantitatively to provide a greater understanding of micropattern formation during μPIP.

7.2 Use of μPIP to Pattern Poly(ethylene glycol) (PEG) on Polymer Substrates

An intrinsic drawback of μPIP in its present form is the lack of control over whether a protein adsorbs to the plasma-exposed or plasma-protected regions of a given substrate. Chapter 4 demonstrates that bovine serum albumin (BSA) adsorbed to the plasma-protected regions of most polymers studied, with poly(hydroxybutyrate/hydroxyvalerate) (PHBV) being an exception. This data indicates that where a protein adsorbs will depend not only on the protein, but also on the substrate and plasma system. However, if the plasma-exposed regions of a polymer substrate could micropatterned with molecules that are resistant to protein adsorption prior to ink-immersion, subsequent protein adsorption will be forced to occur on the bare, unpatterned substrates regions. As poly(ethylene

glycol (PEG) is commonly conjugated to surfaces to make them more protein resistant,[1-3] the ability to micropattern PEG using μPIP prior to biomolecular ink-immersion would make μPIP a more universal micropatterning method that could successfully applied any polymer substrate, provided that the substrate is susceptible to plasma modification. For example, oxygen plasma is known to incorporate hydroxyl groups onto polymer surfaces. Amine-terminated PEG could be used to conjugate PEG to the plasma-induced hydroxyl groups, thus, making the plasma-exposed regions resistant to further protein adsorption.

7.3 Further Development of μPIP for Gradient Generation

The ability of μPIP to form poly-L-lysine gradients on polymer substrates is illustrated in Chapter 6. However, forming microgradients of other relevant biomolecules (e.g., laminin, collagen) will be more challenging, especially if the biomolecules adsorb to the plasma-protected (i.e., more hydrophobic) regions of a given substrate. As poly-L-lysine preferentially adsorbs to the plasma-exposed regions of PDMS and PMMA, the individual gradient strips were separated by bare regions in contact with the PDMS stamp, and thus, protected from the oxidative effects of plasma during treatment. However, if using inks that adsorb to the plasma-protected regions, gradients would appear very different: the gradient effect would run in the opposite direction (i.e., biomolecule concentration would *increase* as the pattern extends towards the substrate interior), and the gradient strips would be separated by spaces that would be homogeneously covered with the given biomolecule. This problem may be overcome, however, by employing a two-step plasma-treatment. If an untreated polymer surface is

initially hydrophobic, it could be totally exposed (i.e., in the absence of a PDMS stamp) to oxygen plasma so that the surface becomes hydrophilic. This hydrophilic surface could then be covered with a modified PDMS stamp (see Chapter 6) and exposed to plasma that will make the surface more *hydrophobic* by incorporating non-polar functionalities. Methane (CH_4) is a potential plasma feed gas that could be investigated as it would be expected to introduce non-polar methyl groups onto an exposed surface during treatment. If the substrate surfaces can be made more hydrophobic by this method, then gradients of any biomolecule, regardless of adsorption characteristics, should be relatively easy to generate.

7.4 Application of μPIP to Non-Polymeric Substrates and Non-Biomolecular Inks

Although this thesis documents the application of μPIP for biomolecular patterning on polymeric substrates, μPIP has the potential to micropattern inorganic substrates using organic-based inks. Whether a substrate is able to be patterned by μPIP depends largely on if the substrate is susceptible to chemical surface modification by plasma. With numerous choices for plasma feed gases besides oxygen, a suitable plasma system can likely be devised for most substrates. In addition, as plasma-treatment chemically modifies a surface by incorporating specific functional groups, traditional wet chemical methods could be used to conjugate other molecules to the plasma-incorporated functional groups, thereby, forming non-biomolecular micropatterns on either polymeric or inorganic substrates. For example, polymer substrates could potentially be

micropatterned with conductive polymers for use in polymer-based electronics or plastic microchips.

7.5 References

(1) Yang, Z.; Galloway, J. A.; Yu, H. *Langmuir* **1999**, *15*, 8405-8411.

(2) Chapman, R. G.; Ostuni, E.; Liang, M. N.; Meluleni, G.; Kim, E.; Yan, L.; Pier, G.; Warren, H. S.; Whitesides, G. M. *Langmuir* **2001**, *17*, 1225-1233.

(3) Liu, V. A.; Jastromb, W. E.; Bhatia, S. N. *J. Biomed. Mater. Res.* **2002**, *60*, 126-134.

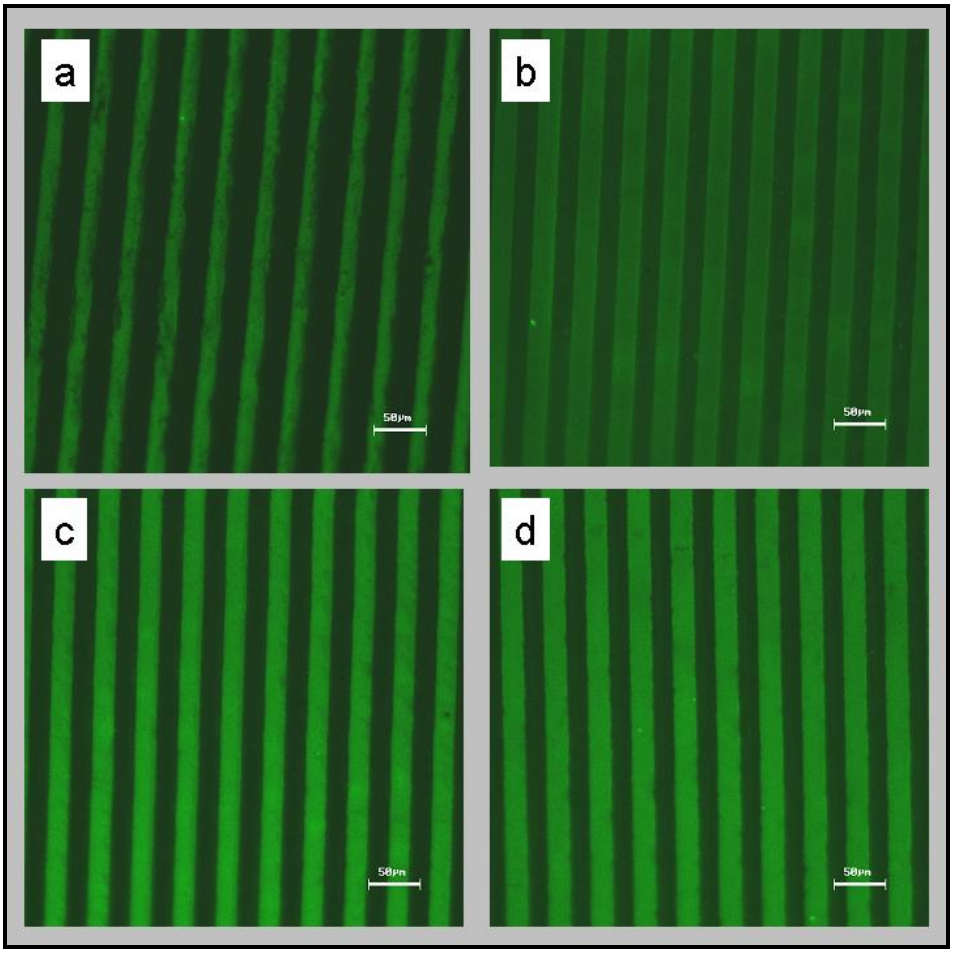

Figure 7-1: Fluorescent micrographs showing the ***effect of ink concentration*** on poly-L-lysine patterns on PMMA at constant plasma-treatment (O_2, 300 W, 300 s), ink-immersion time (60 s), PBS rinse time (20 s), and fluorescence-imaging parameters: (a) 1 μg/mL, (b) 10 μg/mL, (c) 100 μg/mL, and (d) 1000 μg/mL. Scale bar indicates 50 μm.

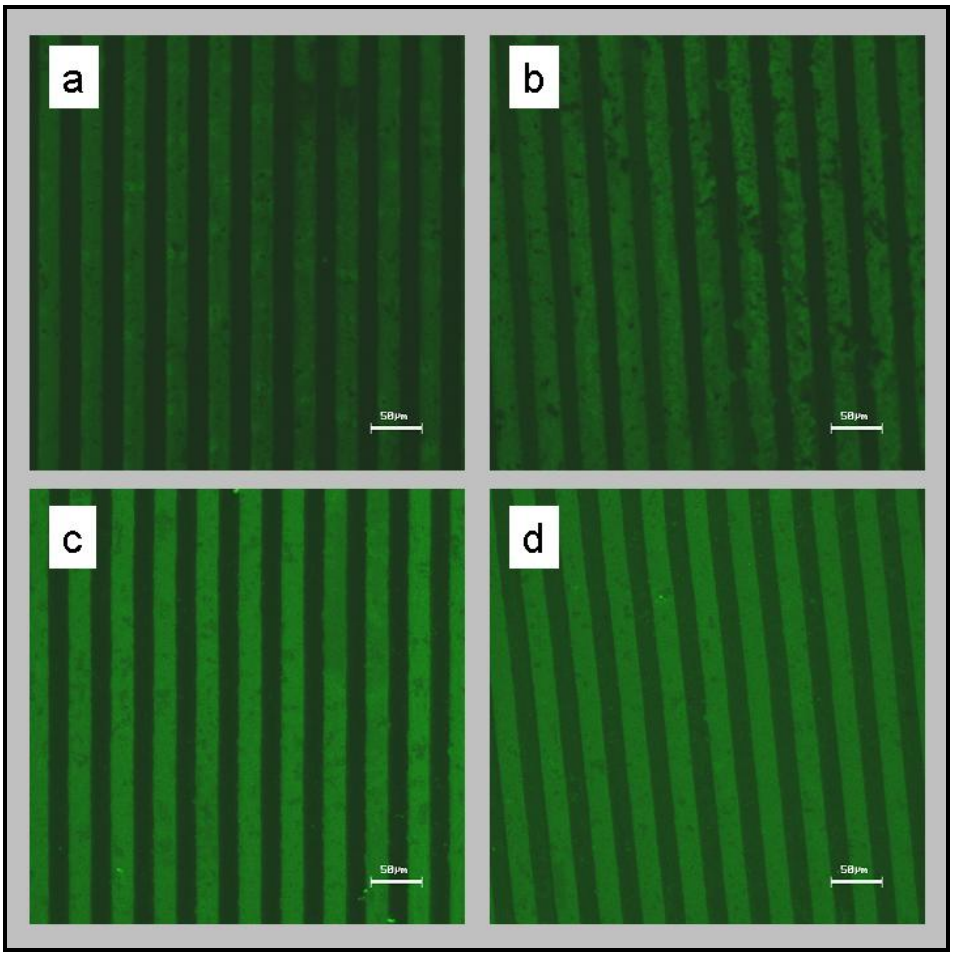

Figure 7-2: Fluorescent micrographs showing the ***effect of immersion time*** on poly-L-lysine patterns on PMMA at constant plasma-treatment (O_2, 300 W, 300 s), PBS rinse time (20 s), and fluorescence-imaging parameters: (a) 5 s (1 μg/mL ink concentration), (b) 600 s (1 μg/mL ink concentration), (c) 5 s (1000 μg/mL ink concentration), and (d) 600 s (1000 μg/mL ink concentration). Scale bar indicates 50 μm.

Curriculum Vita

BRYAN A. LANGOWSKI

EDUCATION

2007	Ph.D. Chemistry The Graduate School-New Brunswick, Rutgers University New Brunswick, NJ
2000	M.S. Forensic Science John Jay College of Criminal Justice, The City University of New York New York, NY
1997	B.S. Administration of Justice Rutgers College, Rutgers University New Brunswick, NJ

PUBLICATIONS

Langowski, B. A., Uhrich, K. E., "Microscale Plasma-Initiated Patterning (μPIP)", *Langmuir* **2005**, *21(23)*, 10509-10514.

Langowski, B. A., Uhrich, K. E., "Oxygen Plasma-Treatment Effects on Si Transfer", *Langmuir* **2005**, *21(14)*, 6366-6372.

Langowski, B. A., Rothchild, R., Sapse, A., "*Ab Initio* Studies of Hindered Rotation of Some Aromatics Rings in *N*-2, 6-Difluorophenyl Imides and Unsubstituted Bridgehead Phenyls", *Spectroscopy Letters* **2001**, *34(2)*, 235-251.